2012

Synthesis of a difluorometric cross-membrane molecular probe for studying amphipathic systems

Danielle Raymond

Synthesis of a Difluorometric Cross-Membrane Molecular Probe for Studying Amphipathic Systems

Danielle M. Raymond

Submitted in Partial Fulfillment

of the Requirements for the Degree

Master of Science in Chemistry

Supervised by

Dr. Christina Goudreau Collison

School of Chemistry and Materials Science

The College of Science

Rochester Institute of Technology

Rochester, New York

2012

Approved: _____

Project Advisor

_____

Department Head

_____

Library

Copyright Release Form

Synthesis of a Difluorometric Cross-Membrane Molecular Probe for Studying Amphipathic Systems

I, Danielle M. Raymond, hereby grant permission to the Wallace Memorial Library, of RIT, to reproduce my thesis in whole or in part. Any use will not be for commercial use or profit.

Signature

Date

Acknowledgements

First and foremost I would like to thank my research advisor and mentor Dr. Christina Collison. With all of your help and encouragement over the last two years I've finally accomplished my goal and I have realized my passion for chemistry is going to expand beyond these next five years and far into my future. I would not have been so successful without your guidance. I would also like to thank the rest of my committee members for all of your imparted wisdom and support: Dr. Cody, Dr. Coleman, Dr. Tan, and the late Dr. Langner who will surely be missed. Thank you to the Chemistry department and staff at RIT as well for financial aid, support, and encouragement.

Secondly, to my family who has been such a crutch I would never have made it this far in my academic endeavors if I didn't have your full support and encouragement. To my Mom and Dad, you have taught me to strive for the best and I've excelled because I know you are always there to catch me if I fall. Thank you for your unconditional love and support. And to Clint, you have been my life-support through all of the late nights and crazy schedules. Thank you so much for your continued support and reassurance.

To my lab mates Jenn Swartzenberg and Anthony Carestia who made working in the lab fun and the time pass quickly, thank you for all of your help! To Morgan Bida and Anthony Mangan, thank you for being my sounding board all of the time. You are the reason I was able to make it through all of the hard work and the friendships we've cultivated over the last two years mean a lot to me. I would also like to thank all of the students who started worked on this project before me mainly Ryan Walvoord, Timothy Liwosz, Brett Granger, and Josh Kolev.

Abstract

A surfactant is an amphiphile which consists of a hydrophobic and hydrophilic end. In nonpolar solvents containing a small amount of water surfactants can form reverse micelles. Extensive research has been done using fluorescent probes to study several properties of these amphiphilic aggregates including mechanism of formation, critical micelle concentration, aggregate number and size, nanopolarity, and viscosity. Dr. Langner's group at RIT proposed the structure of a difluorometric, ratiometric probe that can transverse the membrane of a reverse micelle created in a system of decane/water/AOT/butyl alcohol. This probe has a dansyl and a coumarin portion making it amphiphilic and could advance future studies in the formation of reverse micelles and the kinetics of their interactions with other compounds. Use of a difluorometric probe helps eradicate the limitations of previously utilized single fluorophore-containing probes involving both their interactions with the aqueous medium, and pinpointing the location in the reverse micelle system.

My research focused on the synthesis and combination of the dansyl chloride and the 7-amino-4-methyl coumarin species through derivatization chemistry of an acid chloride into an amide. This thesis will serve to highlight various synthetic methods employed by previous undergraduate students in the Collison group as well as my work towards the synthesis of the difluorometric compound which can serve as a probe for various amphipathic systems including reverse micelles. The derivatization chemistry to successfully synthesize this molecule is covered in detail and two difluorometric probes with varying hydrocarbon chain lengths are reported.

Abbreviations

AcOH- Acetic acid
AOT- Sodium bis(2-ethylhexyl)sulfosuccinate, or Aerosol-OT
AuO- Auramine O
nBuLi- *n*-Butyllithium
$(COCl)_2$- Oxalyl chloride
CBr_4- Tetrabromomethane
CCl_4- Carbon tetrachloride
CF_3CH_2OH- 2,2,2-trifluoroethanol
$CHCl_3$- Chloroform
CH_2Cl_2- Dichloromethane
CH_3CN- Acetonitrile
CMC- Critical micelle concentration
C_nOPTPP- (Alkoxyphenyl) tripheylporphyrins
Cs_2CO_3- Cesium carbonate
CTAB- Cetyltrimethylammonium bromide
$CuSO_4$- Copper(II) sulfate
DCM- Dichloromethane
dH_2O- Distilled water
DMA- 4-(Dimethylamino)pyridine
DMF- Dimethylformamide
DMS- Dimtheylsulfoxide
DMSO-d_6- Deuterated dimethyl sulfoxide
DNA- Deoxyribo nucleic acid
Dns-Phe- Dansylated phenylalanine
D_2O- Deuterium oxide
DPA- Dipicolylamine
EtOAc- Ethyl Acetate
EtOH- Ethanol
Et_2NH- Diethylamine
Et_3N- Triethyl amine
HCl- Hydrochloric acid
H_2CrO_4- Chromium(VI) oxide
HMPA- Hexamethylphosphoramide
H_2O_2- Hydrogen peroxide
H_2SO_4- Sulfuric acid
IMP- Most widely recognized metallo-β-lactamase
IR- Infrared spectroscopy
KH- Potassium hydride
$KMnO_4$- Potassium Permanganate

KOAc- Potassium acetate
LC/MS- Liquid chromatography/ mass spectrometry
MBL- Metallo-β-lactamase
MeCN- Acetonitrile
MeOH- Methanol
$MgSO_4$- Magnesium sulfate
MHz- Megahertz
MsCl- Methanesulfonyl chloride
$Na(AcO)_3BH$- Sodium triacetoxyborohydride
NaI- Sodium iodide
NaOH- Sodium hydroxide
NMR- Nuclear Magnetic Resonance Spectroscopy
PCC- Pyridinium chlorochromate
PCl_5- Phosphorous pentachloride
$PdCl_2$ (dppf)- 1,1′-Bis(diphenylphosphino)ferrocene]dichloropalladium(II)
PET- Photoinduced electron transfer PPh_3 Triphenylphosphine
iPr_2EtN- *N*,*N*-Diisopropylethylamine
RAW264- Macrophage-like, Abelson leukemia virus transformed cell line
RIT- Rochester institute of technology
ROH- Alcohol with chain length R
ROS- Reactive oxygen species
RT- Room temperature
$SOCl_2$- Thionyl chloride
TBS- *Tert*-butyldimethylsilyl
TBDMSCl- *Tert*-butyldimethylsilyl chloride
TEA- Triethylamine
THF- Tetrahydrofuran
TLC- Thin Layer Chromatography
TPEN- N,N,N,N- tetrakis(2-pyridylmethyl)ethylenediamine
UV- Ultraviolet

Table of Contents

List of Figures

List of Schemes

List of Tables

CHAPTER 1: INTRODUCTION

Amphiphiles containing both a hydrophobic and hydrophilic component make up secondary micelle structures under critical micelle concentrations in organic/aqueous mixtures. In an attempt to study such reverse micelle systems in a bulk solution of a nonpolar organic solvent containing a small amount of water, Dr. Langner et. al proposed an amphipathic difluorometric probe linking both a dansyl and coumarin component with a hydrocarbon tether (Figure 1).

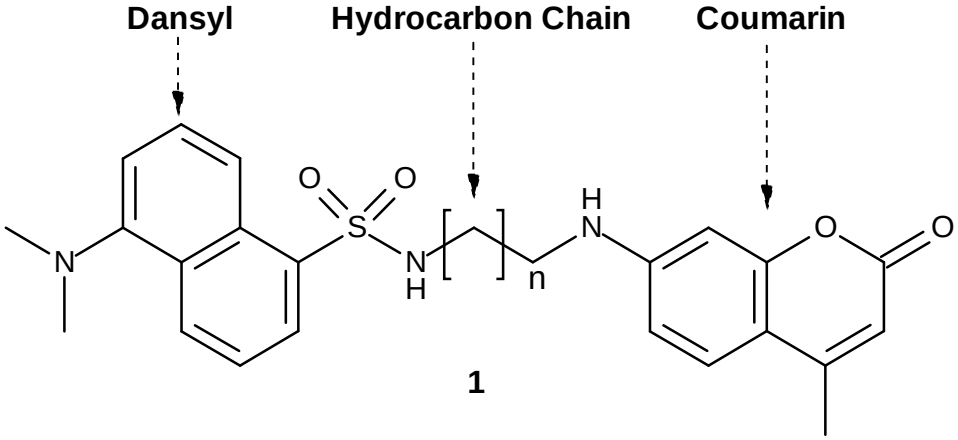

1

Figure 1. Proposed structure of a difluorometric probe of reverse micelles containing dansyl and coumarin components

With sufficient evidence in the literature to support the fluorometric capabilities of both dansyl and coumarin individually as probes to study types of amphipathic systems, this is the first probe to combine their solvatochromic and ratiometric capabilities together. The advantages of this difluorometric probe can help remove the limitations of pinpointing the probe inside of the reverse micelle when only one chromophore is present. Herein the successful synthesis and characterization of probes

44 and **46** are reported and several synthetic attempts of these difluorometric probes are described.

1.1 Amphipathic Systems: Micelles and Reverse Micelles

A surfactant is an amphiphilic compound which means it contains both a hydrophilic (water soluble) and hydrophobic (water insoluble) component. Depending on their nature, surfactants can be classified as cationic, anionic, zwitterionic, or non-ionic species. These surfactants can form many larger aggregates including micelles, reverse micelles, monolayers, bilayers, and vesicles (Figure 2).[1]

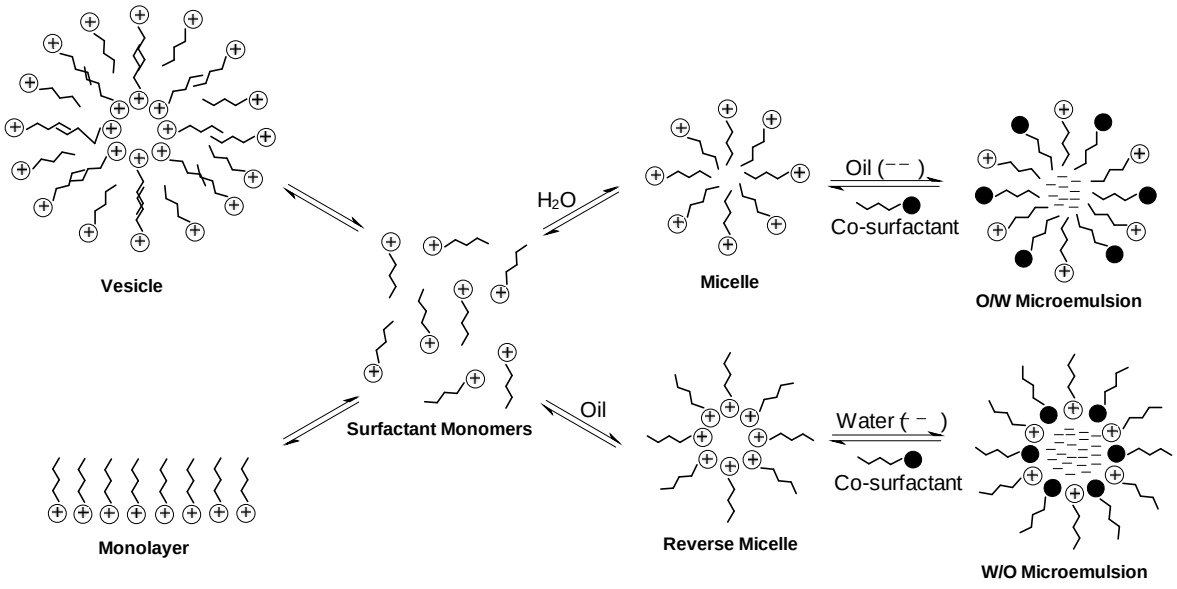

Figure 2. Examples of amphipathic aggregates

Micelles form beyond a certain concentration in water known as the critical micelle concentration (CMC). The polar head groups of the surfactants will line up and be in contact with the outer bulk of the aqueous solution while the inner core of the micelle is formed by the hydrophobic chains (Figure 3). The polar head groups of the monomers arrange randomly so the surface of a micelle is not a smooth one.[1]

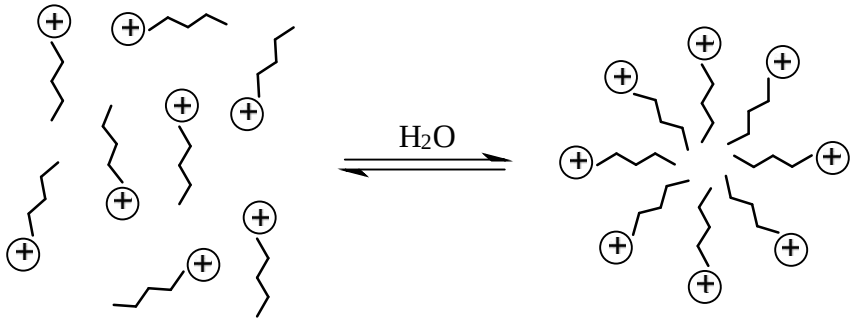

Figure 3. A micelle aggregate

Reverse micelles are the opposite composite; in nonpolar solvents containing small amounts of water the polar head groups are directed towards the center entrapping the water while the hydrophobic tails extend outward toward the bulk of the non-aqueous solution (Figure 4).

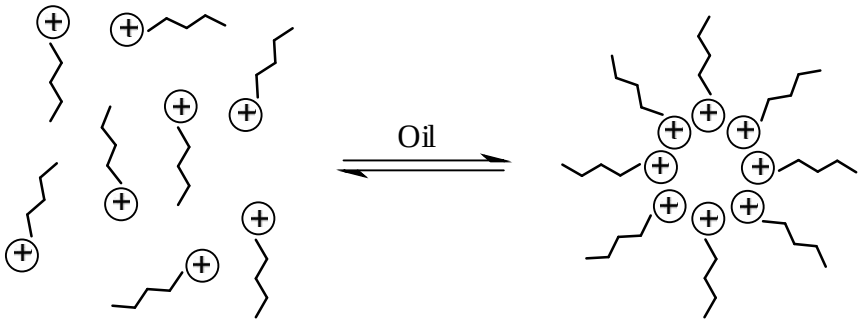

Figure 4. A reverse micelle aggregate

The water content inside of a reverse micelle has been extensively studied and was found to be different from that of ordinary bulk water; it is heterogeneous in nature and its properties will change as a function of R_w which is defined as $\frac{[H_2O]}{[surfactant]}$ and will change with increasing distance from the polar head layer.[1] As such, it is important to have methods to investigate the formation, kinetics, composition, etc. of these amphipathic systems. There are certain characteristics which allow some molecules to determine parameters like these better than others.

1.2 Fluorescent Probes and Their Characteristics for Studying Surfactants

Recently, fluorescence spectroscopy has been used to study characteristics of surfactant assemblies and determine parameters such as critical micelle concentration[3], nanopolarity[4], viscosity[5], aggregation number[6], size of aggregates[7], etc. When a ground state molecule (S_0) is excited by the absorption of photons from incident light, this creates an excited singlet state (S^*) with multiple vibrational levels. This molecule can then degenerate to the lowest vibrational level of the excited singlet state (S_1) through thermal relaxation. The energy contained in this excited state can be emitted in different radiative and non-radiative pathways as illustrated in the Jablonski diagram (Figure 5). Non-radiative processes include internal conversion (IC) and intersystem crossing (ISC). Radiative processes include, but are not limited to, phosphorescence (the process occurring from T_1 to S_0 where T is a triplet state formed from the absorption of energy producing unpaired spins) and fluorescence (the process from S_1 to S_0 where S is a singlet state formed from energy absorption producing paired spins).[2]

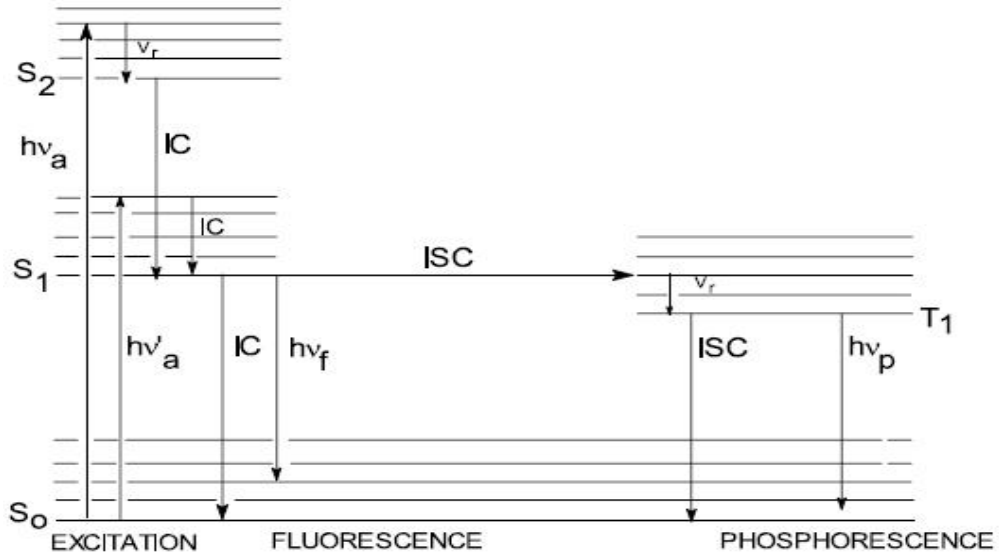

Figure 5. Jablonski diagram describing radiative and non-radiative pathways

The emission process known as fluorescence has been used to study the dynamics of surfactant aggregate formation using, as a probe, molecules that fluoresce at a particular wavelength. This can be done with the measurement of the changes of the emission properties of the fluorescent probe such as spectral distribution (maximum wavelength or maximum intensity), quantum yield, or fluorescence lifetime during the transition from the monomeric stage of the surfactants to the formation of the aggregate. These measurements are quantitatively related to various experimental factors by two different expressions[2]:

$I_f = I_0 (1 - 10^{-\varepsilon c l})\varphi_f$ where I_f is the fluorescence intensity, I_0 is the intensity of the light, ε is the molar absorptivity, c is the molar concentration of the solute, l is the path length (cm), and φ_f is the quantum yield of fluorescence.

$I_{f(t)} = I_{f(0)} exp^{-t/\tau}$ where $I_{f(0)}$ is the initial fluorescence intensity at time t=0, $I_{f(t)}$ is the fluorescence intensity at time t, and τ is the average fluorescence lifetime of the excited singlet state. Responses of the fluorometric probes are sensitive to changes in the microenvironment in which they are contained so that they can display distinct luminescent properties.

There are specific characteristics that are desirable for a fluorescent probe to exhibit. Such characteristics include a rigid framework and a small number of coupled vibrational energy levels in which the excitation energy can be lost. Organic molecules typically used as probes absorb energy in the 250-260nm region. A fluorescent probe can be characterized as intrinsic, extrinsic, or covalently bound. Intrinsic probes allow a system to be observed without any kind of chemical perturbation and it only occurs when the system to be studied contains an intrinsic fluorophore such as tryptophan[8] or

phenylalanine[9] present in proteins. Some probes can be covalently bound to the system being studied but those not covalently bound are known as extrinsic fluorescent probes. There have been several organic molecules employed as fluorescent probes in order to study aggregates such as micelles[10], reverse micelles[11], microemulsions[12], liposomes[13], monolayers[14], and bilayers[15]. Of these various aggregates, reverse micelles are of particular interest due to their use as a medium to study chemical and biological reactions.[16]

1.3 Fluorescent Probe Examples to Study Reverse Micelles

Fluorescence spectroscopy has been used extensively and is a viable way to determine the structure of reverse micelles based on the study of the nature of the water that is enclosed. Valeur et al. was able to study the acid-base reactivity of water inside of a reverse micelle of sodium dioctylsulfosuccinate commonly known as AOT[17] which is the most commonly used surfactant in reverse micelle research (Figure 6). Three fluorescent probes were used to study this acid-base reactivity: 2-naphthol (NOH), sodium-2-naphthol 6-sulphonate (NSOH), and potassium 2-naphthol-6,8-disulphonate (NDSOH) (Figure 7).[18] Using these fluorescent probes, Valeur was able to determine the rate constants of deprotonation and recombination in the aqueous medium of the reverse micelle (Figure 8) as well as their exact location in the aggregate.[1,18]

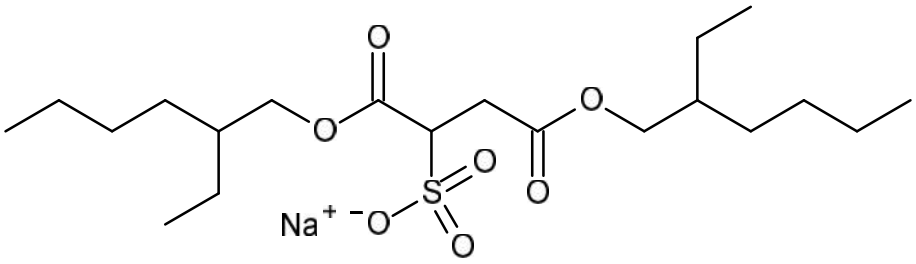

AOT

Figure 6. Structure of an AOT surfactant monomer

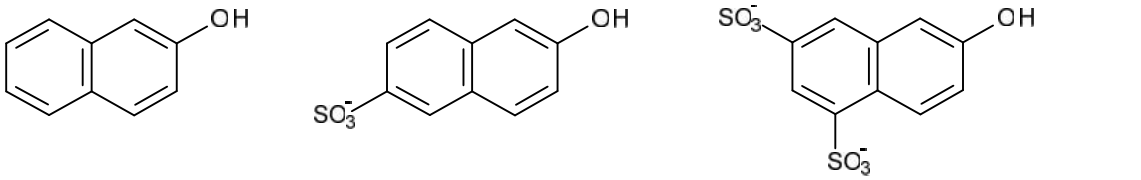

2-Naphthol (NOH) **2-Naphthol-6-Sulfonate (NSOH)** **2-Naphthol-6,8-Disulfonate (NDSOH)**

Figure 7. Structures of NOH, NSOH, and NDSOH

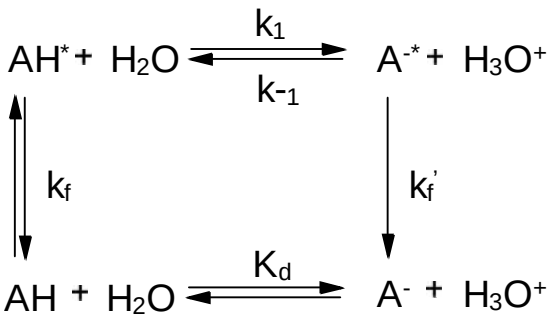

Figure 8. The proton-transfer reaction studied by the NOH derivatives

Kevan et al. synthesized a series of (alkoxyphenyl) triphenylporphyrins (C_nOPTPP) which have varying chain lengths (Figure 9). These probes were used to investigate the photo-induced electron transfer to the interface water in both AOT and CTAB/ROH (cetyltrimethylammonium bromide) reverse micelles.[11]

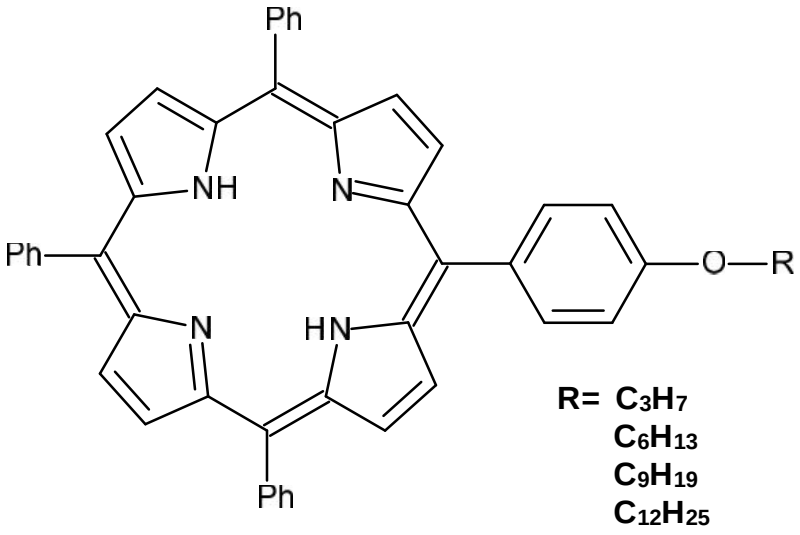

Figure 9. Series of porphyrin based C_nOPTPP probes with varying chain lengths

The photoyield of this reaction was correlated to the alkyl chain length of the porphyrins, the cationic or anionic interface charge of the reverse micelles, and the length of the cosurfactant alcohol used in the CTAB/ROH micelles. With increasing chain lengths of the C_nOPTPP moiety there was a decrease in photoyield due to an increased distance between the porphyrins and the interface water as there was more hydrophobic interactions between the nonpolar chains. Similar results were found when changing from C_4OH to C_8OH in the CTAB/ROH system; with increasing hydrophobic interactions there was an increase in the interaction distance between the porphyrins and the interface water which lowered photoyields (Figure 10). The cationic interface charge of CTAB/ROH produced higher photoyields than the anionic interface charge of the AOT reverse micelles. Overall, Kevan and co-workers showed that shorter chain lengths of both the porphyrin and cosurfactant alcohol, and a cationic reverse micelle interface charge are all optimal conditions for efficient electron transfer through the interface of a reverse micelle.[11]

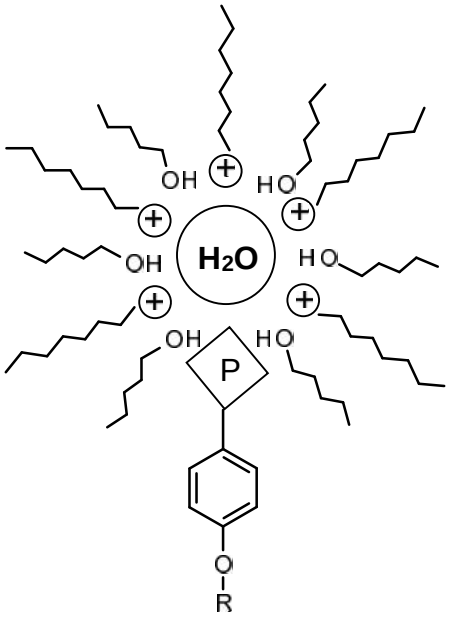

Figure 10. The C_nOPTPP probes used to study the electron transfer through the interface of a reverse micelle of a CTAB/ROH reverse micelles as a function of porphyrin moiety (P) chain length and ROH co-surfactant chain length

Polarity and microviscosity of the water contained inside of a reverse micelle have also been studied using fluorescent probes. A measurement of the viscosity inside of a micelle is based on the measurement of the fluorescent properties which depend on the mobility of the probe in its environment.[2] Hasegawa and co-workers determined the microviscosity of the water in an AOT reverse micelle as a function of R_w ($\frac{[H_2O]}{[\text{surfactant}]}$) using a viscosity-sensitive fluorescent probe Auramine O (AuO) (Figure 11). The fluorescence quantum yield of AuO was found to increase with increasing solvent viscosity when it was solubilized in the reverse micelle core. The microviscosity of the water pool decreased rapidly below $R_w = 10$, then the microviscosity changed gradually until the solution became thick at $R_w = 50$.[19]

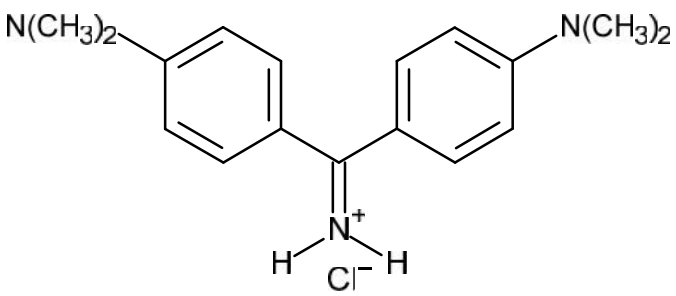

Auramine O (AuO)

Figure 11. Structure of AuO used to study the microviscosity of water inside of an AOT reverse micelle

The aggregation number or number of surfactants constituting a surfactant assembly can also be determined using fluorescence spectroscopy. This determination can be accomplished by monitoring the decrease in fluorescence intensity of the probe by a quencher inside of the aggregate either by steady-state fluorescence quenching or time-resolved fluorescence quenching. Turro and Yekta applied this steady-state fluorescence quenching to measure the decrease of fluorescence intensity of a micelle bound probe as a function of quencher concentration and fitted it to this equation: $\ln \frac{I}{I_0} = \frac{N[Q]}{C_s} - CMC$ where C_s and $[Q]$ is the total concentration of the surfactant and quencher respectively and *N* supplies the aggregation number.[2,20]

Given the uses of a fluorescent probe to study reverse micelles, Langner and coworkers designed a difluorometric probe consisting of both a dansyl and coumarin moiety in order to probe surfactant assemblies (Figure 12). Dansyl and coumarin are two aromatic compounds that each have their own fluorescent capabilities that allow them to probe assemblies such as micelles, reverse micelles, and proteins effectively. There are

several examples in literature of the ability of these compounds to probe such structures. Together, they have the ability to enhance the capabilities of a singular probe.

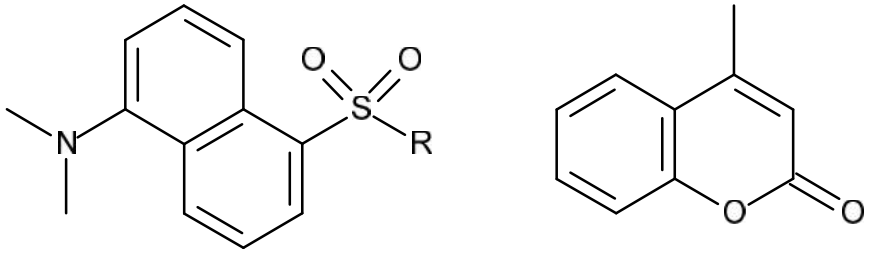

Dansyl **Coumarin**

Figure 12. Dansyl and Coumarin aromatic compounds which display individual fluorescent characteristics

1.4 Introduction to Fluorescent Probes Consisting of Dansyl and Coumarin

Dansyl compounds are environmentally sensitive and known to exhibit large Stokes shifts along with varying fluorescent quantum yields when exposed to changing local environments.[21] Dansyl chloride exhibits an absorbance maximum at 372 nm in chloroform (when derivatized with n-butylamine) and an emission maximum at 492 nm. Dansyl chloride is a well-known solvatochromic compound which exhibits a shift in wavelength in its absorbance and emission spectra in the presence of different solvent polarities.[21] Coumarin and its 7-amino derivatives are known to exhibit high intensity fluorescence and are relatively easy to synthesize. 7-Amino 4-methylcoumarin has an absorbance maximum at 350 nm and an emission maximum at 430 nm.[22] There are several examples in literature which will be discussed in more detail in the next sections that provide information on how these two compounds have been used as fluorescent probes.

1.5 Fluorescent Probes Containing a Dansyl Component

Kurosaki and coworkers synthesized a group of fluorescent probes (dansylC_nSHs) with a thiol group as a Zn^{II} ligand and a dansyl group as the fluorophore in order to detect IMP-1 (Figure 13).[23] IMP-1 is one of the most widely recognized metallo-β-lactamases (MBL's) which are created by various pathogenic bacteria and can catalyze the hydrolysis of the β-lactam ring of β-lactam antibiotics. Often times MBL's are not susceptible to β-lactamase inhibitors and therefore it is important to be able to detect the presence of IMP-1 in infectious bacteria for effective chemotherapy at initial stages of a disease. In order to test whether or not these probes were effective at detecting IMP-1 the measurement of the fluorescence emission spectra was completed with 1 μM dansylC_nSHs with varying concentration of IMP-1. It was found that with varying concentrations of the MBL, the fluorescence intensity of the probes also increased and the most blue-shifted spectra of the dansyl probes was seen in dansylC_4SHs indicating that this was the most efficient detector of IMP-1. It was also found by x-ray crystallography and electron density mapping that the main interaction of the dansylC_4SHs and the IMP-1 was between the naphthyl ring and a Trp64 residue while the thiol group was coordinated to two Zn^{II} molecules which caused a strong interaction between the two and ultimately inhibition of the IMP-1 was observed.[23]

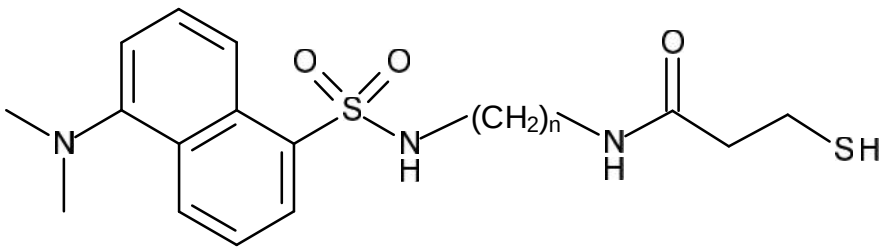

Figure 13. Dansyl probes with varying chain lengths, a dansyl fluorophore, and a thiol Zn^{II} ligand

Another example of fluorescent dansyl probes is seen in Hohsaka's work. It had been found that aromatic non-natural amino acids with vertically extended side groups are good substrates for protein systems. Hohsaka synthesized four different dansyl amino acids (Figure 14).[24]

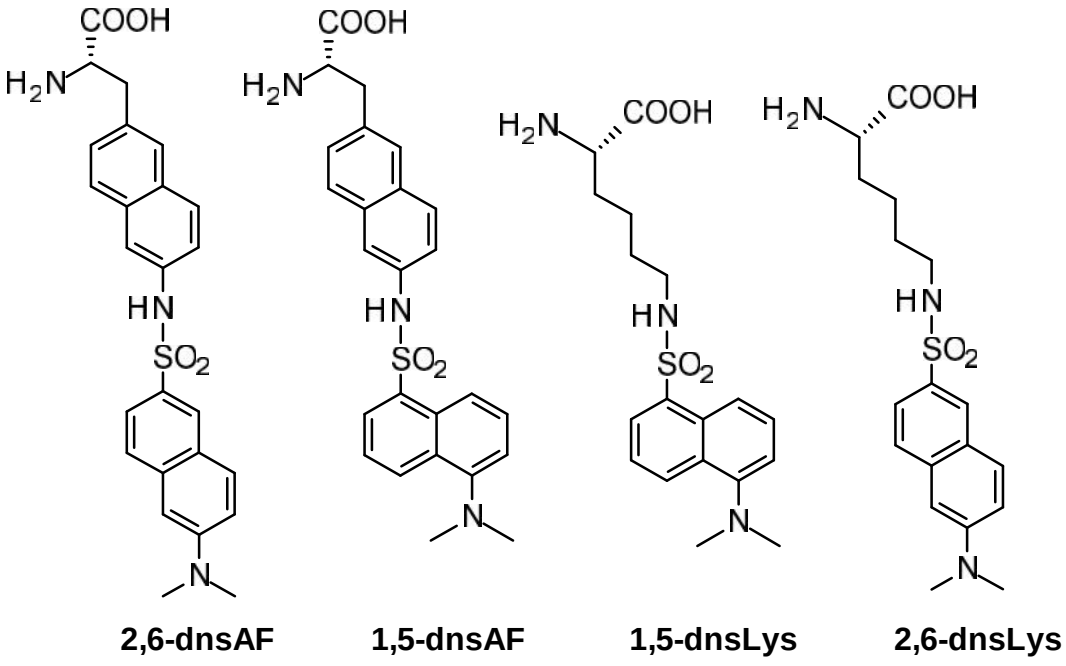

Figure 14. Dansylated amino acid derivatives

First the ability to incorporate these dansyl amino acids into proteins was tested using a streptavidin expression system. Western blotting of the *in vitro* translation of the

streptavidin molecule revealed that the dansyl amino acids were incorporated into the protein successfully with 2,6-danysl-aminophenylalanine (2,6-dnsAF) appearing to be the best substrate producing a higher yield of the streptavidin protein. The 2,6-dnsAF was then incorporated into seven different positions in the streptavidin protein (Figure 15). After observing the fluorescence spectra of the seven dansyl streptavidin mutants, a trend was observed in the varying value of λ_{max}. The blue-shifted fluorescence observed when the dansyl compounds were in the blue shaded positions in the protein (residues W75, W79, and L124) suggests that those positions were hydrophobic. This was also confirmed by the x-ray crystallographic structure. In the red shaded positions of the protein (residues E44, E51, and W120), a red-shifted fluorescence of the probes was observed suggesting that these dansyl amino acid derivatives were now in hydrophilic regions in the aqueous solvent. At the Y43 position a slightly more red-shifted fluorescence was observed than originally predicted but from Figure 15, B it is clear that there is a pocket within the protein structure that exposes this residue to a more hydrophilic environment. With the fluorescent data of these probes positively responding to their microenvironment, Hohsaka et al. showed how this was a useful technique for probing protein structures.[24]

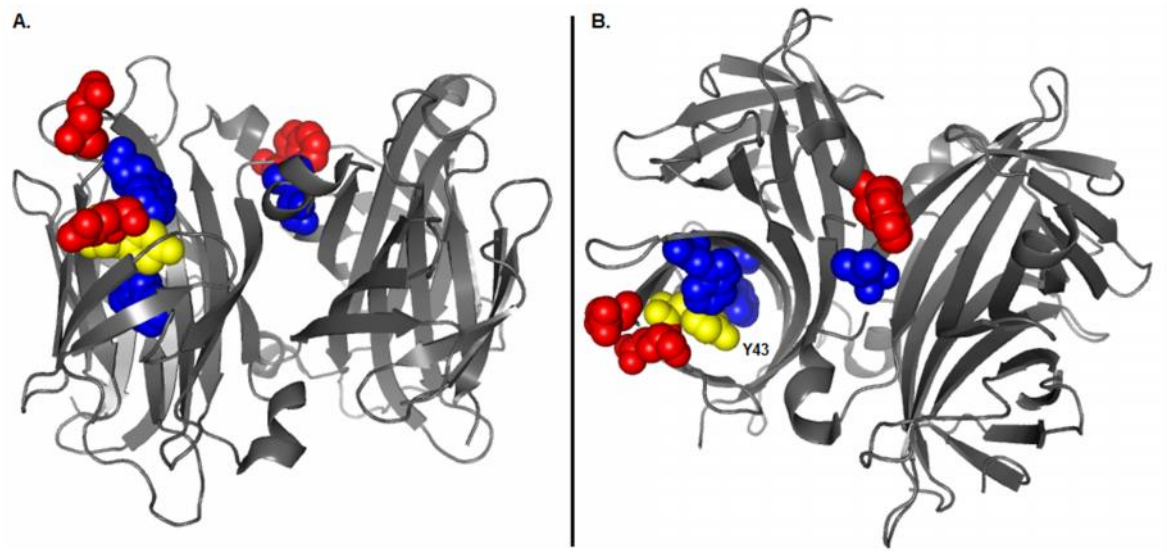

Figure 15. The 7 different positions of 2,6-dnsAF incorporated in the Streptavidin protein

Also using dansyl amino acid derivatives, Takeuchi and co-workers provided specific information on fluorescent enhancement in micelles. Using Dns-Phe (dansyl phenylalanine) it was found that the fluorescent intensity increased as a function of concentration of anionic surfactant used. The fluorescent enhancement was even greater in the presence of a cationic surfactant using Dns-Phe. Enhancement was also seen while using a surfactant with a longer chain length due to a more hydrophobic microenvironment inside of the micelle causing less fluorescence quenching by water.[25]

Similarly, O'Connor and co-workers has shown a 25-fold enhancement of fluorescence emission intensity of this dansyl compound upon the addition of either one equivalents of acid or 4 equivalents of Zn^{2+} ion (Figure 16).[21]

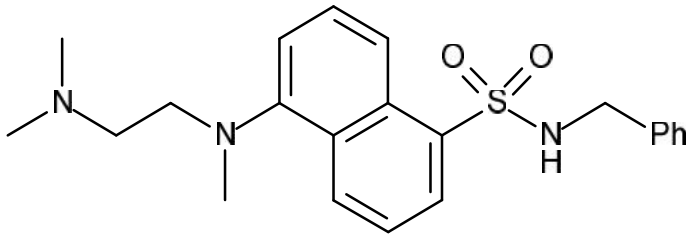

[a] λ_{ex} = 344 nm
[a] λ_{em} = 502 nm

Figure 16. Dansylated compound that exhibits fluorescence enhancement in the presence of 1.0 equivalence of acid or 4.0 equivalence of Zn^{2+}

Upon protonation or coordination of the basic aliphatic amine, a source of intramolecular quenching of the pendant amine is removed. PET analysis confirmed the regiochemical effect of this quenching and PET occurred readily with this dansylated fluorescent probe. Using this type of probe, the change in fluorescence intensity could be measured to monitor proton or ion flux in a solution or polymer.[21]

1.6 Fluorescent Probes Containing a Coumarin Component

Similar to dansyl chloride, other useful aromatic compounds used as fluorescent probes are coumarins which are known to be strongly fluorescent and easy to derivitize. Mizukami and co-workers used a 7-hydroxy coumarin based probe for the ratiometric fluorescence imaging of cells based on its ability to coordinate Zn^{2+}. A series of 5 coumarin-based probes were synthesized in the search for a ratiometric fluorescent probe using 7-hydroxycoumarin as the fluorophore and Dipicolylamine (DPA) as the metal ligand (Figure 17).[26]

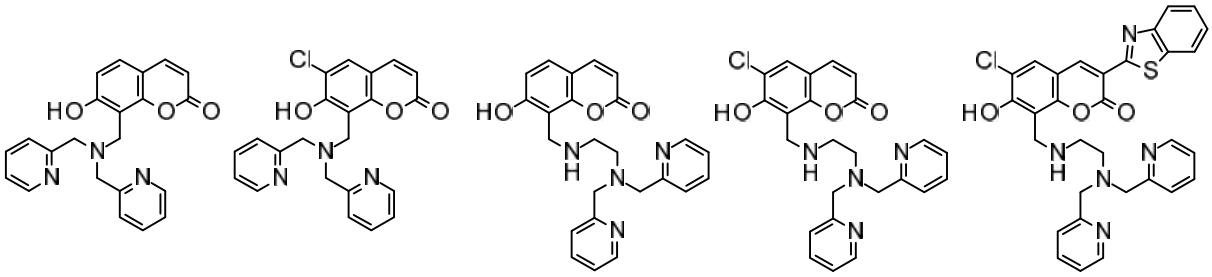

2 **3** **4** **5** **6**

Figure 17. Five coumarin based fluorescent probes for the ratiometric fluorescence imaging of Zn^{2+} coordinating cells

When the oxygen atom of these coumarin probes binds to Zn^{2+} the excitation spectra are expected to shift according to their electron-donating ability and whether or not the hydroxy group is protonated under the experimental conditions. If the phenol form is dominant, a red shift in the spectrum would be expected, whereas a blue shift would be expected if the phenolate form was dominant. With probe **2** it was apparent that the hydroxyl group was participating in the binding of Zn^{2+} as a shift toward longer wavelengths was observed in the excitation spectrum under the pH 7 buffered reaction conditions. The addition of the chlorine at the 6-position as seen in probe **3** produced a blue shift in the excitation spectrum indicating that the phenolate predominates. Probes **4** and **5** produced ratiometric points around 382 and 377 nm in the presence of Zn^{2+} but could only be excited by UV light which would damage living cells. Probe **6** was the first probe to produce blue-shifted excitation spectra with ratiometric excitation in the visible light region. This probe was then introduced to RAW264 cells and the ratiometric fluorescent signal was measured at F_{380}/F_{450} with the changing of intracellular Zn^{2+} concentration. As the Zn^{2+} concentration increased, the fluorescent ratio (F_{380}/F_{450}) increased as well. When TPEN was added to decrease the concentration of Zn^{2+} in the

cells, the fluorescent ratio value decreased back down to the original level. This was the first ratiometric probe for the Zn^{2+} detection in living cells excitable by visible light.[26]

Another use of coumarin-based fluorescent probes is seen by Du Ý et al. to detect hydrogen peroxide, a stable reactive oxygen species (ROS). Hydrogen peroxide is involved in cellular redox signaling in regulating many diseases and can cause oxidative damage to cells. A good coumarin-containing compound for ROS detection is umbelliferone. However, this probe has a short excitation wavelength that could result in photo-damage to cells. It was proposed by Wang and co-workers that 'click' modification of coumarin could be used as a way to easily manipulate coumarin's spectroscopic properties. In light of Wang's synthesis of a fluorescent product which was converted from a non-fluorescent parent compound via 'click' modification[27], Du Ý synthesized an analogous compound **7** (Figure 18).[28]

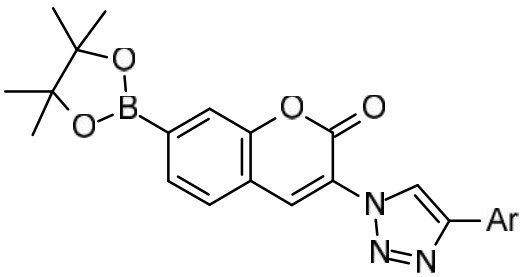

7

Figure 18. Synthesized coumarin containing compound **7** for detecting hydrogen peroxide

Compound **7** was then tested for its ability to detect hydrogen peroxide under near physiological conditions and upon addition of H_2O_2 the non-fluorescent parent compound **7** was converted to the fluorescent compound **8** which displayed a five-fold increase in fluorescence intensity (Figure 19). Fluorescent compound **8** was also found to have a

concentration-dependent response to the increase of hydrogen peroxide as well as greater affinity for hydrogen peroxide over several other ROS compounds.[28]

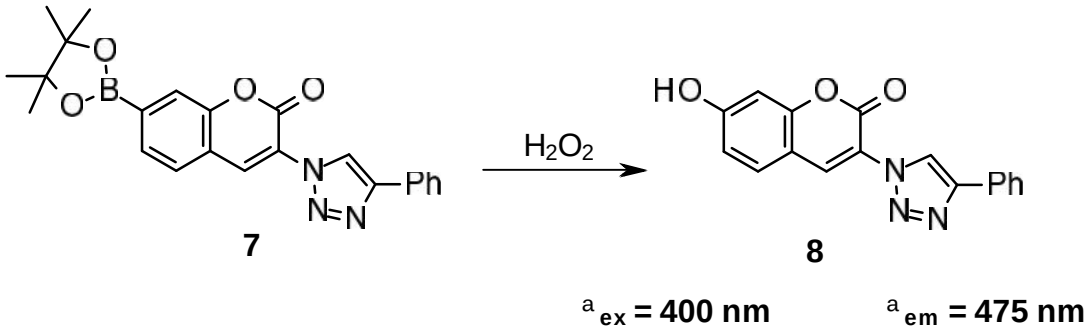

Figure 19. Reaction of a non-fluorescent compound **7** with H_2O_2 to produce fluorescent compound **8** which is H_2O_2 responsive

Similarly, Singh and co-workers used a coumarin-based probe to detect hydroxyl radicals in the vicinity of DNA molecules. Coumarin molecules were conjugated to polyamine compounds in order for coumarin to act as a hydroxyl radical indicator (Figure 20). The polyamine would act as a DNA-specific ligand which would closely tether the probes to the DNA backbone so that the hydroxyl radical could be quantified.[29]

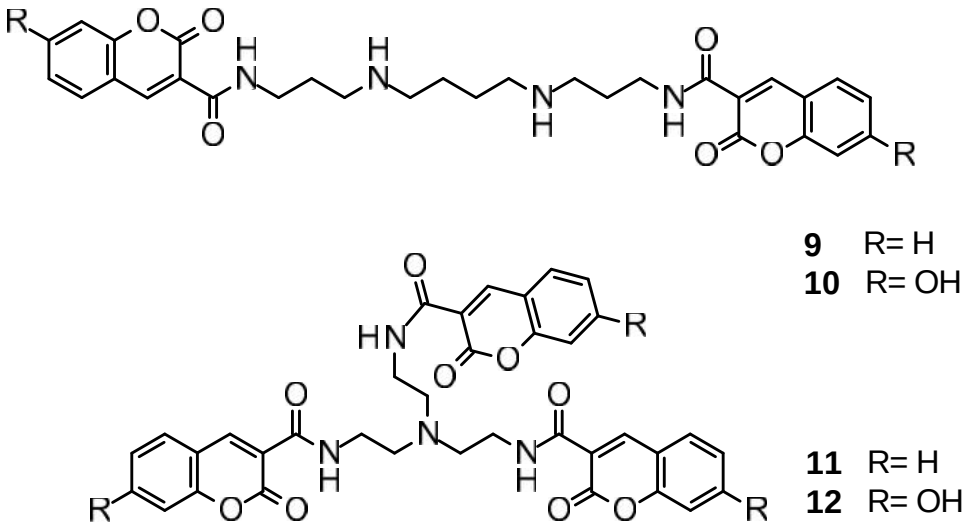

Figure 20. Coumarin/polyamine compounds for the detection of hydroxy radicals in close proximity to DNA molecules

Docking studies did reveal that these coumarin probes were involved in a ligand-DNA complex held together by H-bonding interactions. Compound **9** was found to bind to DNA and other negatively charged molecules, whereas coumarin carboxylic acids and other previous compounds of similar function could not, which shows the usefulness of this probe in efficiently detecting and quantifying hydroxyl radicals within a radius of 6 nm from the DNA which is the diffusion range of the radicals.[29]

1.7 Proposal of a Fluorometric Probe Containing Dansyl and Coumarin Components

Given dansyl and coumarin-derived compounds to make fluorescent probes for various biological and amphiphilic aggregate systems, Dr. Langner and co-workers at RIT proposed a difluorometric cross-membrane probe (**1**) containing both the dansyl and the coumarin components to study reverse micelles (Figure 21).

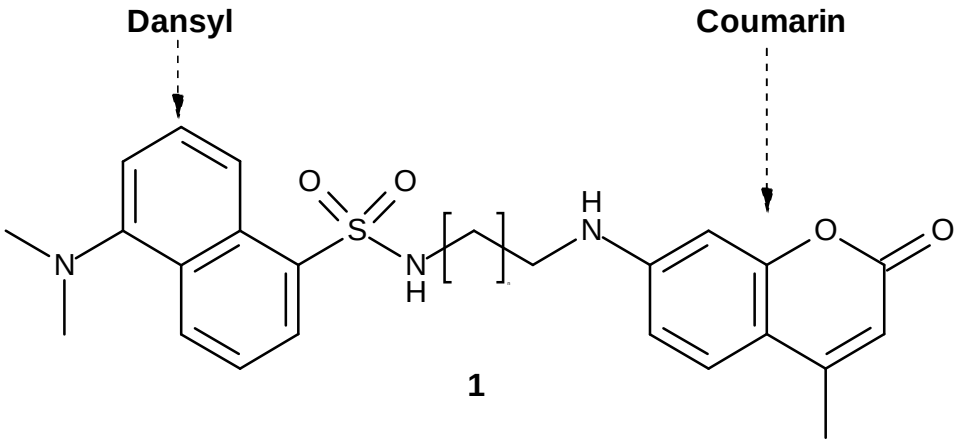

Figure 21. Dansyl and Coumarin containing probe proposed for the ratiometric fluorescence imaging of micelle/reverse micelle aggregates

A probe of this nature would have several attractive properties as a fluorometric probe for amphiphilic systems. This type of probe would be expected to produce ratiometric and solvatochromic results. The fluorescence could be measured of both the dansyl and the coumarin portions providing ratiometric fluorescence and a color change would be exhibited with a change in position of the absorption or emission bands of the dansyl portion with respect to changing solvent polarity. Using the coumarin portion as a control as its fluorescence would not be expected to change with solvent polarity, the solvatochromic fluorescence of the dansyl portion could provide valuable information about the changing environments around the probe as a reverse micelle is formed at the CMC. Both the dansyl and the coumarin portions are opposite compositions making the dansyl portion hydrophobic with a logP = 3.02 (based on dansyl chloride) and the coumarin portion hydrophilic with a logP = 1.25 (based on 7-amino 4-methylcoumarin). With varying carbon chain lengths between the two compounds in the same structure, Dr. Langer proposed that the coumarin portion of the molecule could be included in a reverse micelle's inner microenvironment, the carbon chain could transverse the reverse micelle

membrane, and the dansyl portion would be free floating in the outer organic bulk of the solution. Such a system could provide valuable information about the kinetics of formation when monitoring the fluorescence of both portions of the molecule during the formation of the reverse micelle. Dr. Langner hoped that this would help remove the limitations of a previously utilized single fluorophore-containing probe. Single fluorophore limitations included difficulty in pinpointing the location of the probe in the reverse micelle system, and determining the probe's interaction with the aqueous medium contained inside the reverse micelle. **Thus, the goal of this research project is to synthesize a difluorometric cross-membrane probe with both a dansyl and coumarin portion separated by varying carbon chain lengths in order to study reverse micelle systems.**

CHAPTER 2: PREVIOUS SYNTHETIC ROUTES

2.1 Ryan Walvoord's Previous Synthetic Work

There have been various synthetic attempts at obtaining the difluorometric probe **1** proposed by Dr. Langner. There are three different components of this probe (Figure 22) that allow for various ways to approach the synthesis. Originally in the first attempt at making a difluorometric probe for this project, 9-Aminoacridine was envisioned as the fluorophore for the hydrophilic portion of the molecule which has comparable fluorescent characteristics to coumarin. When the first student began work on this difluorometric probe synthesis in the Collison group, this was the intended target:

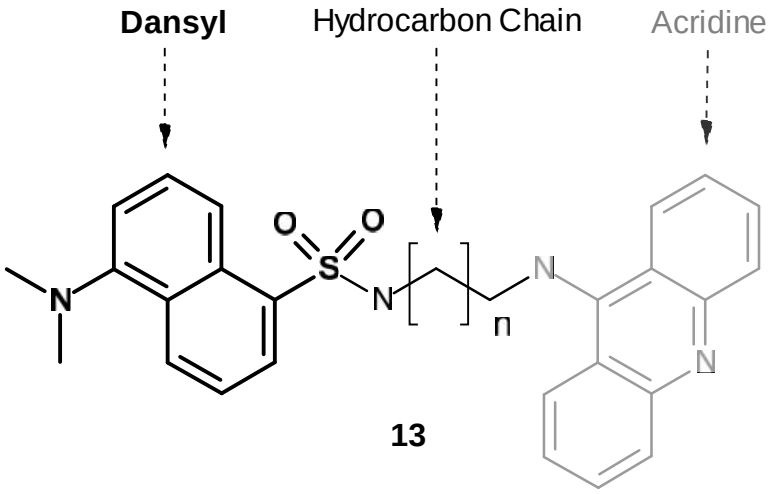

Figure 22. The three components of the first proposed difluorometric probe

Several strategies were investigated by previous undergraduate students in the Collison group to synthesize this novel probe. The first person to work on this synthesis was Ryan Walvoord (BS, 2006). Ryan focused on making the long hydrocarbon chain first. The design involved making a 7-carbon tether with two different functional groups on either end (Scheme 1). These functional groups would allow for controlled placement

of the two components in this difluorometric probe. The triflate could act as a good leaving group making one end of this molecule highly electrophilic whereas the alkyne on the other end could be treated with a base in order to make it very nucleophilic.

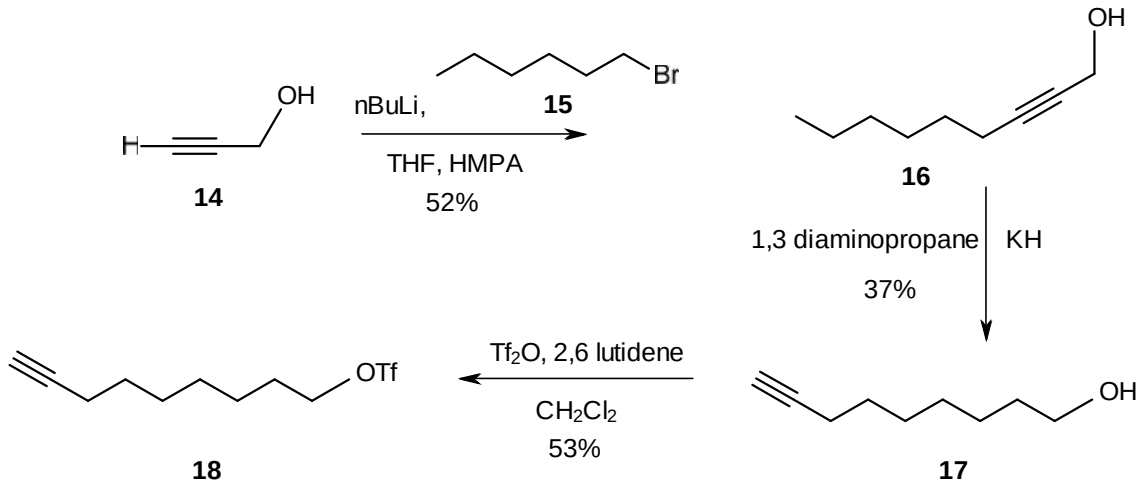

Scheme 1. Synthetic scheme to produce the functionalized hydrocarbon chain of the difluorometric probe

Starting with commercially available propargyl alcohol (**14)**, nBuLi was added to form the alkynate and then reacted with 1-bromohexane (**15**) to produce alcohol **16** (52% yield). Next the alkyne was treated with 1,3-diaminopropane and KH in order to walk the alkyne to the terminal end of the hydrocarbon chain giving alcohol **17** (37% yield). Scheme 2 shows how the amine acts as an alkyne transfer facilitator from one end of the hydrocarbon chain all the way to the terminal end of the carbon chain. Lastly, the alcohol was converted to an effective leaving group using TBDMSCl and giving triflate **18** (53% yield).

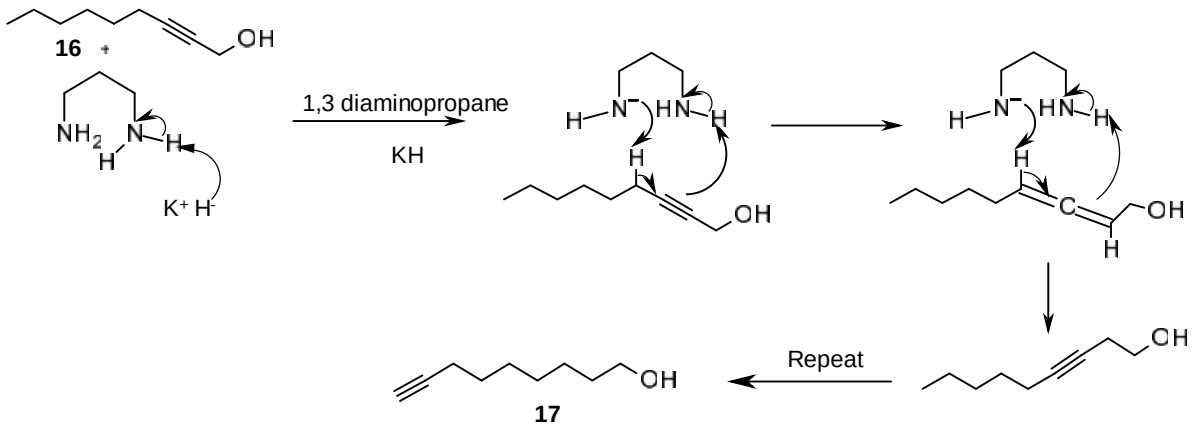

Scheme 2. Mechanism of traveling alkyne using 1,3-diaminopropane and KH

Ryan's synthetic strategy centered around the successful synthesis of the di-functional carbon tether. Strategy A first involves the coupling of 9-aminoacridine (**19**) to the triflate (**18)** end followed by dansyl incorporation at the alkyne. Strategy B is the reverse of strategy A and attempts to couple the dansyl moiety to the alkyne with a TBS protected alcohol (**27**) first followed by an S_N2 reaction with 9-aminoacridine (**19**). Strategy C eliminates the use of the long tether and the chemistry of coupling the 9-aminoacridine (**19**) to the mesylate of the dansyl component (**26**) is proposed (Scheme 3).

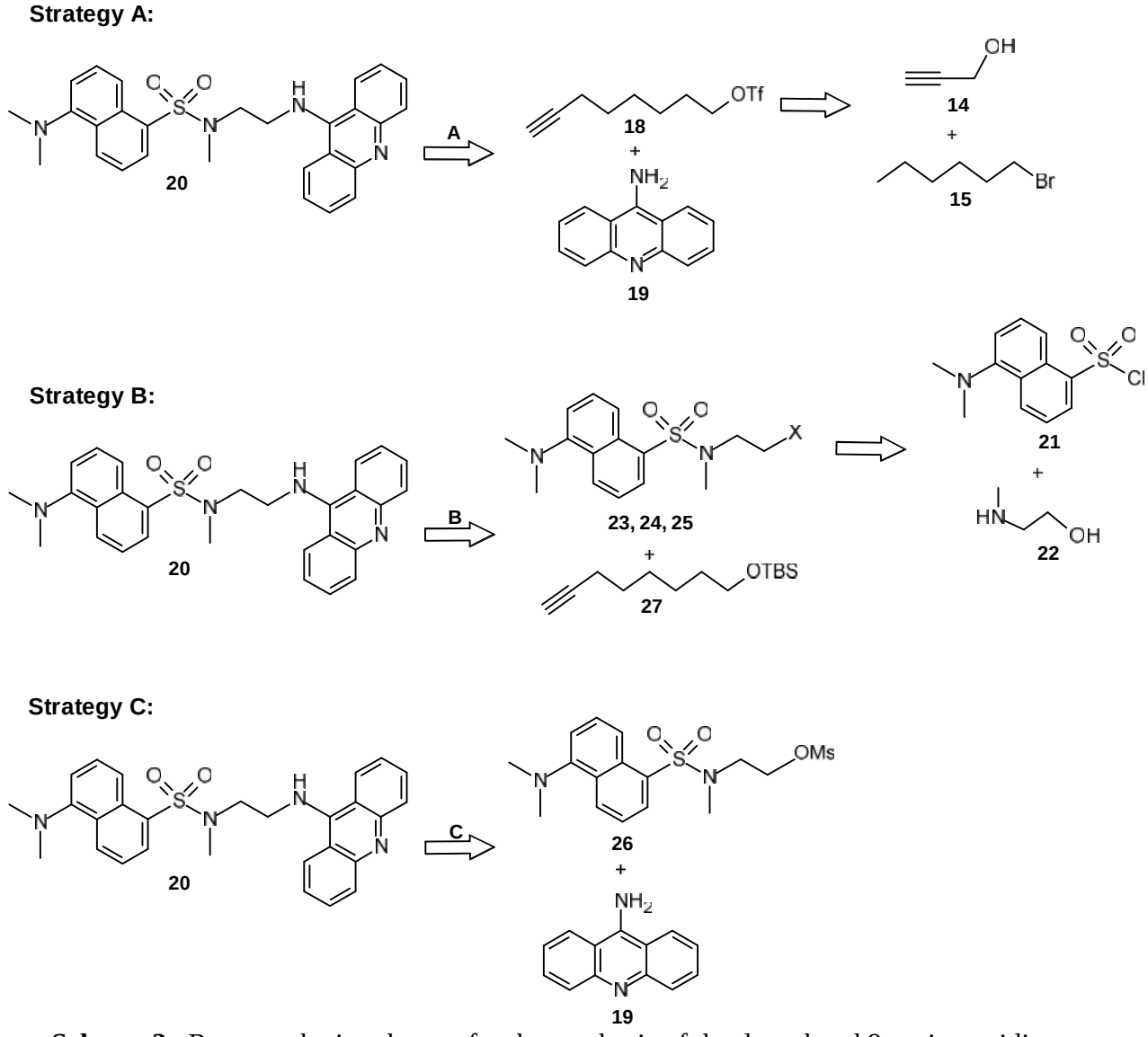

Scheme 3. Retrosynthetic schemes for the synthesis of the dansyl and 9-aminoacridine difluorometric probe

Unfortunately, no reaction took place between 9-aminoacridine and triflate **18** and the starting 9-aminoacridine (**21**) was recovered which prompted Ryan to attempt a different approach (Scheme 4). Synthetic pathways to create the dansyl component of the fluorometric probe with varying leaving groups to utilize in S_N2 reactions to combine the components of this fluorometric probe.

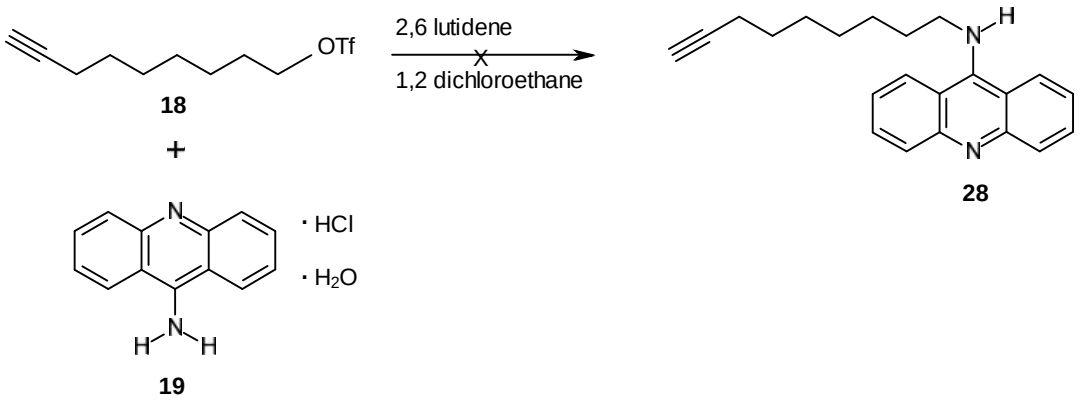

Scheme 4. First attempt to couple the hydrocarbon chain with 9-aminoacridine (**19**)

The next approach Ryan took was utilizing the alkyne end of the hydrocarbon chain in order to attach it to the dansyl component (Scheme 3, **B**). Dansyl chloride is commercially available and relatively inexpensive so a two-step synthesis was employed to create the sulfonamide directly attached to the dansyl component and then to convert the hydroxyl group into something more electrophilic (Scheme 5).

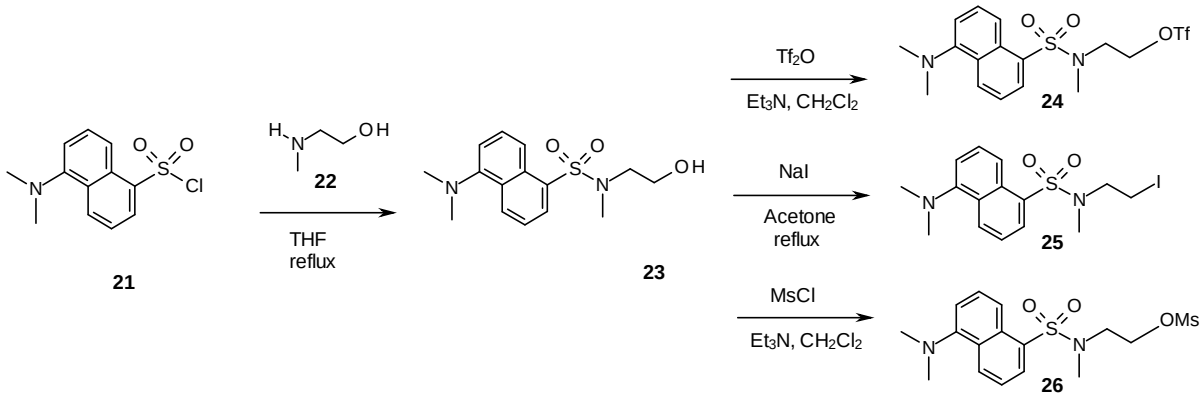

Scheme 5. Synthetic pathways to create the dansyl component of the fluorometric probe with varying leaving groups to utilize in S_N2 reactions

With compounds **24-26** in hand (40-50% yields), Ryan protected alcohol **17** as a silyl ether (**27**) and then deprotonated terminal alkyne **27** using nBuLi. This reactive alkynate intermediate was then treated with the electrophilic dansyl portion (**24**, **25**, or

26, Scheme 6). None of these reactions produced the dansylated compound and starting materials were recovered.

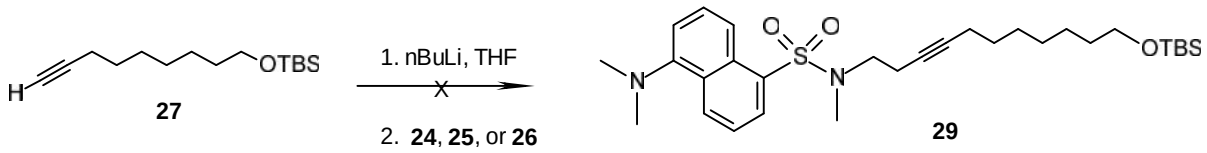

Scheme 6. S_N2 reaction of the hydrocarbon chain and the dansylated compounds functionalized with different leaving groups

Similarly, Ryan attempted to attach the 9-aminoacridine directly to the dansyl component (Scheme 3, **C**) by replacing the mesylate on compound **26** in an S_N2-type reaction (Scheme 7). This reaction was attempted in ethyl acetate with sodium bicarbonate as the base and in THF with potassium hydride as the base but in both cases the product was never detected and starting 9-aminoacridine (**19**) was recovered, most likely this was due to low nucleophilicity of the amine.

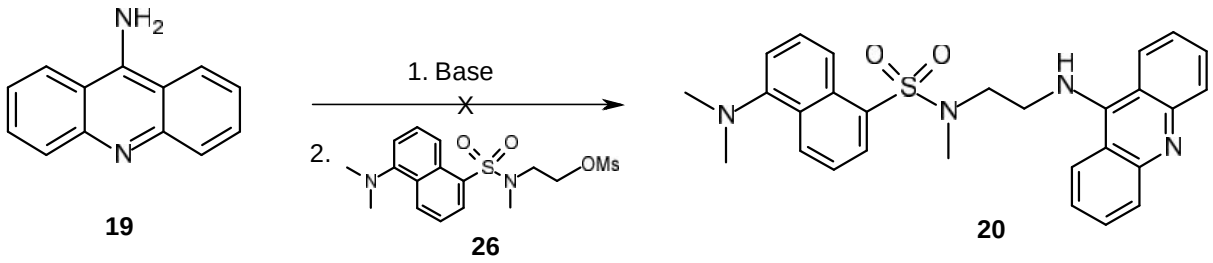

Scheme 7. S_N2 reaction between 9-aminoacridine (**19**) and the dansylated compound **26** to produce a difluorometric probe with a short hydrocarbon chain separating the fluorophores

After several attempts, a sweep of the literature indicated that 9-aminoacridine was not often utilized in S_N2 type reactions. 9-Aminoacridine was found to participate

more in nucleophilic aromatic substitutions and often times the reactivity of the carbon attached to the amino group is employed.[30,31] Another problem with using this molecule was the adverse health effects; 9-aminoacridine is highly toxic and not favorable to work with . This is when Dr. Langner's group proposed the switch from 9-aminoacridine to 7-amino 4-methylcoumarin; a compound far less toxic and much easier to handle. The literature revealed several hits on fluorometic probes containing this coumarin component.[28,29,32,33] Furthermore, the log P value of the 7-amino 4-methylcoumarin is lower than that of 9-aminoacridine which was also encouraging given the scope of this project and the goal of encapsulation inside of a reverse micelle.

2.2 Timothy Liwosz and Brett Granger's Previous Synthetic Work

With a new product in mind, several new synthetic routes were designed and investigated.

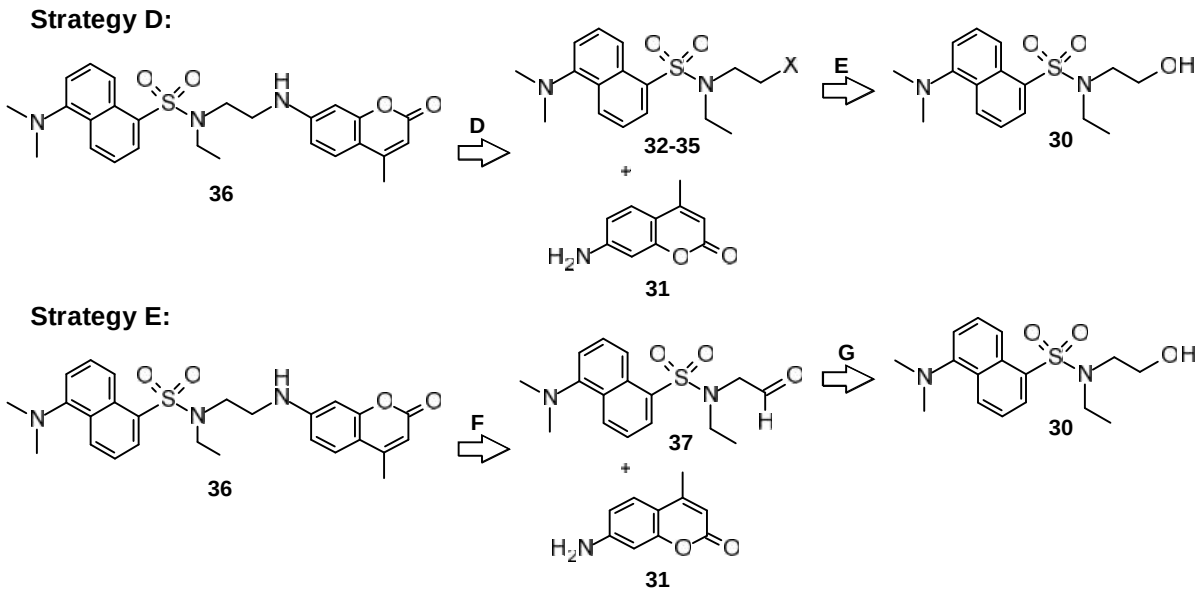

Scheme 8. Retrosynthetic schemes for the synthesis of the dansyl and coumarin difluorometric probe

Undergraduates Timothy Liwosz and Brett Granger (2007-2008) focused on synthetic steps **D** and **E** (Scheme 8, Strategy **D**). Both of these routes were similar to Ryan's attempts with 9-aminoacridine utilizing an S_N2 reaction of the amine of 7-amino 4-methylcoumarin to replace an electrophilic component on the dansyl component. The retrosynthetic plan in Tim and Brett's work eliminated the alkyne chemistry and focused on the previous success of forming a sulfonamide. This chemistry would be used as the primary way of connecting the tether to the dansyl moiety. Tether length and subsequent coumarin coupling would be the challenges to this new plan.

First 2-(ethylamino)ethanol was reacted with dansyl chloride (**21**) to produce sulfonamide **30** in a 60% pure yield. The switch to 2-(ethylamino)ethanol from the methylated derivative previously utilized by Ryan was for commercial availability reasons. Next, bromination of the hydroxyl group using CBr_4 and PPh_3 was achieved followed by the replacement of the bromine with iodine. Finally, coupling was attempted

between coumarin **31** and bromide **32** in an S_N2 reaction (Scheme 9). As in Ryan's work, the final product **36** was not detected and starting materials were recovered. Tim and Brett synthesized several other dansyl sulfonamides containing other leaving groups (Figure 23).

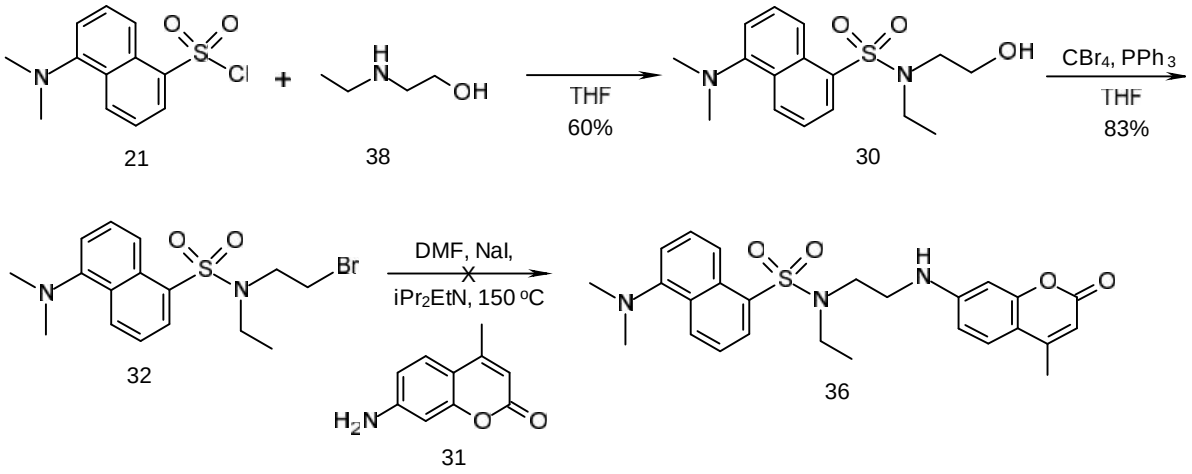

Scheme 9. Synthetic scheme to produce a difluorometric probe containing the dansyl and coumarin fluorophores

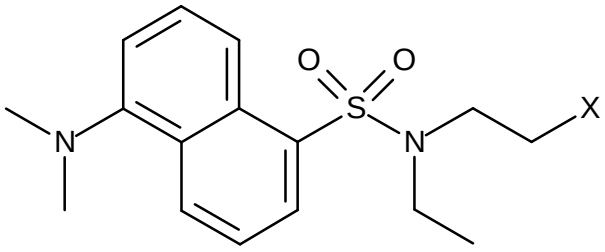

32: X=Br
33: X=Cl
34: X=I
35: X=OTf

Figure 23. Dansylated sulfonamides containing different leaving groups for the S_N2 reaction with 7-amino 4-methylcoumarin

With these new electrophilic dansyl compounds in hand, their reaction with 7-amino 4-methylcoumarin was investigated under several different reaction conditions (Table 1). Several different bases, solvents, and reaction conditions were utilized in order to couple these two components to give the final difluorometric probe, however, the desired product was never detected under any of these reaction conditions and in most cases the starting materials were recovered.

Table 1. Different reaction conditions using 7-amino 4-methylcoumarin as a nucleophile in an S_N2 reaction with different electrophilic dansyl components

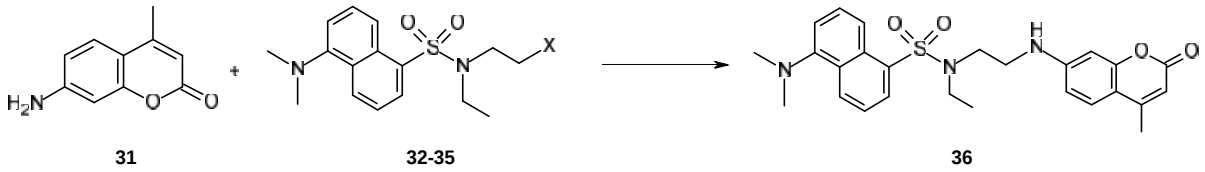

31 **32-35** **36**

Dansyl Component	Solvent	Temp.	Time	Base	Result
32	CH3CN	Reflux	24 hr	Hunig's Base	S.M. Recovered
32	DMF	150°C	48 hr	Hunig's Base	S.M. Recovered
32	CF3CH3OH	100°C	48 hr	No Base	S.M. Recovered
33	CH3CN	Reflux	24 hr	Hunig's Base	S.M. Recovered
34	CH3CN	Reflux	48 hr	Cs2CO3	S.M. Recovered
34	CH3CN	Reflux	48 hr	Et3N	S.M. Recovered
34	CF3CH3OH	Reflux	30 hr	No Base	S.M. Recovered
34	DMSO	120°C	2 hr	Cs2CO3	Decomposed S.M.
35	DMF	150°C	24 hr	Hunig's Base	S.M. Recovered

This prompted an analysis of a literature search in order to find a solution to this reactivity problem. 7-Amino 4-methyl coumarin was found to participate 25% of the time in S_N2 chemistry with a halogen and 75% of the time with an aldehyde or acid chloride. This led to an alternative synthetic approach to synthesizing the probe through

steps **F** and **G** (Scheme 8, Strategy **E)**. Oxidizing alcohol **30** to an aldehyde instead of conversion to a leaving group was thought to enhance the electrophilicity and thus increase the reactivity with the coumarin. If an aldehyde could be synthesized on the dansyl component, then a reductive amination could be used to attach the coumarin.

2.3 Josh Kolev's Previous Synthetic Work

Josh Kolev (2009) was the first person on this project to successfully synthesize a dansyl component containing an aldehyde functional group. He attempted several different oxidation conditions to oxidize the hydroxyl group to the carboxylic acid as well as directly to the aldehyde. An analogous system was found in a literature search which converts an alcohol in close proximity to a sulfonamide into a carboxylic acid so Josh attempted these and several other oxidation conditions (Table 2).[34]

Table 2. Oxidation conditions to convert the hydroxyl group on the dansyl component to a carbonyl functionality

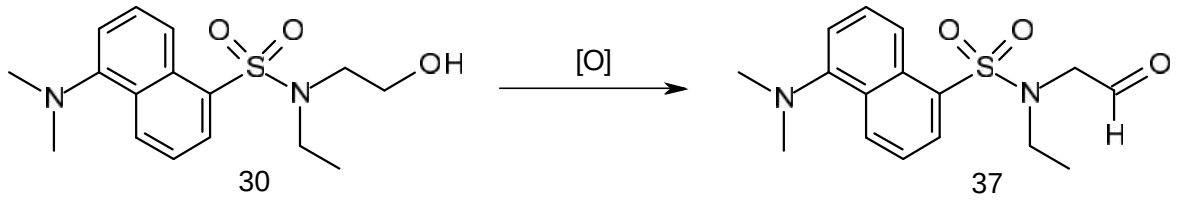

30 37

Dansyl Component	Oxidation Conditions	Product	Result
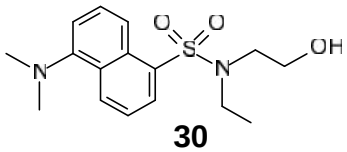 **30**	MnO_2 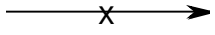 KOH	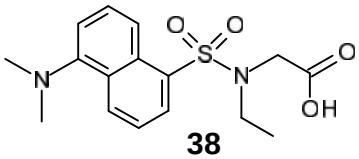 **38**	Starting Materials Recovered
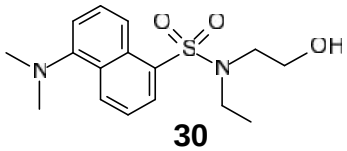 **30**	PCC 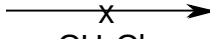 CH_2Cl_2 (37% Max)	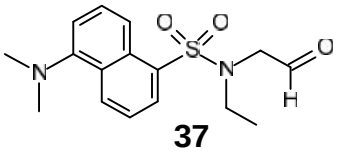 **37**	Product detected by NMR
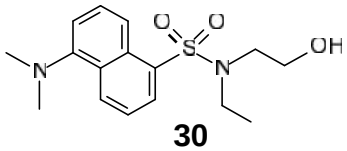 **30**	$(COCl)_2$ 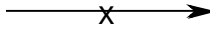 DMSO, CH_2Cl_2 (50%)	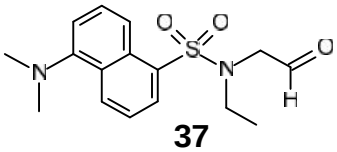 **37**	Product detected by NMR

Josh's attempts to oxidize the hydroxyl group to the carboxylic acid were not successful and his yield of aldehyde was not very high when oxidizing to the aldehyde using PCC. The first oxidation to work with decent yields employed the Swern oxidation using oxalyl chloride and DMSO as the catalyst.

The crude NMR of aldehyde **37** was fairly clean thus this approach seemed promising for the synthesis of this difluorometric probe. The next step would be the reductive amination between the 7-amino 4-methyl coumarin and compound **37**. Josh attempted this reductive amination however the amide was not detected by any NMR or

LC/MS data. Solubility issues seemed to arise as a solid formation was observed after the addition of the sodium triacetoxyborohydride; however, upon dissolving some of this solid in DCM, starting 7-amino-4-methyl coumarin was recovered.

Given the progress to this point, I began work on the synthesis of the coumarin-based probe on the heels of Josh Kolev's success with the Swern oxidation. The question at this point became whether or not it was possible to accomplish the reductive amination between the 7-amino 4-methylcoumarin and aldehyde **37**. I began by repeating the synthesis of alcohol **30** and aldehyde **37** to optimize yields and further investigate the reductive amination.

CHAPTER 3: CURRENT SYNTHETIC ROUTE

3.1 Retrosynthetic Pathways Explored

My work began with synthesizing compounds **30** and **37** in order to attempt the reductive amination. Below is an account of all of my synthetic attempts to make the difluorometric probe. A retrosynthetic account can be found below in Scheme 10 which shows all of my attempts to synthesize this compound which will be discussed in more detail in the following section.

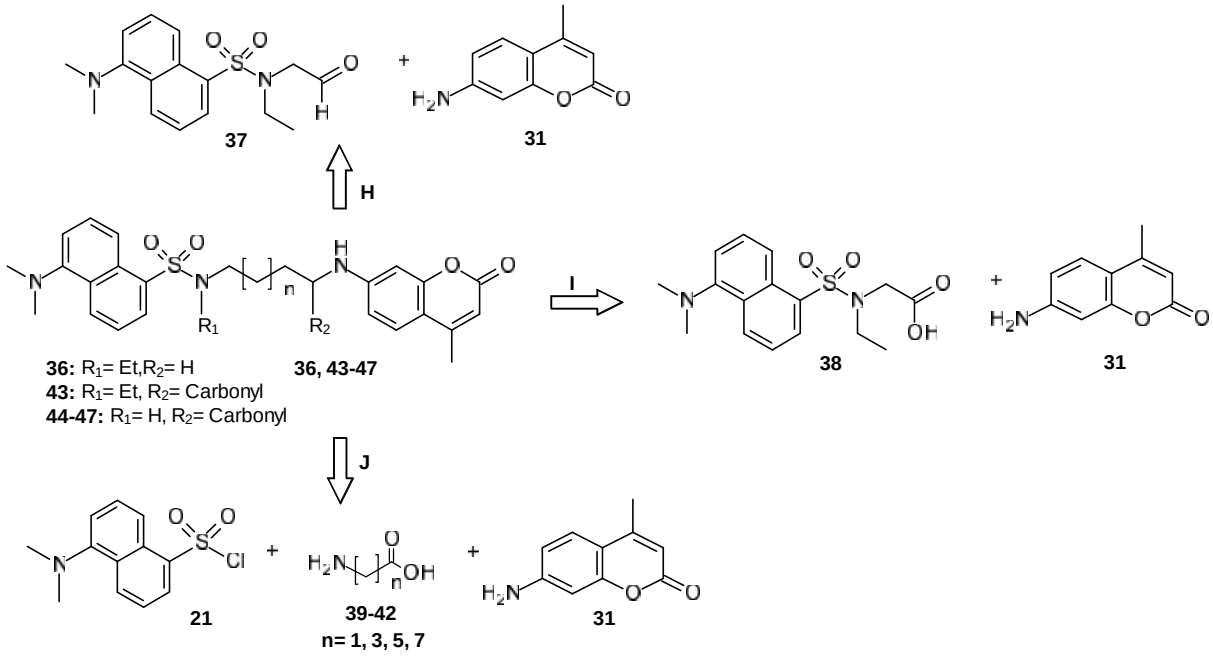

Scheme 10. My retrosynthetic attempts at synthesizing the dansyl/coumarin difluorometric compound

3.2 Results and Discussion

Following retrosynthetic pathway **H**, **I**, and **J** (Scheme 10) I focused first on reductive amination with the dansyl aldehyde (Scheme 10, **H**). First, commercially available dansyl chloride (**21**), was refluxed with amino alcohol **38** in THF to afford sulfonamide **30** in 98% crude yield (Scheme 11).

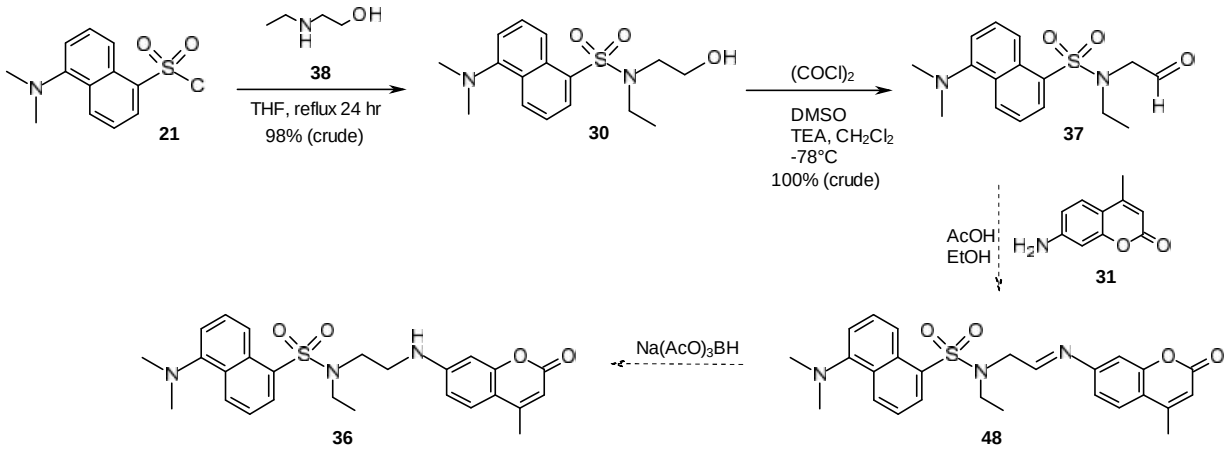

Scheme 11. Synthetic scheme to synthesize the dansyl/coumarin difluorometric probe including a Swern oxidation and a reductive amination

With an increased equivalency of amino alcohol **38** from 1.2 to 1.7, the derivatization reaction occurred more rapidly and, as a result, did not have to run overnight to give complete conversion to the product. A 98% yield of alcohol **30** was obtained as a fairly pure yellow oil and did not require further purification. The Swern oxidation was then performed on the primary alcohol **30**. In my hands, the yield for this step was improved dramatically. Josh's attempts afforded a 50% yield while my best efforts gave quantitative yields. This was accomplished by making sure that all solvents were freshly distilled before use and a fresh bottle of oxalyl chloride was employed. After use, all of the solvents and reagents were flushed with argon to keep them under an

inert atmosphere. Some solvents remained after the reaction often making the crude yield exceed 100%. However, the resulting aldehyde **37** was very pure and was used without purification.

Before attempting the reductive amination again with the 7-amino 4-methylcoumarin, a model reaction was completed first. A reductive amination was attempted between the aldehyde **37** and aniline (**49**) (Scheme 12). Aniline was chosen because it resembles the coumarin amine we wanted to use in the reaction and it is significantly less expensive than 7-amino 4-methylcoumarin. It was our hypothesis that the reductive amination we desired would not proceed if the model reaction with aniline didn't work. The amine in aniline is more electron-rich in comparison to the amine of 7-amino 4-methylcoumarin and thus more nucleophilic.

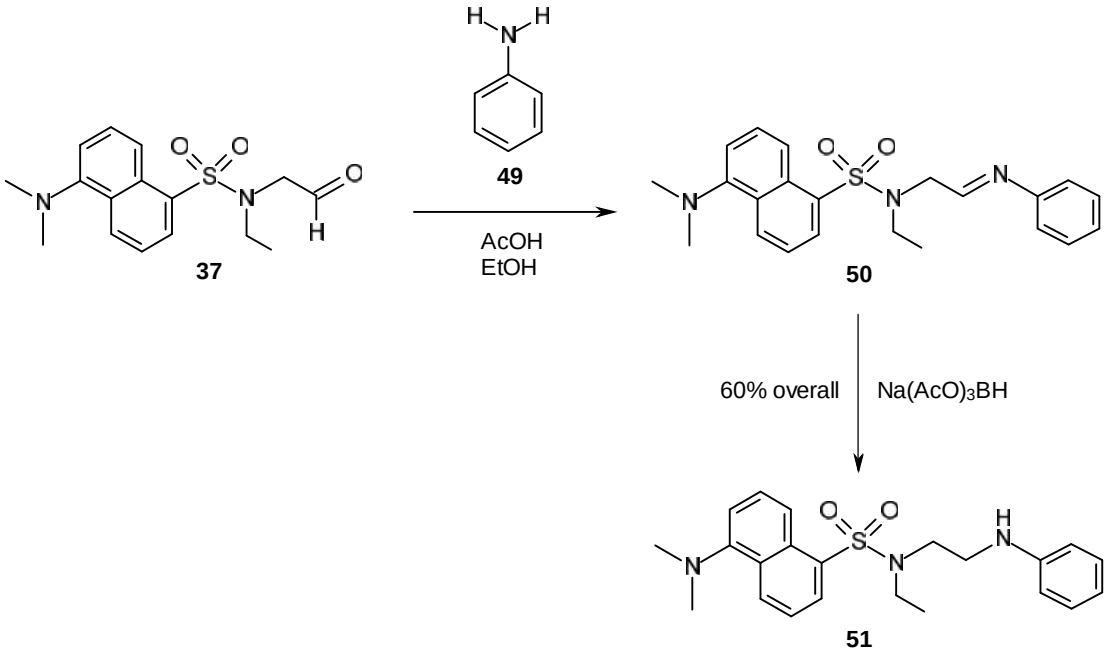

Scheme 12. Reductive amination with aniline (**49**) as the model reaction for 7-amino 4-methylcoumarin

Reductive amination with aniline using acid-catalyzed conditions to form imine **50** and subsequent reduction using sodium triacetoxyborohydride gave amine **51** in a 60% yield (over two steps) which was promising for the reaction between aldehyde **37** and 7-amino 4-methylcoumarin.

When reductive amination was attempted using 7-amino 4-methylcoumarin as the amine, no product was detected by NMR (Scheme 13). The number of equivalents of amine was adjusted (5 and 2.5 equivalents) and neither case afforded any desired product. In all cases run analogously to the aniline model study, only starting coumarin was recovered.

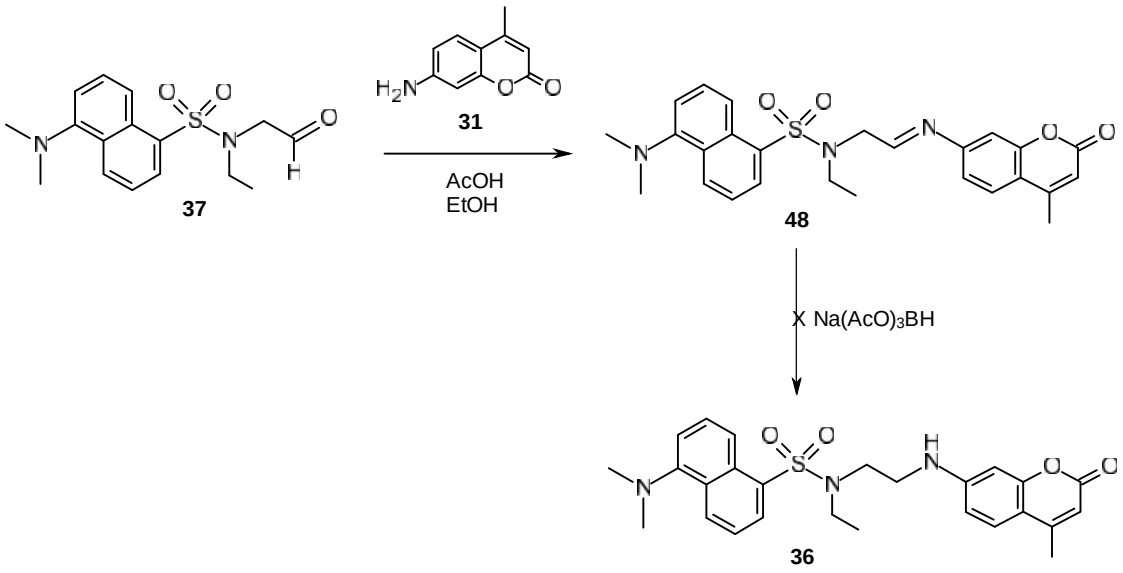

Scheme 13. Attempted reductive amination using 7-amino 4-methylcoumarin (**31**) as the amine

Since the reductive aminations attempted did not involve isolation of the imine intermediate prior to hydride introduction, it was difficult to know exactly what the issue with the reaction was. In order to identify the possible problems in the failed reductive amination, the reaction was stopped after the addition of acetic acid and 7-amino 4-

methylcoumarin in an effort to isolate the imine. An ^{1}H NMR revealed mostly 7-amino 4-methylcoumarin starting material which means the imine was not forming in the first step of this reaction preventing the reductive amination from occurring. As expected, it is believed that the nucleophilicity of the coumarin amine is lower and is sluggish in forming the imine with the dansyl aldehyde **37** even in the presence of heat. Since the coumarin portion must remain as part of the target, the strategy next became enhancing the elctrophilicity of the dansyl portion (Scheme 10, **I**).

A second look was taken at Josh's previous attempts at the oxidation of compound **30**. If the oxidation from the hydroxyl group to the carboxylic acid could be achieved then the carboxylic acid could be converted to highly electrophilic acid chloride which should be much more reactive towards the amine of 7-amino 4-methylcoumarin (Scheme 14).[35,36]

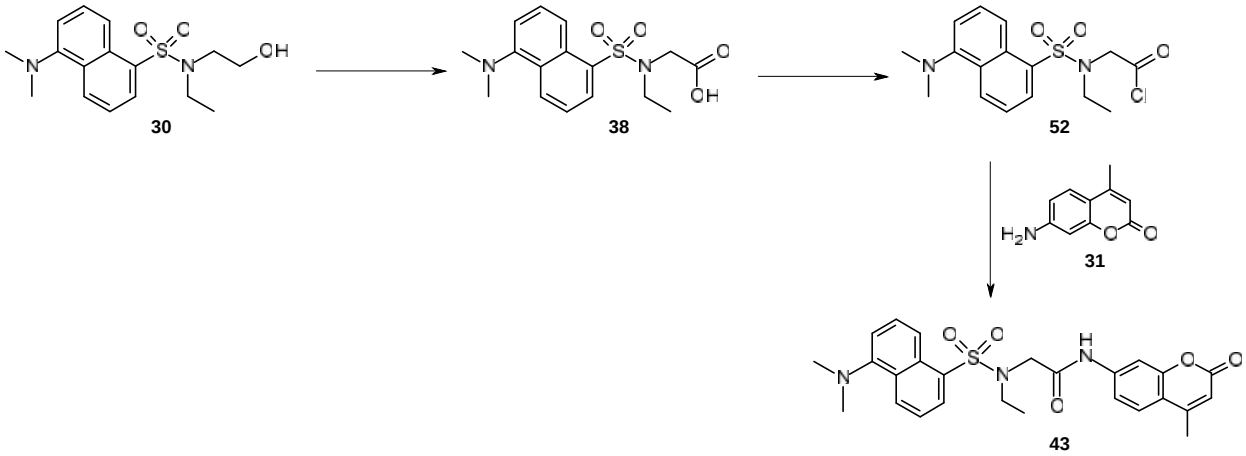

Scheme 14. New route envisioning the derivatization of the carboxylic acid **38** into acid chloride **52** which can participate in an S_N2 reaction with 7-amino 4-methylcoumarin (**31**) as the nucleophile

A literature search provided reactions of similar acid chloride systems containing a sulfonamide which were able to be oxidized to the carboxylic acid so these reaction conditions were attempted on our dansyl alcohol **30**.[37,38,39] The first oxidation used the Jones reagent. Several different procedures were followed and many changes to the reagents, reaction conditions, and work ups were made and can be found in Table 3.

Table 3. Different procedures used to attempt oxidation of compound **30** to carboxylic acid **38**

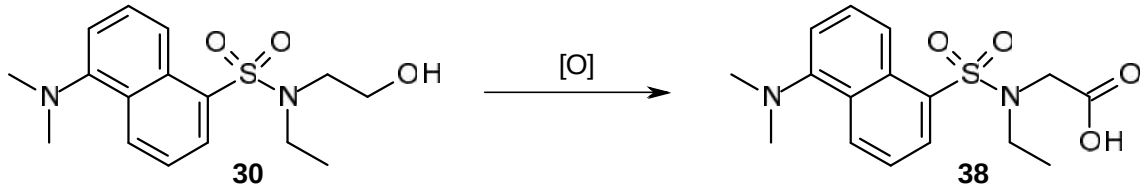

30 **38**

Entry	Oxidative Conditions	Reaction Conditions	Time	Results
1	8N Jones Reagent/Acetone	Stirred at RT	1 hr	Products Unrecoverable*
2	8N Jones Reagent/Acetone	Stirred at RT	7 hr	Products Unrecoverable*
3	8N Jones Reagent/Acetone	JR added drop wise, stirred at RT	10 hr	Products Unrecoverable*
4	8N Jones Reagent/Acetone	JR added over 30 min, stirred at RT	24 hr	Products Unrecoverable*
5	8N Jones Reagent/Acetone	JR added over 30 min, stirred at RT	36 hr	Products Unrecoverable*
6	3M Jones Reagent/Acetone	JR added over 30 min, stirred at RT	6 hr	Products Unrecoverable*
7	2.65 M Jones Reagent/Acetone	JR prepared in situ at 0°C, stirred at RT	6 hr	Products Unrecoverable*
8	CrO_3/H_5IO_6/MeCN	Reagents added at 0°C, stirred at RT	5 hr	Starting Materials Recovered
9	$KMnO_4$/Acetone/H_2SO_4	$KMnO_4$ added at 0°C, stirred at RT	2 hr	No Product Detected
10	$KMnO_4$/TBAB/AcOH/DCM	Reflux	6 hr	Starting Materials Recovered
11	$KMnO_4$/Acetone/H_2O	Reflux	6 hr	Starting Materials Recovered
12	PCC/HCl/DCM	Stirred at RT	24 hr	Aldehyde Detected by NMR
13	PCC/H_2SO_4/DCM	Stirred at RT	24 hr	Aldehyde Detected by NMR

*Upon acidification of the basic aqueous layer and extraction with various organic solvents, aromatic peaks were not observed in the organic extractions by ^{1}H NMR. Any product formed was unrecovered from the aqueous layer.

In each effort to oxidize the alcohol **30** using Jones reagent, the product was not detected using ^{1}H NMR. In fact, several NMR's did not show any signs of aromatic peaks at all in the crude mixture (Table 3, entries **1-7**). In these cases it was believed that if the product was forming, it was trapped in the aqueous layer seeing as it would be a highly polar compound containing both a sulfonamide and a carboxylic acid in close proximity. LC/MS of the water layer neither provided a mass that identified the carboxylic acid nor the starting alcohol. However, a zoomed in NMR of the aqueous layer did show that there were possibly some peaks in the aromatic region. This led to a different problem; if the product was in the aqueous layer it was not easily extractable using standard acidification and extraction techniques which means that this would not be an ideal way to obtain acid **38**.

The next attempt to achieve the oxidation was using $KMnO_4$. Again several different procedures were followed based on a literature search of similar compounds.[40,41,42,43] Oxidations using $KMnO_4$ did not afford the carboxylic acid product. Generally, $KMnO_4$ oxidations gave recovery of the starting alcohol **30** in high yields (60-80%) indicating that no reaction was taking place (Table 3, entries **9-11**).

Another oxidation attempt employed chromium trioxide and periodic acid as per a paper by Hanessian and co-workers (Table 3, entry **8**).[44] The result of this oxidation attempt was similar to our reactions using Jones reagent where there were no aromatic peaks found in the proton NMR of the organic layer. The last entries **12** and **13**

describes our last attempt to oxidize to the carboxylic acid based on Snaith and co-workers analogous oxidation where they used HCl or H_2SO_4 with PCC in the presence of a primary alcohol resulting in the over-oxidation to the carboxylic acid.[45] When the same reaction conditions were applied to our alcohol **30**, carboxylic acid **28** was again not detected by NMR. A mixture of starting alcohol **30** and the aldehyde **37** was found in both cases.

At this point, we knew that the amine was not highly nucleophilic and as such a highly electrophilic system needed to be employed. Further, oxidations to form the carboxylic acid proved impractical. Thus, a third route was devised incorporating the idea of increasing the electrophilicity of the dansyl portion while circumventing challenging oxidations (Scheme 10, **J**). This route envisioned a new linker for the hydrocarbon tether between the two molecules. Commercially available amino acids were hypothesized to both add to the dansyl chloride moiety via the amine as well as convert to the acid chloride via the carboxylic acid (Scheme 15).

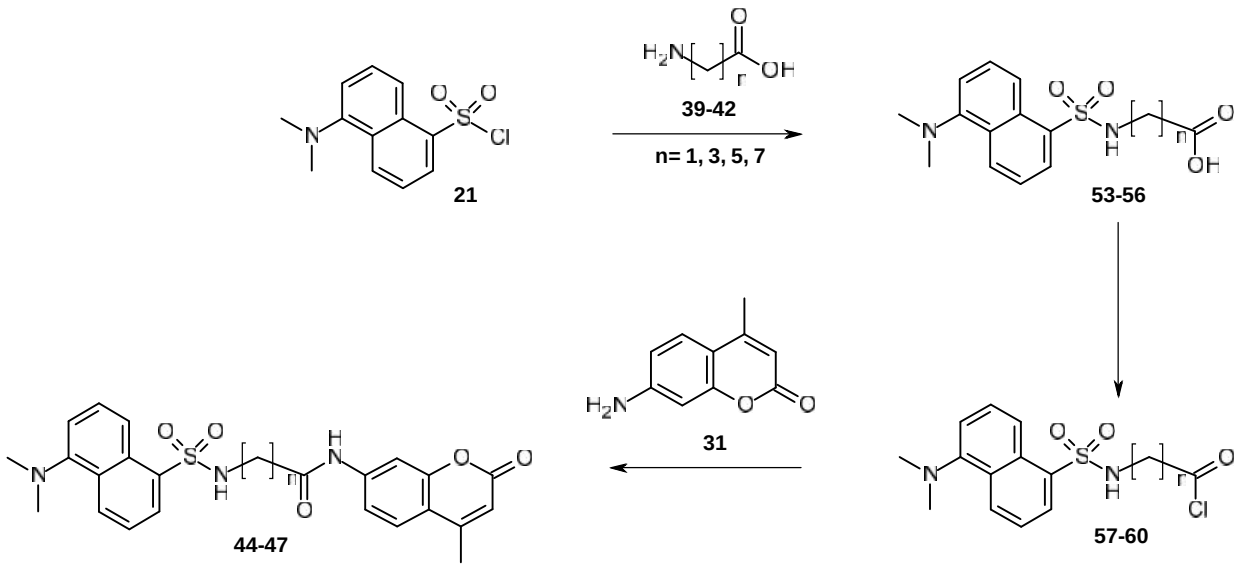

Scheme 15. New route to utilize derivatization chemistry to create a highly electrophilic dansyl component to react in an S_N2 reaction with the 7-amio 4-methylcoumarin (**31**)

A solubility test on glycine which would be used to form the shortest tether between components found that only water afforded its solubility out of several different solvents including MeOH, EtOH, EtOAc, $CHCl_3$, CH_2Cl_2, MeCN, and DMSO. Since the acid chloride would be highly water sensitive, a literature search was done to find a procedure to forgo this. Work by Levine and co-workers show glycine converting to glycyl chloride hydrochloride using PCl_5 in CCl_4 (Scheme 16).[46]

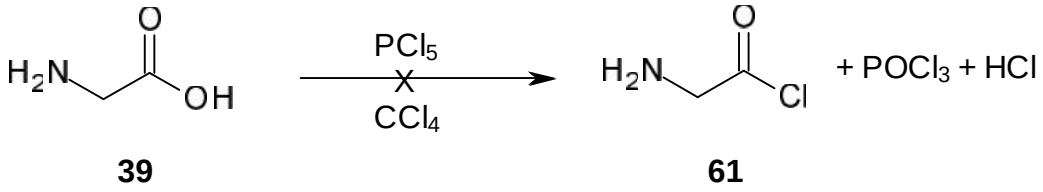

Scheme 16. Synthesis of glycyl chloride (**61**) using PCl_5

Our attempt at repeating this procedure gave a solid product that by IR was not the starting material. However, according to Levine and co-workers, the glycyl chloride product could be recrystallized from acetyl chloride. Our isolated solid was not soluble in

acetyl chloride indicating that it may not have been the acid chloride product **61**. Upon attempting to use solid in a derivatization reaction with the 7-amino 4-methylcoumarin, the coumarin was recovered from the reaction.

Since working with the glycine to produce the glycyl chloride was difficult since glycine is not soluble in many solvents other than water, it was thought that solubility issues could be addressed by first coupling glycine (**39**) to the dansyl moiety (Scheme 17).

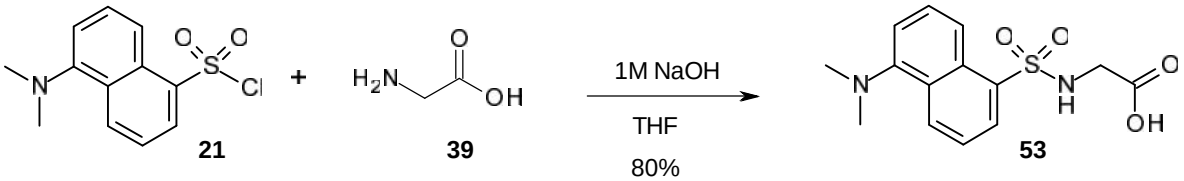

21 **39** **53**

Scheme 17. S_N2 reaction between glycine (**39**) and dansyl chloride (**21**) under basic conditions

Initial attempts began with commercially available dansyl chloride (**21**) and glycine (**39**) in a 1M solution of NaOH and THF, to give acid **53** as a yellow solid (57% yield). After tweaking the procedure to include concentrating the aqueous layer after all of the starting dansyl chloride had been converted to product as shown by TLC, and adding freshly-made cold 5M HCl to the aqueous layer to precipitate the product as a yellow solid, the yields improved up to 80%, and the product became easier to collect.

With acid **53** in hand, the synthesis of the acid chloride was then attempted. The first reaction aimed at producing the acid chloride involved refluxing the starting carboxylic acid with thionyl chloride in a solution of DCM for three hours (Table 4, entry **1**). This

reaction was difficult to monitor via TLC due to large streaks from the reaction mixture. After concentrating the solution, the crude product was used directly in the next step without further purification. Assuming that the acid chloride had formed a small amount was added to a solution of 7-amino 4-methylcoumarin pre-mixed with Et_3N and the reaction was refluxed for 2 hours followed by stirring overnight at room temperature. After 12 h, TLC revealed the presence of starting material with little evidence of any new product formation. Upon full work up, an ^1H NMR proved that there was indeed predominantly 7-amino 4-methylcoumarin remaining. This led us to believe that the acid chloride was not in fact produced from the thionyl chloride reaction.

Table 4. Reaction conditions to synthesize the dansyl sulfonamide acid chloride **57** to participate in an S_N2 reaction with 7-amino 4-methylcoumarin (**31**) as the nucleophile

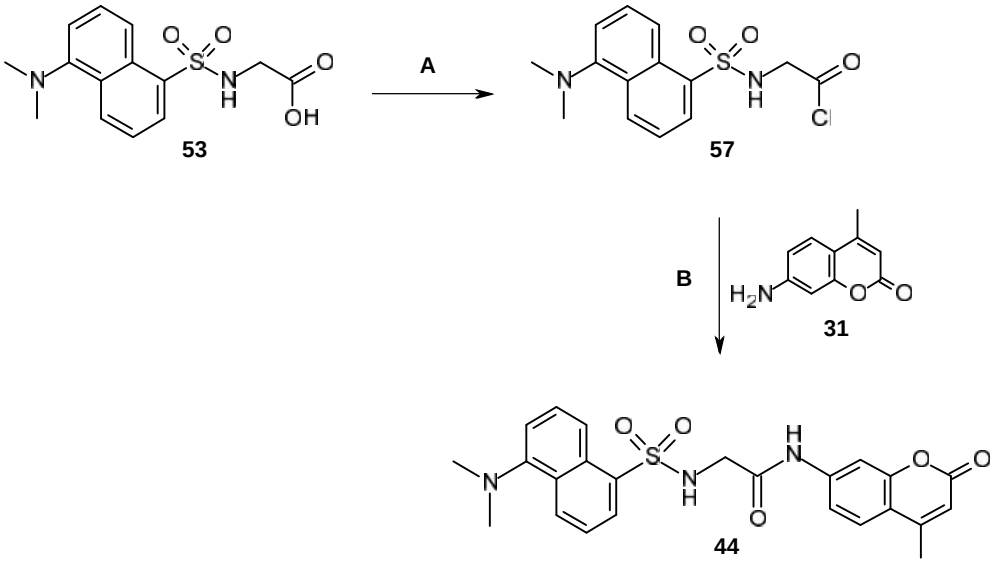

Entry	Reaction Conditions (A)	Result After B
1	$SOCl_2$/DCM	S.M. Recovered
2	$(COCl)_2$/Cat. DMF/THF	Product Detected

Next a Vilsmeier reaction with oxalyl chloride and DMF was employed to convert the starting carboxylic acid (**53)** to the acid chloride (**57**) (Table 4, entry **2**). Following the Vilsmeier reaction, all of the solvent was removed *in vacuo* to afford a dark yellow solid which was used immediately in the next reaction with 7-amino 4-methylcoumarin without further purification so as to keep as little moisture as possible from getting into the compound and to reduce any decomposition (Scheme 18).

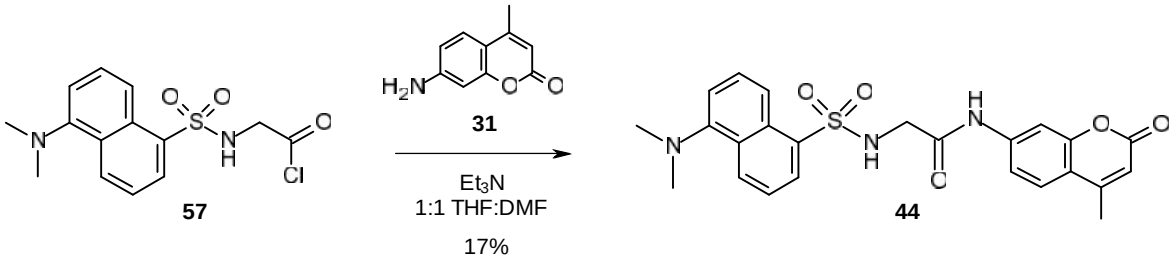

Scheme 18. Derivatization of acid chloride **57** to amide **44** using 7-amino 4-methylcoumarin

The TLC after 12 h still showed coumarin **31** present but it also showed the addition of a new spot below that of coumarin. Thus, upon working up the reaction and taking an ^{1}H NMR of the solid product in DMSO it was found that there was a significant increase in the number of aromatic peaks compared with the NMR of dansyl acid **57** and 7-amino 4-methyl coumarin. This was promising for the formation of amide **44**. The new spot was isolated by column chromatography and characterized. Upon taking an LC/MS, ^{1}H NMR, ^{13}C NMR, IR, and high resolution MS, the product was confirmed to be amide product **44** ($C_{24}H_{23}O_5N_3S$) with a molecular weight of 465.14 g/mol containing a dansyl and a coumarin component with one CH_2 separating the two components in a 17% yield.

With the ability to synthesize this difluorometric compound successfully, the same procedure was envisioned using a different commercially available starting material but with a longer carbon chain in between the amine and acid functional groups. Sigma Aldrich commercially supplies γ-aminobutyric acid (**40**) , 6-aminocaproic acid (**41**) , and 8-aminooctanoic acid (**42**) as relatively inexpensive starting reagents. The first step of this synthesis was then applied to each of these compounds (Scheme 19).

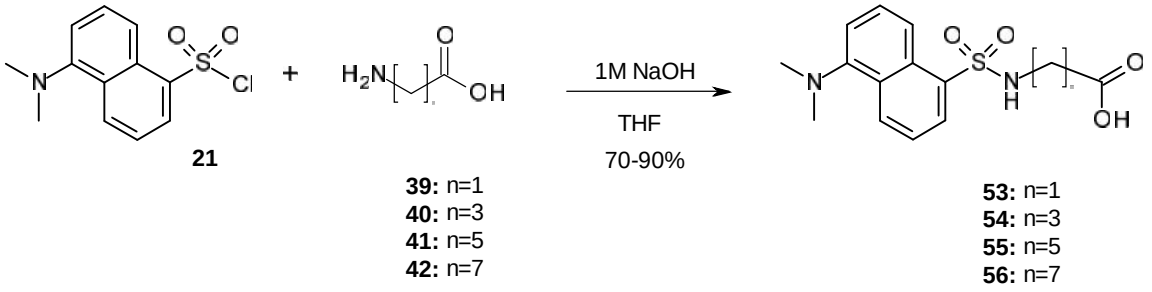

Scheme 19. Reaction of 1-, 3-, 5-, and 7-carbon chain length amino acids with dansyl chloride (**21**)

Each of these compounds was identified using ^{1}H NMR and produced between 70-90% yields. High vacuum was sometimes required to remove all of the aqueous solvent from the compounds before using any of them in the next step. The 5-carbon dansylated carboxylic acid **55** was chosen as the next compound to advance through the synthesis so there would be one short and one long carbon chain difluorometric compound to compare once fluorescent characterization began. Next the carboxylic acid **55** was converted to the acid chloride using the Vilsmeier method to produce acid chloride **59** in a 92% yield (Scheme 20).

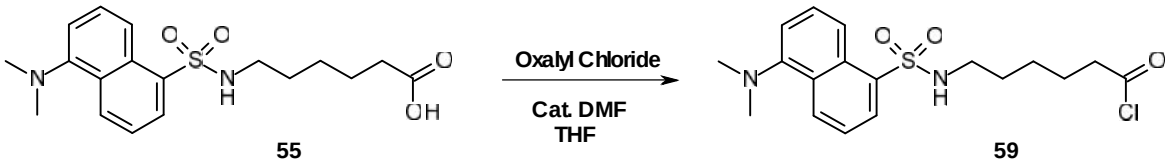

55 59

Scheme 20. Vilsmeier reaction of carboxylic acid **55** with oxalyl chloride and DMF to produce acid chloride **59**

Before attempting to couple compound **59** with 7-amino 4-methylcoumarin, a small amount of the dark yellow solid product was removed and reacted with Et_2NH in a solution of dry DCM. After removing all of the solvent *in vacuo*, the solid product was tested by ^1H NMR. The presence of the acid chloride **59** was supported by the detection of compound **62** (Figure 24) indicating the reaction between the Et_2NH and the acid chloride had taken place. With this supporting evidence of acid chloride **59** it was quickly used in the next synthetic step. Acid chloride **59** was charged with 7-amino 4-methylcoumarin (**31**) in a 1:1 solution of THF and DMF in Et_3N to afford amide **46** (Scheme 21).

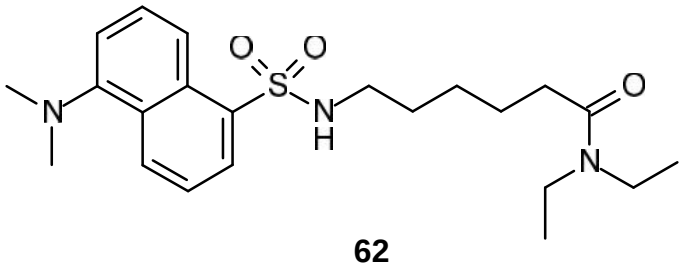

62

Figure 24. Compound **62** detected after the reaction of acid chloride **59** with diethylamine

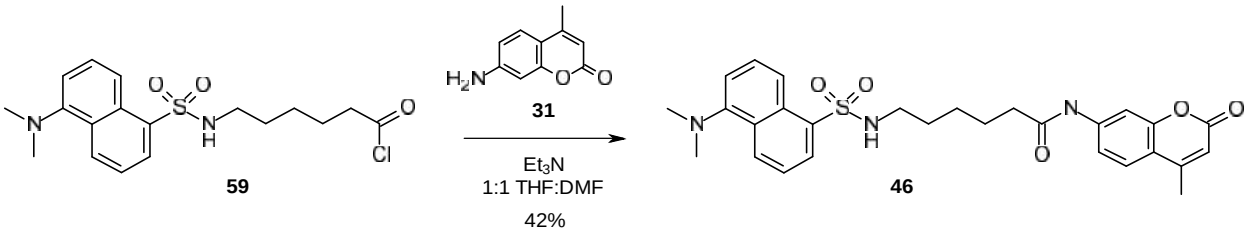

Scheme 21. S_N2 reaction between acid chloride **59** and 7-amino 4-methylcoumarin (**31**)

Again the TLC showed some starting coumarin after stirring overnight but a new product spot was found as well. After column chromatography purification, amide **46** was isolated in a 42% yield and identified ($C_{28}H_{31}O_5N_3S$) with a molecular weight of 521.21 g/mol characterized by LC/MS, ^{1}H NMR, ^{13}C NMR, IR, and high resolution MS. The higher yield can be attributed to its slightly higher solubility in THF than the one-carbon tethered amide **44.**

Given our success, it was now our focus to repeat these experiments so as to produce more materials for fluorometric characterization. Upon doing so, problems were detected in the first synthetic step. Instead of producing the yellow solid carboxylic acid **53** after acidifying the aqueous layer, a yellow oily product crashed out of the solution but could not be collected by vacuum filtration. All of the aqueous solution had to be removed by placing it on the high vacuum for several days upon which a yellow solid resulted matching the NMR of the previously made acid **53.** However, this acid product was far less pure than the first attempt. Using this resulting acid **53** to convert to the acid chloride **57** did not yield the same solubility trend in THF as previously observed. Upon testing the starting dansyl chloride (**21**) by ^{1}H NMR it was found that it had slightly begun to degrade but it still only produced one spot on a TLC plate so column chromatography purification is not going to be practical for removing any degraded

products. Thus it is noted that care must be taken with the handling and storage of dansyl chloride.

3.3 Future Work

A significant future step will be the synthesis of the remaining 3- and 7-carbon chain difluorometric compounds. In particular, the 7-carbon tether appears to be long enough to cross most decane/water/AOT/butyl alcohol reverse micelles.

Another future endeavor will be the completion of the fluorescent characterization of the 1- and 5-carbon chain probes that have been synthesized in this work. General fluorescent data needs to be obtained for both the fluorophores individually as well as for the 1- and 5-carbon chain difluorometric probes. Similar to a paper in 1993 by Hawker et al., we would like to obtain fluorescent data for the molecular probes in a variety of solutions ranging from non-polar solvents to highly polar solvents. In Hawker's research the widely studied solvatochromic probe 4-(N,N-dimethylamino)-1-nitrobenzene was attached to the core of 6 generations of [G-X]-N(Me)-Ph-NO_2 dendritic molecules in order to establish the nature of the probe in the microenvironment around the dendritic macromolecules (Figure 25).[47]

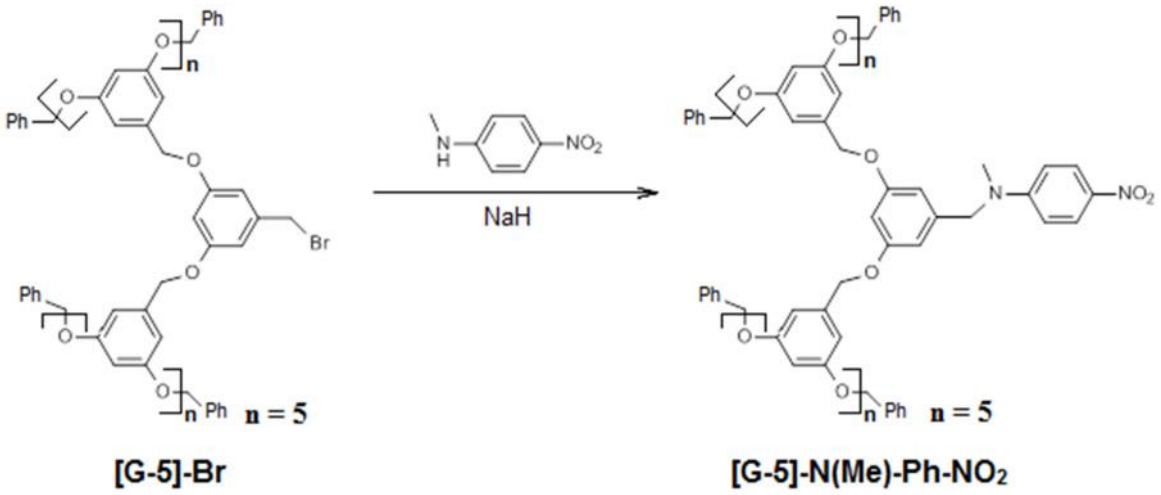

Figure 25. Synthesis of the 5th generation [G-X]-N(Me)-Ph-NO_2 dendritic molecule

UV-vis analysis of the 6 generations of dendrites containing the probe was performed in a variety of solvents from CCl_4 to DMSO. It was found that upon increasing the molecular weight and size of the dendrimers, the absorbance maximum experienced a bathochromic shift. A plot of the λ_{max} vs. the generation number experiences a large discontinuity between the third and fourth generation in the non-polar solvents which is characteristic of the transition from the extended form of the dendrimers to the globular structure.[47]

Similarly to Hawker's research, Mishra et al. conducted a similar experiment using a dansyl group attached to the focal point of novel glycerol-based polyether dendrimers.[48] In order to determine the solvent effect on the emission maximum of the dansylated dendrimers, the fluorescence was measured in a variety of solvents with different polarites. Through this research it was evident that there was in fact a solvatochromic shift in the emission maximum for all three generations of the dansylated polyether dendrimers tested. Similarly to Hawker's work, there was not as large of a bathochromic shift seen in the fluorescence emission from the second to third generation

of the dendrimers which meant there was a structural change going on in the dendrimers which was shielding the dansyl portion from the bulk of the polar solvent.[48]

This provided an interesting basis for fluorescent characterization of our difluorometric probes. Dr. Tan's research group has begun collecting data on both the dansyl and the coumarin components individually in a series of solvents ranging from low to high polarity. The next step will be to subject our 1- and 5-carbon chain fluorometric probes to the same conditions and measure the λ_{max} of each component in the molecule to note any changes from the pure components. The dansyl component is expected to show a solvatochromic shift in fluorescence emission with changing polarities whereas the coumarin portion should have a constant fluorescence emission maximum. The final step would be to mix these probes with a micelle/reverse micelle system and re-measure the λ_{max} to see if any changes can be measured and whether or not any inferences can be made about the microenvironment around the aggregate. The advantages/disadvantages of having a 1- vs. a 5-carbon chain separating the dansyl and coumarin components of the probe can also be discovered with this system as the ideal chain length which will allow for the ratiometric fluorescent imaging of these systems is still unknown. This could have positive implications in the field of ratiometric fluorescent probes used to study amphipathic systems.

3.4 Conclusion

Two potential difluorometric molecules have been synthesized and characterized. Each can be used as a probe for amphipathic aggregates such as micelles and reverse micelles. Dansyl- and coumarin-containing probes have been reported in literature but

this is the first time these two components have been reported in the same molecule for use as a fluorometric probe to study a reverse micelle system. With further characterization and experimentation it is hopeful that these molecules can be used to study micellular systems by encapsulating the hydrophilic coumarin component inside of the reverse micelle core while the hydrocarbon tether straddles the bilayer and the hydrophobic dansyl portion remains in the bulk organic solution. The ratiometric changes in fluorescence between the dansyl and coumarin can then be monitored to provide value information about these types of aggregates.

Circumventing previous synthetic downfalls including the difficult oxidation of the dansylated sulfonamide in order to couple it with the coumarin portion of the molecule, we have employed a 3 step synthesis of these difluorometric molecules beginning with two commercially available components. Before these molecules can be used to study amphipathic systems, basic fluorometric data must be collected for each compound. This data is being procured by Dr. Tan's research group at RIT and is in the preliminary stages. Once the fluorescence data is recorded for these compounds it is hopeful that the synthesis can be improved and the 3- and 7-carbon chain probes can be fully synthesized and characterized.

EXPERIMENTALS

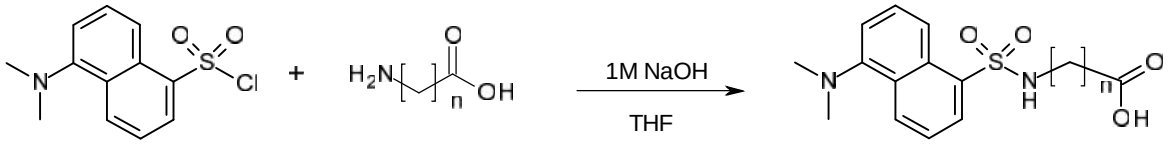

General Procedure: To an oven dried round bottom flask a stir bar and 1.15 equivalence of the solid amino acid was added. To this flask 1.35 equivalence of 1M NaOH was added and the solution stirred until all of the amino acid dissolved. Next, 1.0 equivalence of dansyl chloride dissolved in 110 equivalence of dry THF (Some remained in suspension) was added dropwise to the NaOH solution. The pH of the solution was monitored and minimal amounts of NaOH were added to keep the pH at 9.0. When TLC (2:1 ethyl acetate: hexanes) showed no dansyl chloride starting material in solution the flask was removed from stirring and the THF layer was concentrated in vacuo. The remaining yellow NaOH solution was cooled in an ice bath and small amounts of freshly made 5M HCl were added dropwise until a yellow solid crashed out of solution. This solid product was collected via vacuum filtration and dried for 30 minutes under high vacuum to remove any aqueous solution.

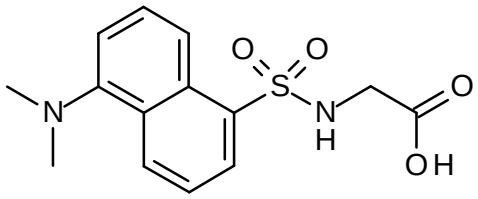

2-(5-(dimethylamino)naphthalene-1-sulfonamido)acetic acid (**53**) (1.008g, 57% yield)

^{1}H NMR: (300 MHz, DMSO-d_6) δ 8.37 (d, *J* = 8.3, 1H), 8.31 (t, *J* = 5.8, 1H), 8.2 (d, *J* = 8.7, 1H), 8.0 (dd, *J* =7.3, 1.1, 1H), 7.5 (mp, 2H), 7.18 (d, *J* = 7.5), 3.5 (d, *J* = 6.1, 1H), 2.75 (s, 6H)

IR: 3510 (w, br), 1332 (m), 1201 (s), 1176 (w), 1157 (w), 1143 (s), 1074 (m), 1024 (m), 786 (s), 626 (m), 574 (m)

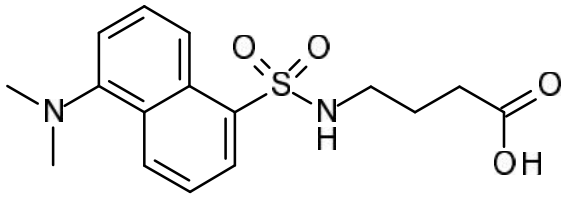

4-(5-(dimethylamino)naphthalene-1-sulfonamido)butanoic acid (**54**) (0.49 g, 98% yield)

^{1}H NMR: (300 MHz, DMSO-d_6) δ 8.3 (d, *J* = 8.3, 1H), 8.2 (d, *J* = 8.7, 1H), 7.9 (d, *J* = 7.5, 1H), 7.8 (mp, 1H), 7.5 (q, *J* = 15.7, 7.8, 2H), 7.2 (d, *J* = 7.2, 1H), 2.75 (s, 6H), 2.69 (mp, 2H), 2.0 (t, *J*= 7.5, 2H), 1.43 (mp, 2H)

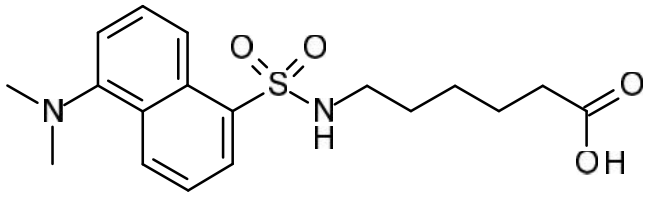

6-(5-(dimethylamino)naphthalene-1-sulfonamido)hexanoic acid (**55**) (0.261g, 97% yield)

^{1}H NMR: (300 MHz, DMSO-d_6) δ 8.36 (d, *J* = 8.7, 1H), 8.2 (d, *J* = 8.7, 1H), 7.9 (d, *J* = 7.4, 1H), 7.79 (t, *J* = 5.1, 1H), 7.5 (q, *J* = 16.4, 8.2, 2H), 7.16 (d, *J* = 7.6, 1H), 2.7 (s, 6H), 2.66 (mp, 2H), 1.89 (t, *J* = 7.1, 2H), 1.16 (mp, 4H), 0.99 (mp 2H)

IR: 3070 (m, br), 2939 (m), 2870 (m), 2337 (w), 2237 (w), 2160 (w), 1712 (s), 1465 (m), 1396 (m), 1319 (s), 1141 (s), 1080 (m), 786 (s), 586 (s)

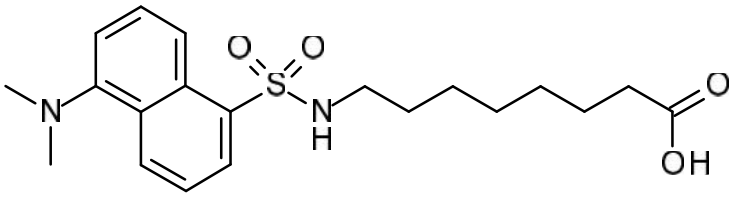

8-(5-(dimethylamino)naphthalene-1-sulfonamido)octanoic acid (**56**) (0.542g, 93% yield)

^{1}H NMR: (300 MHz, DMSO-d_6) δ 8.39 (d, *J* = 8.8, 1H), 8.2 (d, *J* = 8.3, 1H), 8.0 (d, *J* = 7.0, 1H), 7.8 (t, *J* = 5.2, 1H), 7.5 (q, *J* = 16.1, 8.0, 2H), 7.2 (d, *J* = 7.5, 1H), 2.7 (s, 6H), 2.6 (q, *J* = 12.4, 6.4, 2H), 2.0 (t, *J* = 7.3, 2H) 1.18 (mp, 4H), 0.90 (mp, 6H)

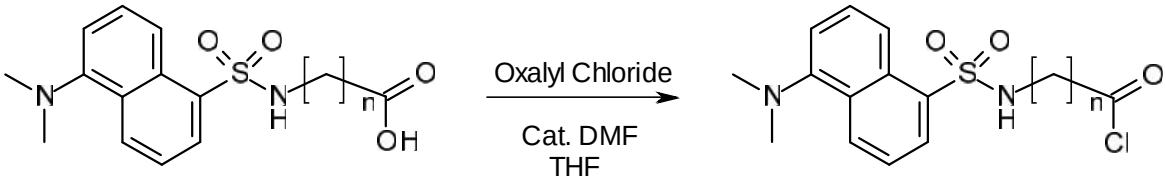

General Procedure: To an oven dried round bottom flask with a stir bar and 1.0 equivalence of the carboxylic acid under argon, 200 equivalence of dry THF was added and stirred for 10 minutes. This solution was cooled to -78°C using a dry ice/acetone bath and 3.7 equivalence of oxalyl chloride was added dropwise to the flask followed by 1-2 drops of DMF. The solution stirred at -78°C for 10-15 minutes then allowed to warm to room temperature. The reaction was monitored by TLC (2:0.5 ethyl acetate: hexanes) and when all of the starting carboxylic acid had disappeared and a new, different color fluorescent spot showed up the reaction was removed and all of the solution was removed in vacuo. The yellow solid was used in the next step without further purification.

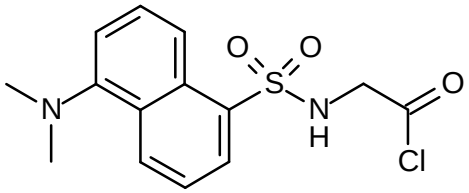

2-(5-(dimethylamino)naphthalene-1-sulfonamido)acetyl chloride (**57**)

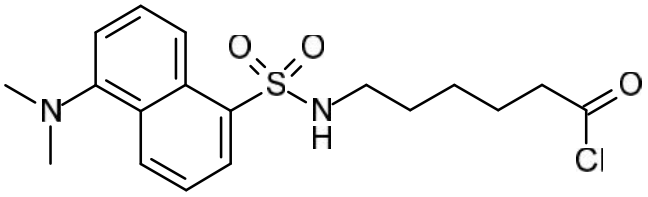

6-(5-(dimethylamino)naphthalene-1-sulfonamido)hexanoyl chloride (**59**)

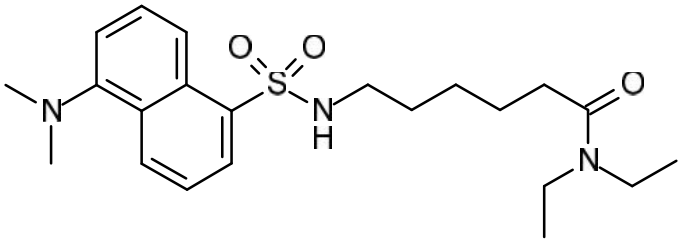

6-(5-(dimethylamino)naphthalene-1-sulfonamido)-N,N-diethylhexanamide (**62**)

Procedure: A small amount of compound **59** (~1mg) was dissolved in dry DCM (1 mL) in a 1 mL round bottom flask and Et_2NH was added dropwise to the solution until the yellow color disappeared and no more exothermic reaction was observed. The solution was then evaporated in vacuo and the resulting solid was dissolved in 1mL of DMSO for ^1H NMR characterization.

^{1}H NMR: (300 MHz, DMSO-d_6) δ 8.35 (d, *J* = 8.6, 1H), 8.2 (d, *J* = 8.6, 1H), 7.9 (d, *J* = 7.4, 1H), 7.5 (q, *J* = 16.4, 8.5, 2H), 7.15 (d, *J* = 7.3, 1H), 2.7 (s, 6H), 2.61 (q, *J* = 14.2, 7.0, 4H), 1.9 (t, *J* = 7.2), 0.99 (t, *J* = 7.4, 6H), 0.90 (mp, 4H), 0.76 (mp, 2H)

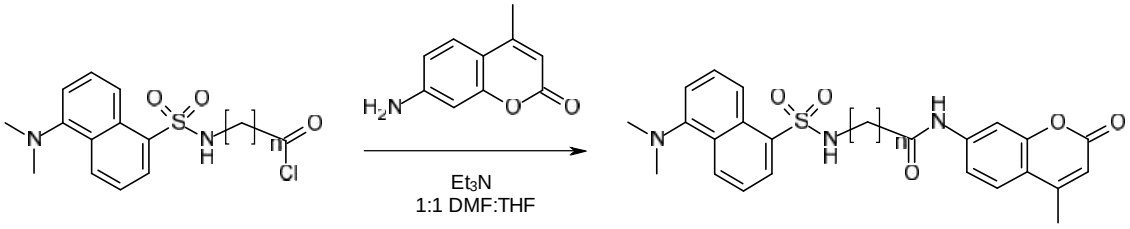

General Procedure: To an oven dried round bottom flask containing a stir bar, 1.0 equivalence of 7-amino 4-methylcoumarin was added and the flask was capped and flushed with argon. The coumarin was dissolved in a 1:1 THF: DMF solution (both freshly distilled, ~30 equivalence each). To this stirring solution, 1.0 equivalence of Et_3N (freshly distilled) was added dropwise and the solution stirred for 10 minutes. Next, a solution containing 1.0 equivalence of acid chloride dissolved in a minimal amount of dry THF was added dropwise to the solution the flask was then fit with a reflux condenser and refluxed for 2 hours. The reaction was then removed from heat and stirred overnight at room temperature. TLC of the reaction (2:1 ethyl acetate: hexanes) showed starting coumarin as well as a new product spot. The solvents were removed in vacuo (some DMF remained), the residual sludge was dissolved in 15 mL of DCM, and the organic layer was washed with dH_2O and Brine to remove the DMF (10 x 25mL). The organic layer was dried with $MgSO_4$, filtered, and evaporated. The crude material was dry packed onto silica gel and column chromatography purification was performed: 1:1 ethyl acetate: hexanes with a slow gradient to pure ethyl acetate).

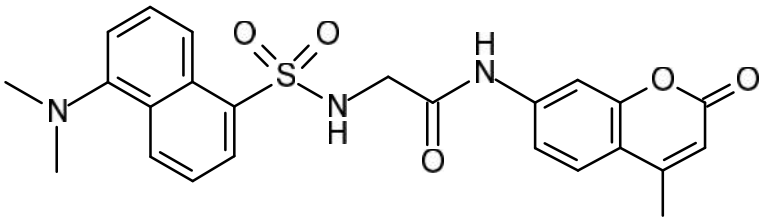

2-(5-(dimethylamino)naphthalene-1-sulfonamido)-N-(4-methyl-2-oxo-2H-chromen-7-yl)acetamide (**44**) (0.048g, 17% yield)

^{1}H NMR: (300 MHz, DMSO-d_6) δ 8.38 (t, *J* = 6.3, 1H), 8.31 (d, *J* = 8.3, 1H), 8.23 (d, *J* = 8.7, 1H) 8.06 (d, *J* = 6.7, 1H) 7.57 (d, *J* = 8.8, 1H), 7.5 (dd, *J* = 8.0, 3.7, 2H), 7.4 (d, *J* = 2.0, 1H), 7.16 (dd, *J* = 10.7, 2.0, 2H), 6.17 (s, 1H), 3.66 (d, *J* = 6.1, 2H), 2.69 (s, 6H), 2.28 (s, 3H)

^{13}C NMR: (300 MHz, DMSO-d_6) δ 168.07, 160.81, 154.36, 153.94, 152.13, 142, 57, 136.76, 130.38, 129.92, 129.84, 129.17, 128.73, 126.77, 124.31, 120.12, 115.94, 115.88, 113.16, 106.35, 46.67, 45.85, 18.82

IR: 3296 (m), 2935 (w), 2823 (w), 1695 (s), 1625 (m), 1616 (w), 1533 (m), 1408 (m), 1392 (m), 1359 (m), 1323 (m), 1143 (s), 852 (m), 785 (s), 563 (m)

HRM/S: *m/z* calculated for $C_{24}H_{23}O_5N_3S$ (M^+) = 466.14 g/mol, found 466.14169

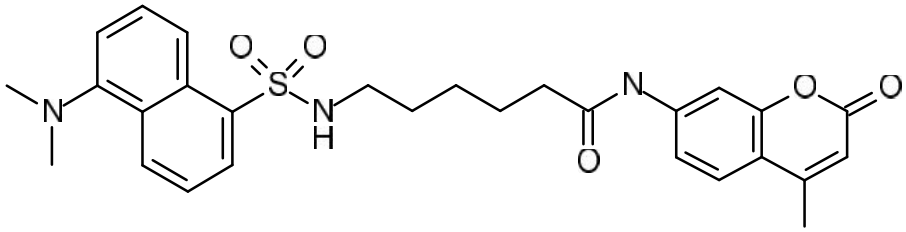

6-(5-(dimethylamino)naphthalene-1-sulfonamido)-N-(4-methyl-2-oxo-2H-chromen-7-yl)hexanamide (**46**) (0.303g, 42% yield)

^{1}H NMR: (300 MHz, DMSO-d_6) δ 8.35 (d, *J* = 8.6, 1H), 8.20 (d, *J* = 8.6, 1H), 8.0 (d, *J* = 7.2, 1H), 7.8 (t, *J* = 5.5, 1H), 7.65 (d, *J* = 1.8, 1H), 7.61 (d, *J* = 8.8, 1H), 7.5 (q, *J* = 17, 8.6, 2H), 7.36 (dd, *J* = 8.8, 1.8, 1H), 7.14 (d, *J* = 7.5), 6.16 (s, 1H), 2.79 (s, 6H), 2.68 (mp, 2H), 2.2 (s, 3H), 2.1 (t, *J* = 7.3, 2H), 1.26 (mp, 4H), 1.08 (mp, 2H)

^{13}C NMR: (300 MHz, DMSO-d_6) δ 172.20, 160.92, 154.52, 153.97, 152.15, 143.44, 136.98, 130.16, 129.93, 129.87, 129.07, 128.61, 126.70, 124.43, 120.00, 115.92, 115.84, 115.59, 112.93, 106.19, 45.89, 43.11, 37.16, 29.80, 26.46, 25.16, 18.82

IR: 3296 (w, br), 2935 (w), 2862 (w), 1697 (s), 1618 (s), 1575 (m), 1519 (m), 1409 (w), 1390 (m), 1309 (m), 1143 (s), 902 (s), 727 (s), 648 (s)

HRM/S: *m/z* calculated for $C_{28}H_{31}O_5N_3S$ (M^+) = 522.21 g/mol, found 522.20654

REFERENCES

(1) Behera, G. .; Mishra, B. .; Behera, P. .; Panda, M. *Advances in Colloid and Interface Science* **1999**, *82*, 1–42.

(2) Misra, P.; Somasundaran, P. In *Interfacial Processes and Molecular Aggregation of Surfactants*; Narayanan, R., Ed.; Advances in Polymer Science; Springer Berlin / Heidelberg, 2008; Vol. 218, pp. 143–188.

(3) Misra, P. K.; Panigrahi, S.; Somasundaran, P. *International Journal of Mineral Processing* **2006**, *80*, 229–237.

(4) Misra, P. K.; Mishra, B. K.; Somasundaran, P. *J Colloid Interface Sci* **2003**, *265*, 1–8.

(5) Somasundaran, P.; Turro, N. J.; Chandar, P. *Colloids and Surfaces* **1986**, *20*, 145–150.

(6) Turro, N. J.; Yekta, A. *J. Am. Chem. Soc.* **1978**, *100*, 5951–5952.

(7) Baden, N.; Kajimoto, O.; Hara, K. *J. Phys. Chem. B* **2002**, *106*, 8621–8624.

(8) Guharay, J.; Sengupta, P. K. *Biochemical and Biophysical Research Communications* **1996**, *219*, 388–392.

(9) Marek, P.; Gupta, R.; Raleigh, D. P. *ChemBioChem* **2008**, *9*, 1372–1374.

(10) Marqusee, J. A.; Dill, K. A. *The Journal of Chemical Physics* **1986**, *85*, 434–444.

(11) Kang, Y. S.; McManus, H. J. D.; Liang, K.; Kevan, L. *J. Phys. Chem.* **1994**, *98*, 1044–1048.

(12) Joseph Georges **1990**, *13*, 27–45.

(13) Paul, B. K.; Guchhait, N. *Journal of Colloid and Interface Science* **2011**, *363*, 529–539.

(14) Grauby-Heywang, C.; Turlet, J.-M. *Journal of Colloid and Interface Science* **2008**, *322*, 73–78.

(15) Matsuki, H.; Goto, M.; Kusube, M.; Tamai, N. *Bulletin of the Chemical Society of Japan* **2011**, *84*, 1329–1335.

(16) Platz, G. *Berichte der Bunsengesellschaft für physikalische Chemie* **1991**, *95*, 103–104.

(17) Flynn, P. F. *Progress in Nuclear Magnetic Resonance Spectroscopy* **2004**, *45*, 31–51.

(18) Bardez, E.; Monnier, E.; Valeur, B. *J. Phys. Chem.* **1985**, *89*, 5031–5036.

(19) Hasegawa, M.; Sugimura, T.; Suzaki, Y.; Shindo, Y.; Kitahara, A. *The Journal of Physical Chemistry* **1994**, *98*, 2120–2124.

(20) N.J. Turro; M. Chow; M.A. Blaustein *J. Am. Chem. Soc.* **1978**, *100*, 5951.

(21) O'Connor, N. A.; Sakata, S. T.; Zhu, H.; Shea, K. J. *Org. Lett.* **2006**, *8*, 1581–1584.

(22) *Molecular Probes Handbook, A Guide to Fluorescent Probes and Labeling Technologies, 11th Edition*; Johnson, I.; Spence, M. T. Z., Eds.; 11th ed.; 2010.

(23) Kurosaki, H.; Yamaguchi, Y.; Yasuzawa, H.; Jin, W.; Yamagata, Y.; Arakawa, Y.; Kurosaki, H.; Yamaguchi, Y.; Yasuzawa, H.; Jin, W.; Yamagata, Y.; Arakawa, Y. *ChemMedChem* **2006**, *1*, 969–972.

(24) Hohsaka, T.; Muranaka, N.; Komiyama, C.; Matsui, K.; Takaura, S.; Abe, R.; Murakami, H.; Sisido, M. *FEBS Letters* **2004**, *560*, 173–177.

(25) Takeuchi, T. *Journal of Chromatography A* **1997**, *780*, 219–228.

(26) Mizukami, S.; Okada, S.; Kimura, S.; Kikuchi, K. *Inorg. Chem.* **2009**, *48*, 7630–7638.
(27) Sivakumar, K.; Xie, F.; Cash, B. M.; Long, S.; Barnhill, H. N.; Wang, Q. *Org. Lett.* **2004**, *6*, 4603–4606.
(28) Du Ý, L.; Ni Ý, N.; Li, M.; Wang, B. *Tetrahedron Letters* **2010**, *51*, 1152–1154.
(29) Singh, A.; Chen, K.; Adelstein, S. J.; Kassis, A. I. *Radiation Research* **2007**, *168*, 233–242.
(30) Gellerman, G.; Waintraub, S.; Albeck, A.; Gaisin, V. *European Journal of Organic Chemistry* **2011**, *2011*, 4176–4182.
(31) Ma, Z.; Day, C. S.; Bierbach, U. *The Journal of Organic Chemistry* **2007**, *72*, 5387–5390.
(32) Choi, M. G.; Hwang, J.; Moon, J. O.; Sung, J.; Chang, S.-K. *Org. Lett.* **2011**, *13*, 5260–5263.
(33) Sun, Y.-Q.; Chen, M.; Liu, J.; Lv, X.; Li, J.; Guo, W. *Chemical Communications* **2011**, *47*, 11029.
(34) Natchus, M. G.; Bookland, R. G.; Laufersweiler, M. J.; Pikul, S.; Almstead, N. G.; De, B.; Janusz, M. J.; Hsieh, L. C.; Gu, F.; Pokross, M. E.; Patel, V. S.; Garver, S. M.; Peng, S. X.; Branch, T. M.; King, S. L.; Baker, T. R.; Foltz, D. J.; Mieling, G. E. *J. Med. Chem.* **2001**, *44*, 1060–1071.
(35) Majumdar, K. C.; Chattopadhyay, B.; Nath, S. *Tetrahedron Letters* **2008**, *49*, 1609–1612.
(36) Bognár, B.; Øz, E.; Hideg, K.; Kálai, T. *Journal of Heterocyclic Chemistry* **2006**, *43*, 81–86.
(37) Armstrong, A.; Bhonoah, Y.; Shanahan, S. E. *J. Org. Chem.* **2007**, *72*, 8019–8024.
(38) Natchus, M. G.; Bookland, R. G.; Laufersweiler, M. J.; Pikul, S.; Almstead, N. G.; De, B.; Janusz, M. J.; Hsieh, L. C.; Gu, F.; Pokross, M. E.; Patel, V. S.; Garver, S. M.; Peng, S. X.; Branch, T. M.; King, S. L.; Baker, T. R.; Foltz, D. J.; Mieling, G. E. *J. Med. Chem.* **2001**, *44*, 1060–1071.
(39) Shen, Z.; Lu, X.; Lei, A. *Tetrahedron* **2006**, *62*, 9237–9246.
(40) Dyer, B. S.; Jones, J. D.; Ainge, G. D.; Denis, M.; Larsen, D. S.; Painter, G. F. *J. Org. Chem.* **2007**, *72*, 3282–3288.
(41) M. Cleij *Journal of Organic Chemistry* **1999**, *64*, 5029–5035.
(42) Roemmele, R. C.; Rapoport, H. *The Journal of Organic Chemistry* **1989**, *54*, 1866–1875.
(43) Solladié, G.; Hugelé, P.; Bartsch, R. *J. Org. Chem.* **1998**, *63*, 3895–3898.
(44) Hanessian, S.; Wang, X.; Ersmark, K.; Del Valle, J. R.; Klegraf, E. *Org. Lett.* **2009**, *11*, 4232–4235.
(45) Bahia, P. S.; Snaith, J. S. *J. Org. Chem.* **2004**, *69*, 3226–3229.
(46) Sumner Levine *Journal of the American Chemical Society* **1954**, *76*, 1382.
(47) Hawker, C. J.; Wooley, K. L.; Frechet, J. M. J. *J. Am. Chem. Soc.* **1993**, *115*, 4375–4376.
(48) Vuram, P. K.; Subuddhi, U.; Krishnaji, S. T.; Chadha, A.; Mishra, A. K. *Eur J Org Chem* **2010**, 5030.

APPENDIX: SPECTRAL DATA OF COMPOUNDS

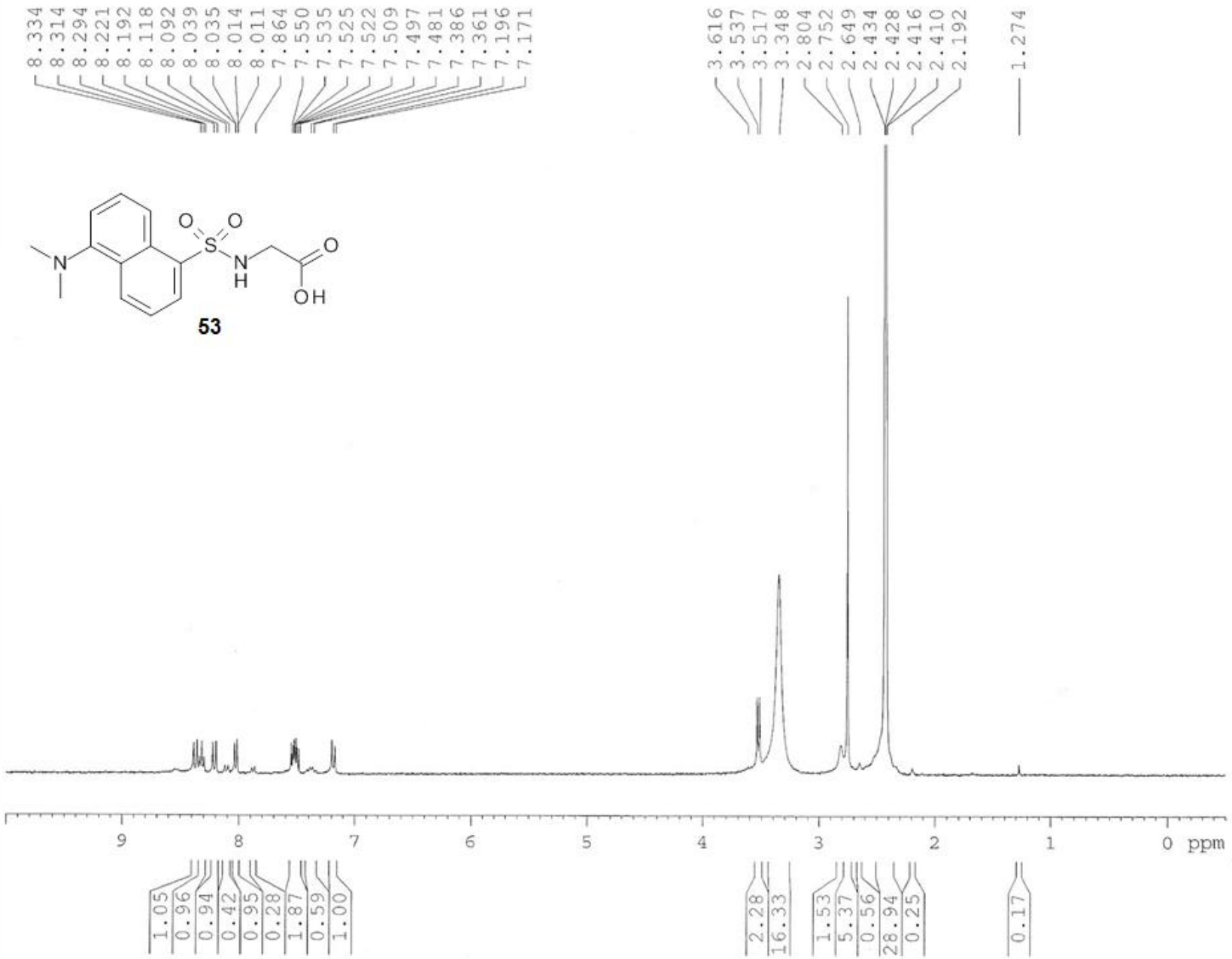
8.334
8.314
8.294
8.221
8.192
8.118
8.092
8.039
8.035
8.014
8.011
7.864
7.550
7.535
7.525
7.522
7.509
7.497
7.481
7.386
7.361
7.196
7.171
3.616
3.537
3.517
3.348
2.804
2.752
2.649
2.434
2.428
2.416
2.410
2.192
1.274
O
O
S
N
H
O
OH
N
53
9
8
7
6
5
4
3
2
1
0 ppm
1.05
0.96
0.94
0.42
0.95
0.28
1.87
0.59
1.00
2.28
16.33
1.53
5.37
0.56
28.94
0.25
0.17

SHIMADZU

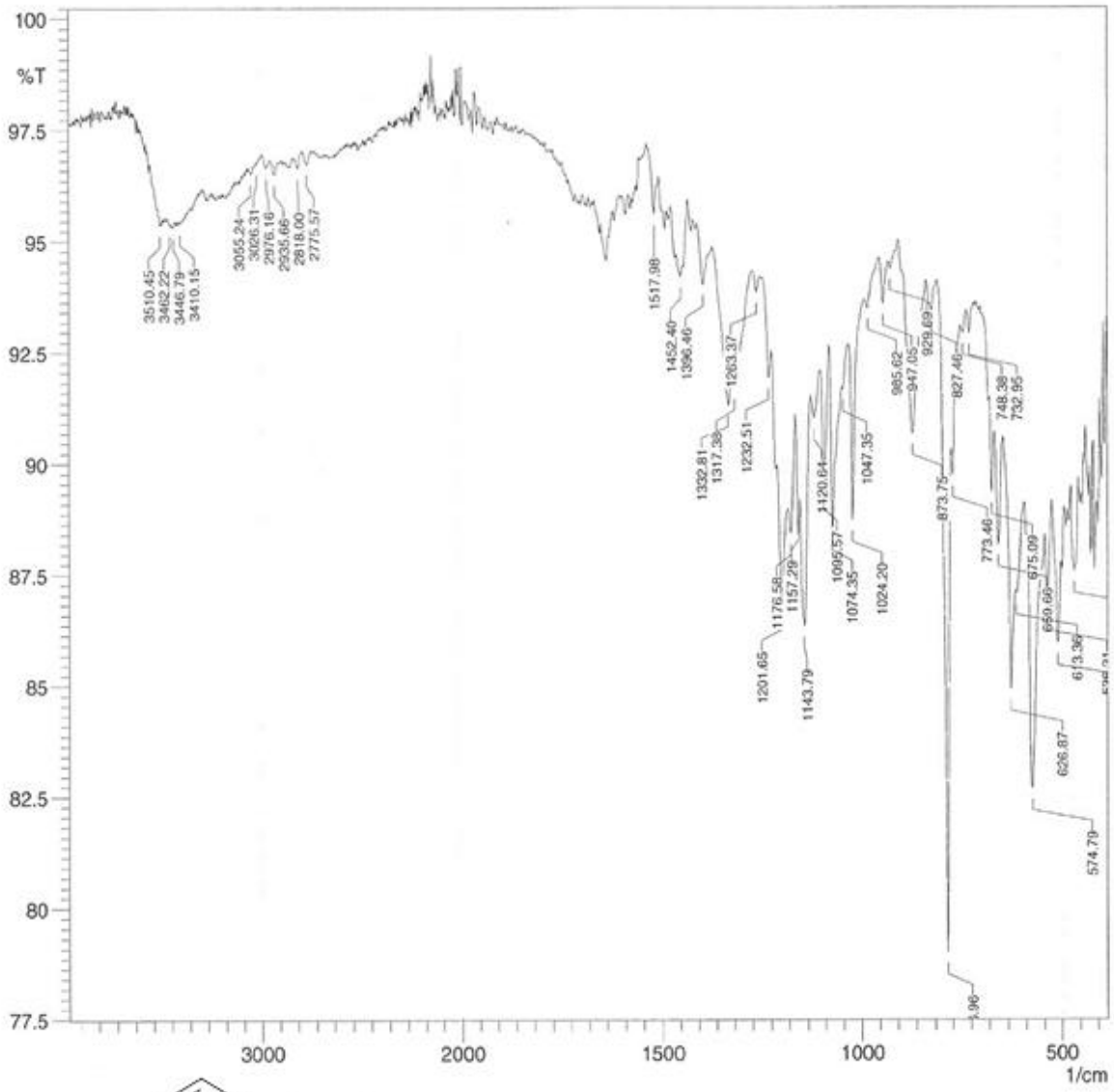

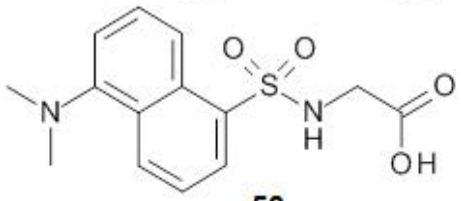

53

Date/Time; 8/8/2011 10:25:44 AM
No. of Scans; 50
Resolution; 4 [1/cm]
Apodization; Happ-Genzel

	Peak	Intensity	Corr. Inte	Base (H)	Base (L)	Area	Corr. Are
1	304.75	75.87	37.87	308.61	300.9	0.26	0.71
2	314.4	36.01	114.72	324.04	310.54	4.3	6.98
3	376.12	82.69	6.31	385.76	374.19	0.74	0.23
4	468.7	87.57	2	476.42	459.06	0.95	0.12
5	509.21	85.95	2.22	524.64	503.42	1.26	0.12
6	536.21	86.73	1.77	542	526.57	0.88	0.07
7	574.79	82.68	5.56	584.43	543.93	2.69	0.5
8	613.36	87.08	0.27	615.29	596	1.06	0.02
9	626.87	84.92	3.3	646.15	617.22	1.69	0.18
10	659.66	88.16	2.44	667.37	648.08	0.94	0.12
11	675.09	89.34	1.76	680.87	669.3	0.52	0.05
12	732.95	92.91	0.56	738.74	723.31	0.47	0.02
13	748.38	92.93	0.32	754.17	740.67	0.42	0.01
14	773.46	89.72	1.1	777.31	756.1	0.8	0.03
15	786.96	79.01	12.07	812.03	779.24	1.84	0.66
16	827.46	93.43	0.3	831.32	813.96	0.48	0.01
17	873.75	90.67	3.52	894.97	840.96	1.84	0.43
18	929.69	94.37	0.22	933.55	918.12	0.38	0.01
19	947.05	93.58	0.97	954.76	935.48	0.51	0.04
20	985.62	93.49	0.38	993.34	956.69	0.97	0.01
21	1024.2	88.72	4.13	1031.92	995.27	1.31	0.18
22	1047.35	91.66	0.17	1049.28	1033.85	0.54	0
23	1074.35	88.54	3.82	1080.14	1051.2	1.27	0.23
24	1095.57	89.45	2.85	1103.28	1082.07	0.87	0.14
25	1120.64	91.02	0.69	1128.36	1105.21	0.9	0.04
26	1143.79	86.34	3.62	1153.43	1130.29	1.25	0.22
27	1157.29	88.78	0.75	1165	1155.36	0.49	0.04
28	1176.58	88.42	1.49	1184.29	1166.93	0.85	0.06
29	1201.65	86.74	2.79	1211.3	1186.22	1.38	0.16
30	1232.51	91.93	1.09	1246.02	1226.73	0.62	0.04
31	1263.37	93.86	0.4	1271.09	1255.66	0.41	0.01
32	1317.38	91.69	0.92	1323.17	1273.02	1.58	0.1
33	1332.81	91.31	1.45	1371.39	1325.1	1.49	0.15
34	1396.46	94.03	1.17	1409.96	1373.32	0.89	0.09
35	1452.4	94.2	0.31	1462.04	1448.54	0.34	0.01
36	1517.98	95.6	1.15	1531.48	1506.41	0.41	0.05
37	2775.57	96.74	0.28	2792.93	2752.42	0.56	0.03
38	2818	96.64	0.28	2833.43	2800.64	0.46	0.02
39	2935.66	96.51	0.29	2958.8	2916.37	0.62	0.02
40	2976.16	96.66	0.11	2999.31	2970.38	0.41	0.01
41	3026.31	96.74	0.04	3028.24	3001.24	0.38	0

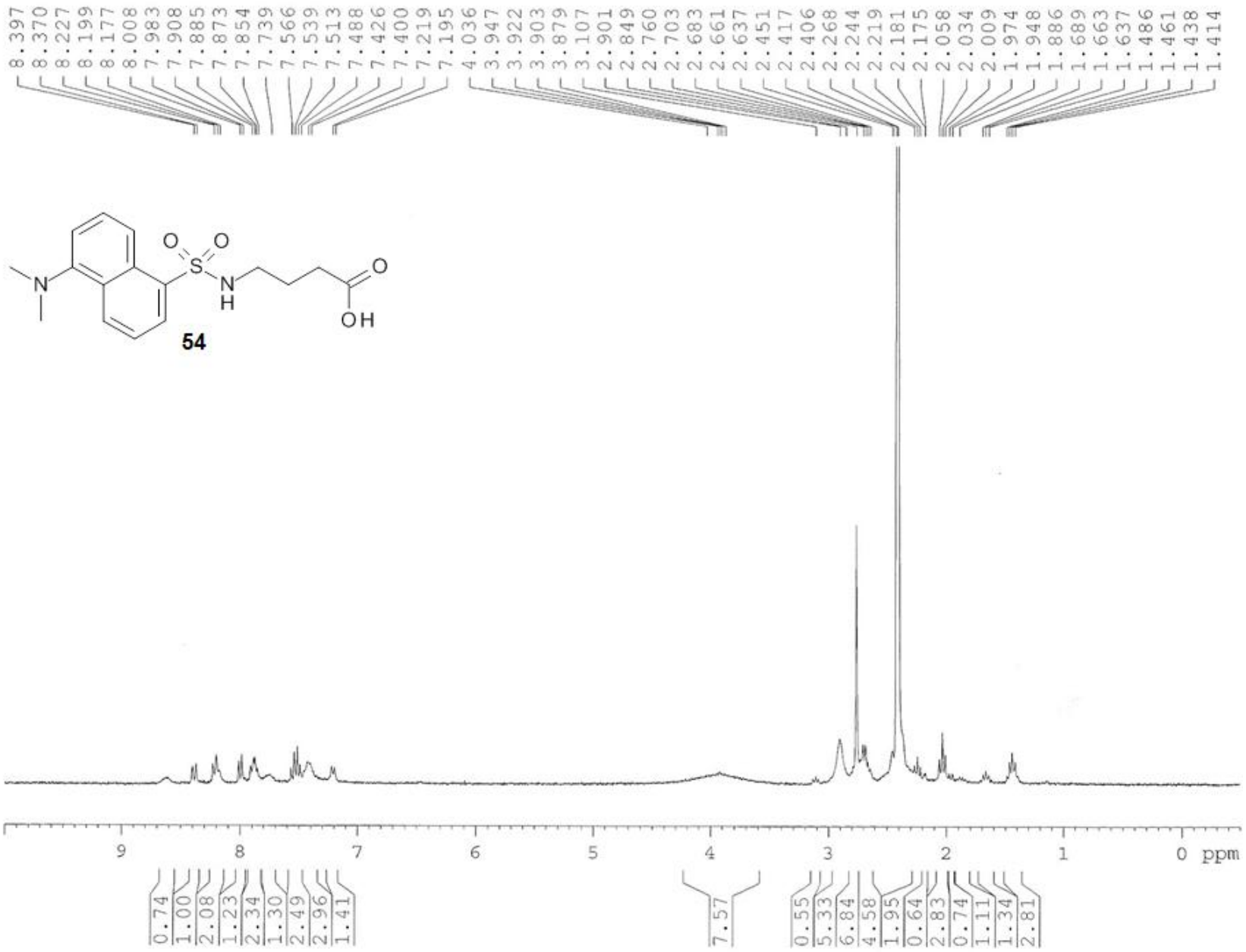
8.397
8.370
8.227
8.199
8.177
8.008
7.983
7.908
7.885
7.873
7.854
7.739
7.566
7.539
7.513
7.488
7.426
7.400
7.219
7.195
4.036
3.947
3.922
3.903
3.879
3.107
2.901
2.849
2.760
2.703
2.683
2.661
2.637
2.451
2.417
2.406
2.268
2.244
2.219
2.181
2.175
2.058
2.034
2.009
1.974
1.948
1.886
1.689
1.663
1.637
1.486
1.461
1.438
1.414
O
O
S
N
H
N
O
OH
54
9
8
7
6
5
4
3
2
1
0 ppm
0.74
1.00
2.08
1.23
2.34
1.30
2.49
2.96
1.41
7.57
0.55
5.33
6.84
4.58
1.95
0.64
2.83
0.74
1.11
1.34
2.81

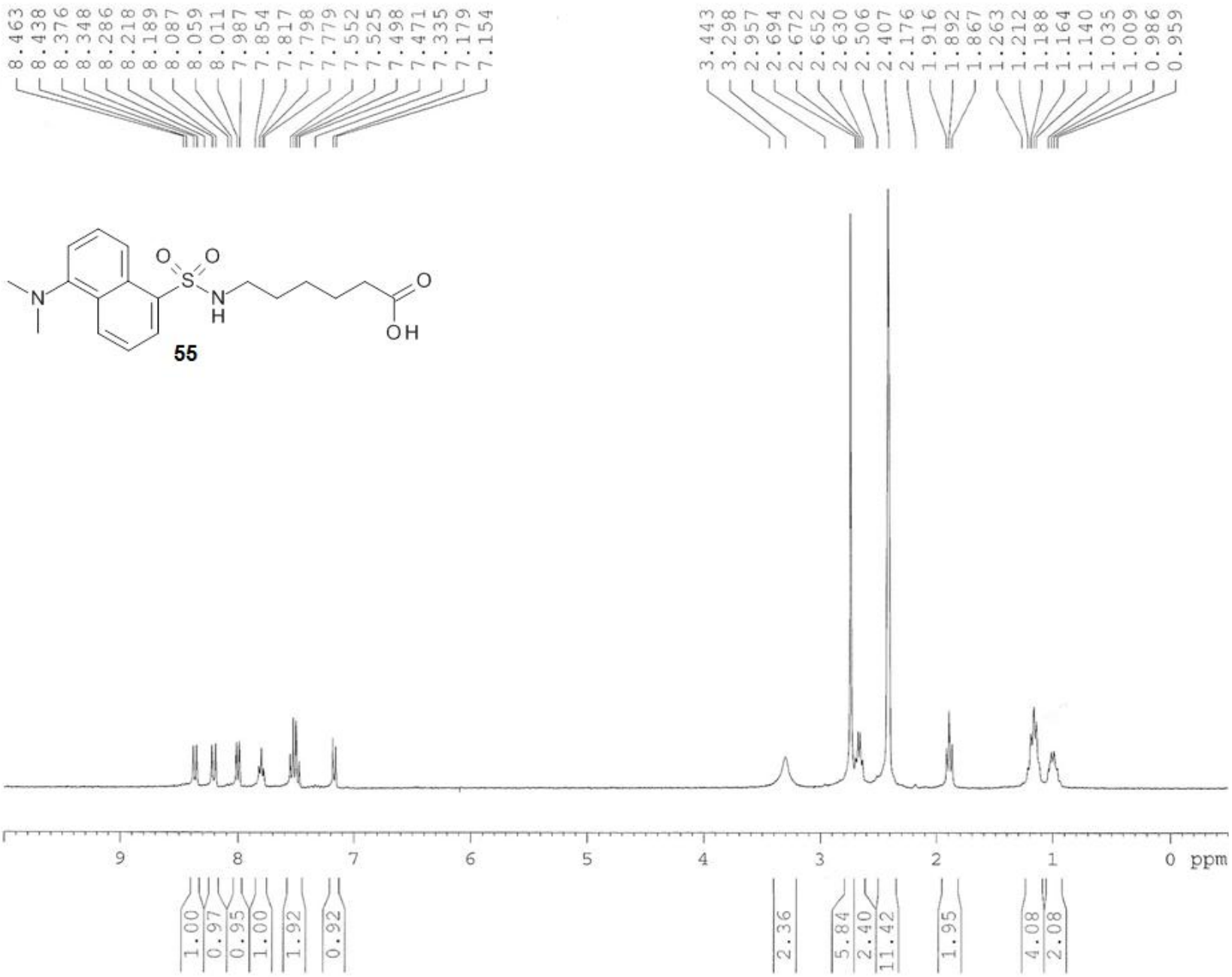
8.463
8.438
8.376
8.348
8.286
8.218
8.189
8.087
8.059
8.011
7.987
7.854
7.817
7.798
7.779
7.552
7.525
7.498
7.471
7.335
7.179
7.154
3.443
3.298
2.957
2.694
2.672
2.652
2.630
2.506
2.407
2.176
1.916
1.892
1.867
1.263
1.212
1.188
1.164
1.140
1.035
1.009
0.986
0.959
O
O
S
N
H
N
O
OH
55
9
8
7
6
5
4
3
2
1
0 ppm
1.00
0.97
0.95
1.00
1.92
0.92
2.36
5.84
2.40
11.42
1.95
4.08
2.08

SHIMADZU

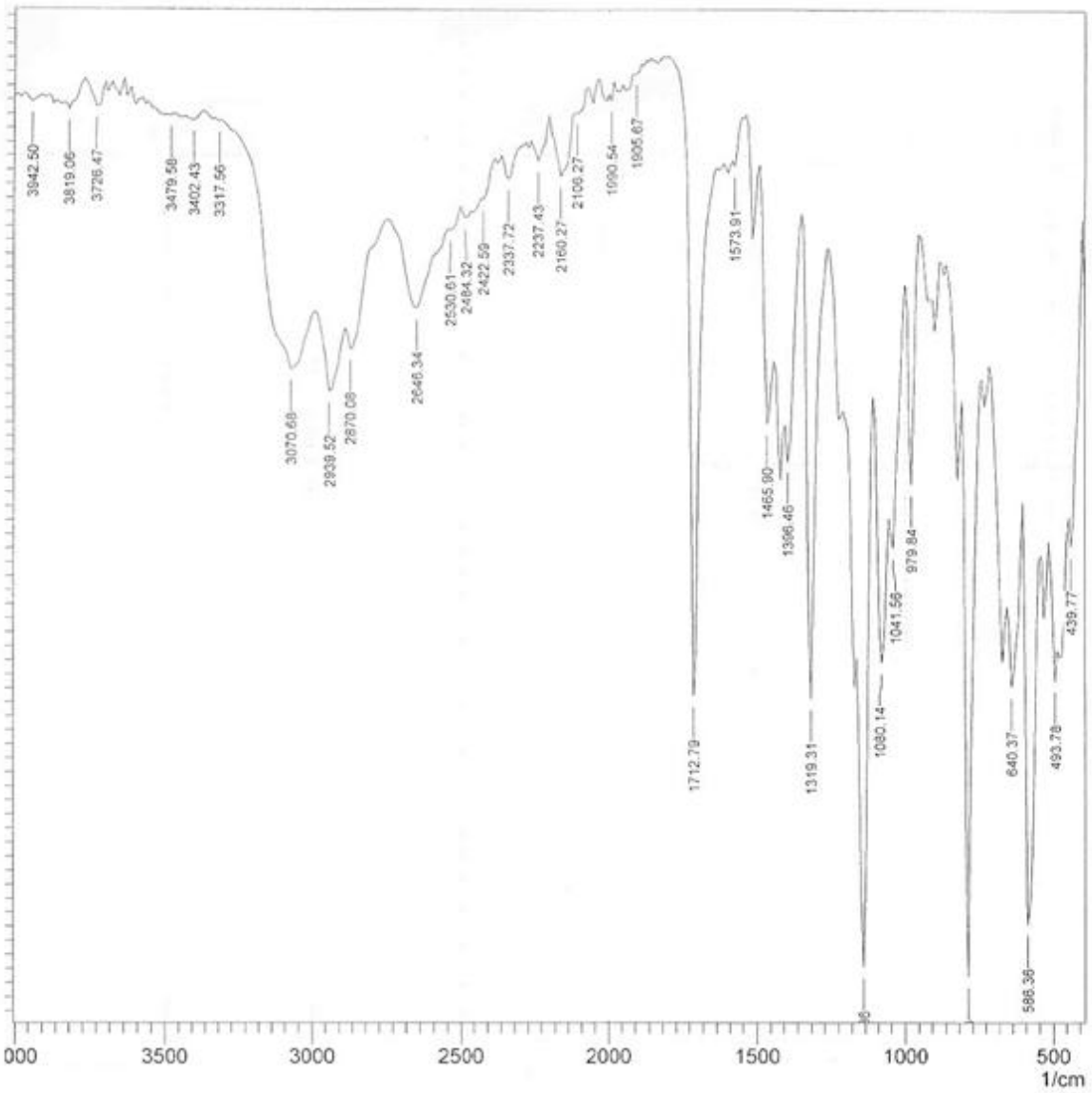

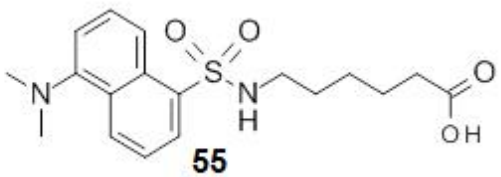

55

Date/Time; 5/14/2012 2:19:21 PM
No. of Scans; 25
Resolution; 16 [1/cm]
Apodization; Happ-Genzel

	Peak	Intensity	Corr. Inte	Base (H)	Base (L)	Area	Corr. Are
1	439.77	88.662	1.113	447.49	408.91	1.718	0.145
2	493.78	86.48	1.969	509.21	455.2	3.198	0.347
3	586.36	82.532	6.586	601.79	547.78	3.757	0.985
4	640.37	86.373	1.603	655.8	609.51	2.744	0.219
5	786.96	81.683	9.475	810.1	748.38	3.683	1.217
6	979.84	89.673	3.332	995.27	956.69	1.456	0.284
7	1041.56	88.64	1.581	1056.99	1002.98	2.301	0.165
8	1080.14	86.78	3.143	1103.28	1056.99	2.583	0.418
9	1141.86	81.84	9.198	1211.3	1111	5.98	1.872
10	1319.31	86.19	7.549	1342.46	1265.3	3.321	1.126
11	1396.46	90.053	1.069	1404.18	1350.17	1.941	0.135
12	1465.9	90.667	2.597	1489.05	1442.75	1.719	0.257
13	1573.91	94.842	0.199	1581.63	1535.34	0.948	0.009
14	1712.79	86.235	9.363	1797.66	1643.35	4.497	1.527
15	1905.67	96.323	0.039	1913.39	1859.38	0.841	0.003
16	1990.54	95.906	0.312	2029.11	1982.82	0.821	0.048
17	2106.27	95.705	0.08	2113.98	2075.41	0.717	0.023
18	2160.27	94.674	0.982	2198.85	2121.7	1.701	0.213
19	2237.43	94.924	0.336	2252.86	2206.57	1.002	0.044
20	2337.72	94.629	0.433	2360.87	2283.72	1.739	0.058
21	2422.59	94.304	0.126	2430.31	2391.73	0.938	0.019
22	2484.32	94.003	0.114	2492.03	2430.31	1.625	0.027
23	2530.61	93.799	0.093	2538.32	2499.75	1.046	0.015
24	2646.34	92.536	1.357	2738.92	2546.04	5.86	0.575
25	2870.08	91.878	0.525	2885.51	2746.63	4.366	0.119
26	2939.52	91.186	1.107	2985.81	2893.22	3.467	0.235
27	3070.68	91.551	1.678	3309.85	2993.52	9.388	0.992
28	3317.56	95.588	0.018	3363.86	3309.85	1.053	0.008
29	3402.43	95.591	0.089	3425.58	3371.57	1.045	0.012
30	3479.58	95.667	0.036	3525.88	3471.87	1.036	0.01
31	3726.47	95.807	0.323	3765.05	3703.33	1.103	0.048
32	3819.06	95.75	0.201	3834.49	3772.76	1.109	0.032
33	3942.5	95.873	0.11	3965.65	3919.35	0.836	0.011

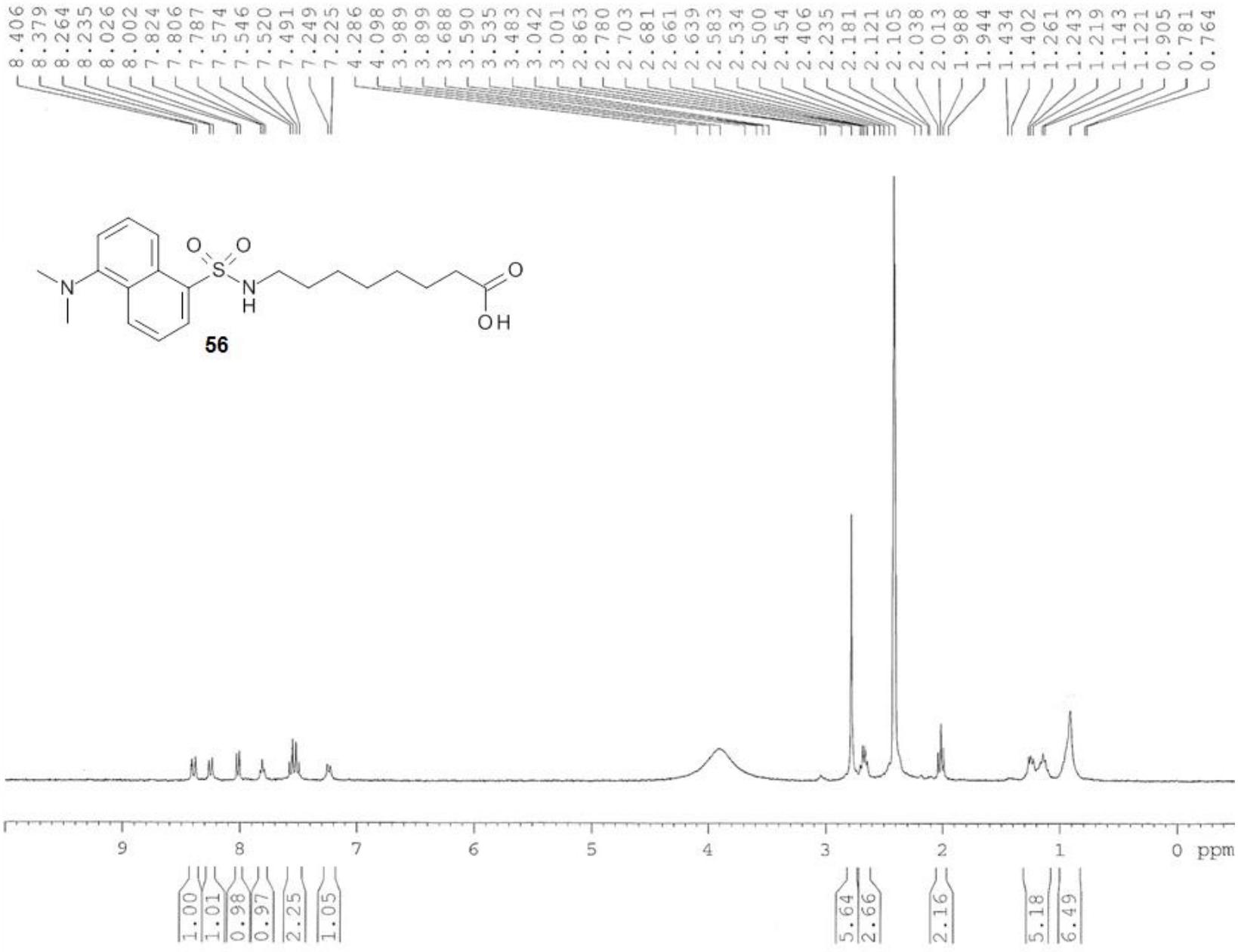
8.406
8.379
8.264
8.235
8.026
8.002
7.824
7.806
7.787
7.574
7.546
7.520
7.491
7.249
7.225
4.286
4.098
3.989
3.899
3.688
3.590
3.535
3.483
3.042
3.001
2.863
2.780
2.703
2.681
2.661
2.639
2.583
2.534
2.500
2.454
2.406
2.235
2.181
2.121
2.105
2.038
2.013
1.988
1.944
1.434
1.402
1.261
1.243
1.219
1.143
1.121
0.905
0.781
0.764
O
O
S
N
H
N
O
OH
56
9
8
7
6
5
4
3
2
1
0 ppm
1.00
1.01
0.98
0.97
2.25
1.05
5.64
2.66
2.16
5.18
6.49

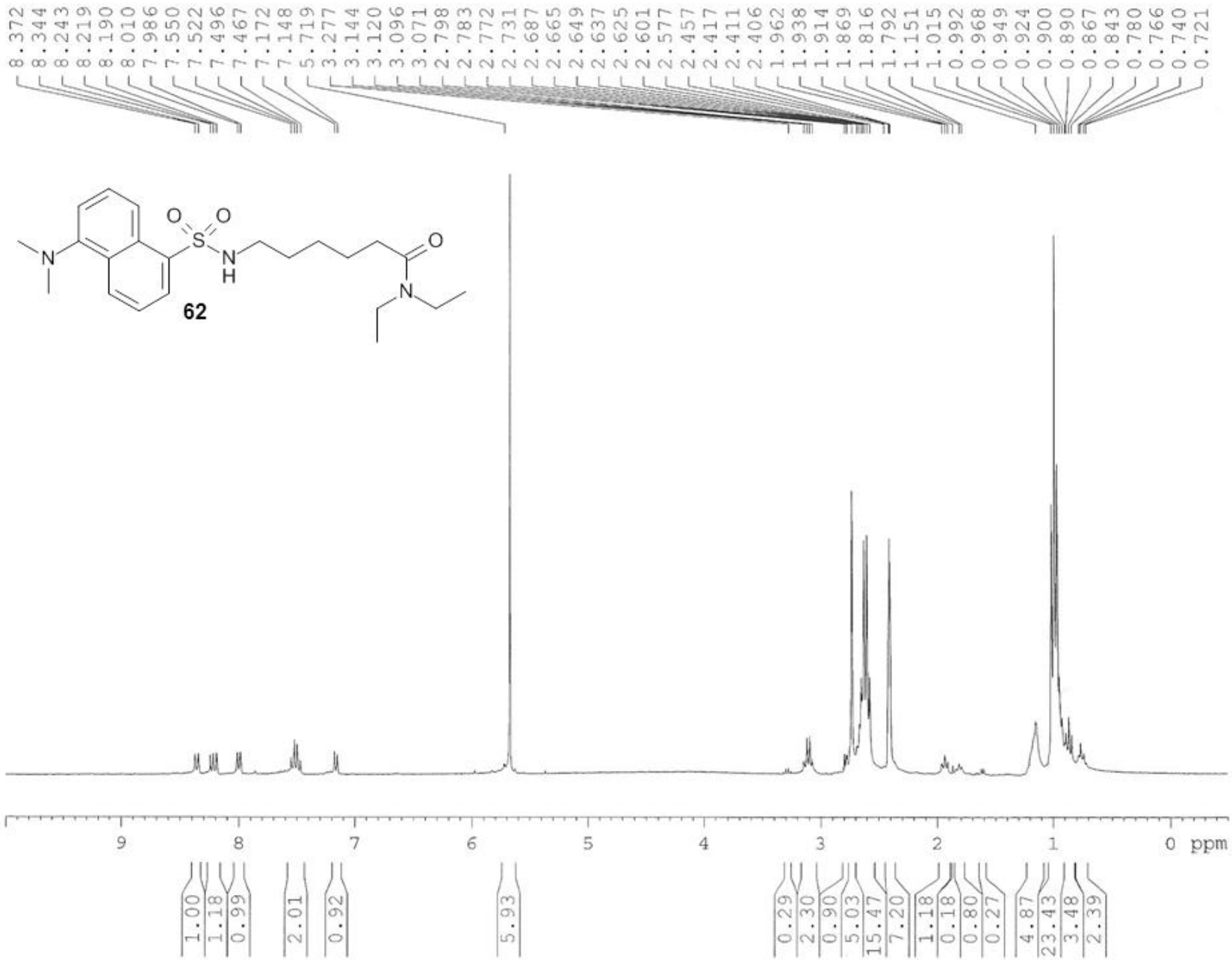
8.372
8.344
8.243
8.219
8.190
8.010
7.986
7.550
7.522
7.496
7.467
7.172
7.148
5.719
3.277
3.144
3.120
3.096
3.071
2.798
2.783
2.772
2.731
2.687
2.665
2.649
2.637
2.625
2.601
2.577
2.457
2.417
2.411
2.406
1.962
1.938
1.914
1.869
1.816
1.792
1.151
1.015
0.992
0.968
0.949
0.924
0.900
0.890
0.867
0.843
0.780
0.766
0.740
0.721
O
O
S
N
H
N
O
N
62
9
8
7
6
5
4
3
2
1
0 ppm
1.00
1.18
0.99
2.01
0.92
5.93
0.29
2.30
0.90
5.03
15.47
7.20
1.18
0.18
0.80
0.27
4.87
23.43
3.48
2.39


8.249
8.221
8.201
8.074
8.050
8.031
7.858
7.838
7.639
7.594
7.565
7.535
7.522
7.507
7.494
7.481
7.470
7.417
7.411
7.208
7.202
7.179
7.173
7.164
7.138
6.990
6.178
6.174
3.676
3.656
3.023
2.916
2.841
2.799
2.736
2.721
2.694
2.644
2.600
2.451
2.417
2.405
2.289
2.181
-0.155
44
9
8
7
6
5
4
3
2
1
0 ppm
1.00
0.98
0.88
0.84
1.00
1.97
0.73
1.85
0.13
0.11
0.76
3.62
0.19
0.27
0.99
0.57
4.10
0.52
0.61
19.96
2.32
0.29

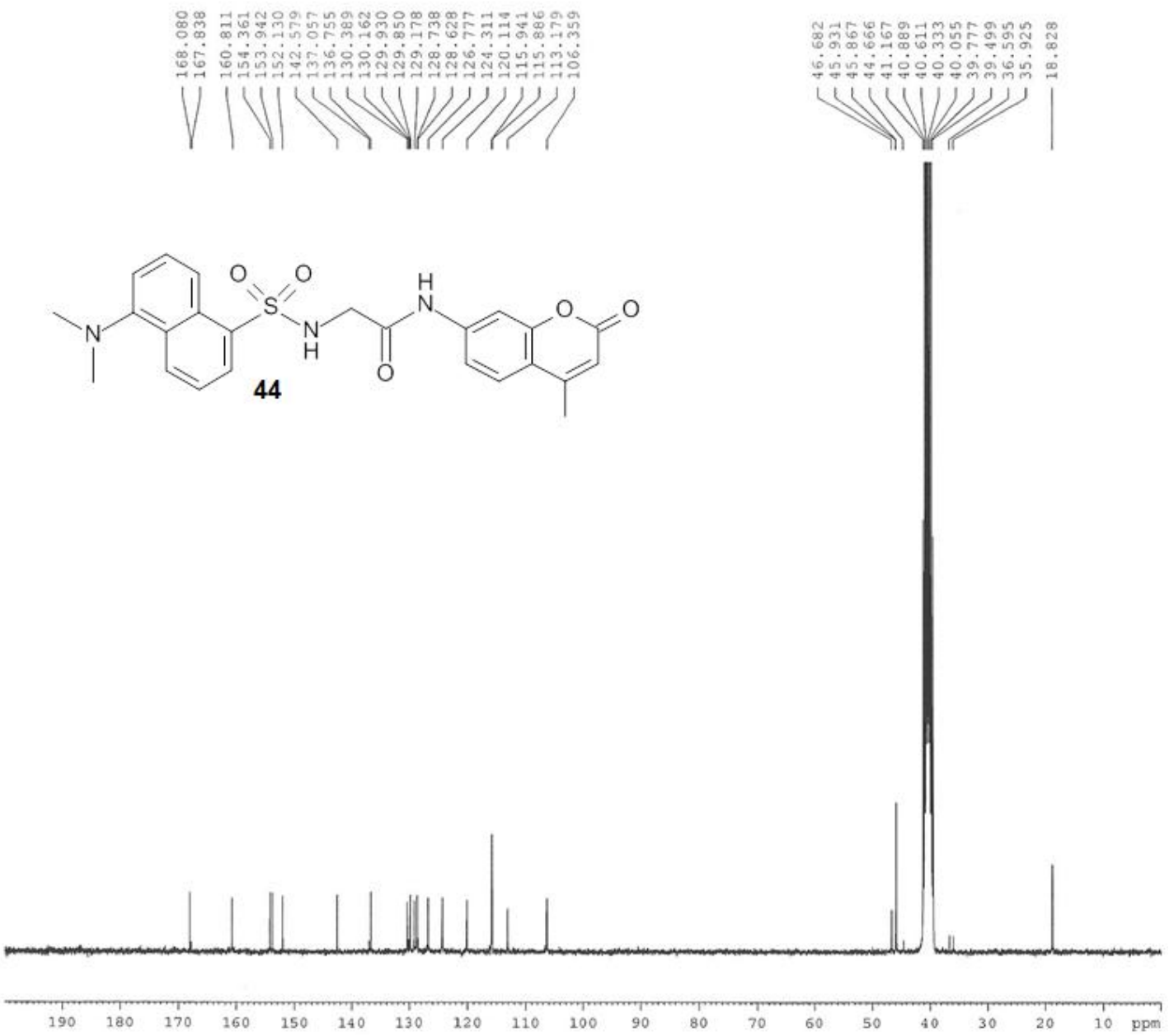
168.080
167.838
160.811
154.361
153.942
152.130
142.579
137.057
136.755
130.389
130.162
129.930
129.850
129.178
128.738
128.628
126.777
124.311
120.114
115.941
115.886
113.179
106.359
46.682
45.931
45.867
44.666
41.167
40.889
40.611
40.333
40.055
39.777
39.499
36.595
35.925
18.828
O
O
S
N
H
N
H
O
O
N
44
190
180
170
160
150
140
130
120
110
100
90
80
70
60
50
40
30
20
10
ppm

SHIMADZU

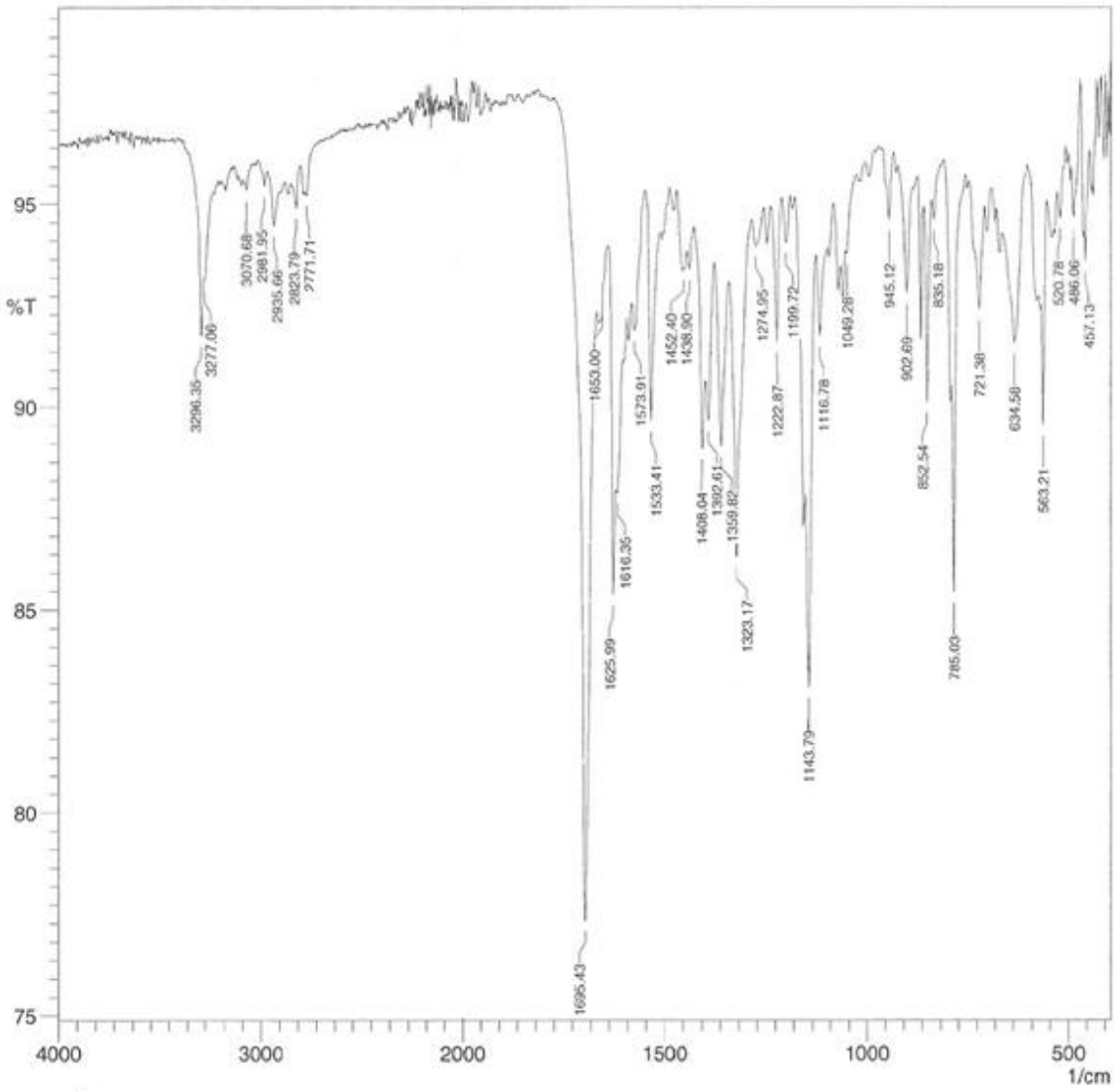

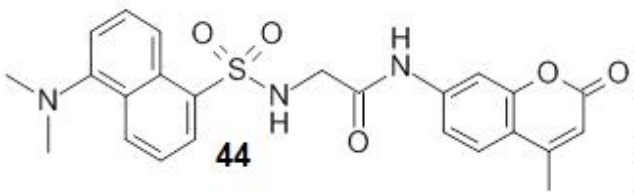

44

Date/Time; 8/17/2011 2:15:49 PM
No. of Scans; 50
Resolution; 4 [1/cm]
Apodization; Happ-Genzel

	Peak	Intensity	Corr. Inte	Base (H)	Base (L)	Area	Corr. Are
1	300.9	48.63	30.86	306.68	298.97	1.09	0.35
2	312.47	36.56	54.19	314.4	308.61	0.94	1.19
3	329.83	23.45	41.05	335.61	327.9	3.13	1.58
4	339.47	29.48	49.25	347.19	335.61	3.1	1.87
5	457.13	93.6	3.34	468.7	447.49	0.47	0.18
6	486.06	94.68	1.8	491.85	470.63	0.39	0.11
7	520.78	94.65	0.96	526.57	507.28	0.39	0.04
8	563.21	89.55	3.7	567.07	555.5	0.41	0.09
9	634.58	91.57	3.49	663.51	601.79	1.76	0.43
10	721.38	92.4	2.67	746.45	709.8	1.01	0.22
11	785.03	85.43	6.02	790.81	758.02	1.07	0.16
12	835.18	94.61	0.61	839.03	819.75	0.4	0.02
13	852.54	90.13	4.78	858.32	840.96	0.55	0.16
14	902.69	92.81	2.78	921.97	889.18	0.8	0.16
15	945.12	94.6	1.7	960.55	933.55	0.53	0.09
16	1049.28	93.79	0.33	1053.13	1026.13	0.6	0.01
17	1116.78	91.76	2.01	1124.5	1097.5	0.84	0.1
18	1143.79	83.1	6.46	1151.5	1126.43	1.31	0.29
19	1199.72	94.05	1.08	1207.44	1190.08	0.43	0.05
20	1222.87	91.61	3.44	1236.37	1209.37	0.76	0.17
21	1274.95	93.97	0.75	1284.59	1255.66	0.74	0.06
22	1323.17	86.31	7.16	1338.6	1286.52	2.13	0.69
23	1359.82	89.03	4.26	1375.25	1340.53	1.37	0.32
24	1392.61	89.66	1.77	1398.39	1377.17	0.82	0.08
25	1408.04	88.98	2.74	1427.32	1400.32	1.01	0.1
26	1438.9	93.4	0.65	1444.68	1429.25	0.42	0.02
27	1452.4	93.38	0.75	1469.76	1446.61	0.64	0.06
28	1533.41	89.66	5.27	1546.91	1512.19	1.12	0.31
29	1573.91	91.88	1.18	1579.7	1548.84	0.9	0.07
30	1616.35	87.88	0.84	1620.21	1604.77	0.77	0.04
31	1625.99	85.37	4.82	1635.64	1620.21	0.82	0.15
32	1653	92.13	0.2	1654.92	1637.56	0.51	0
33	1695.43	77.35	16.33	1768.72	1668.43	4.2	1.92
34	2771.71	95.22	0.31	2781.35	2731.2	0.9	0.01
35	2823.79	94.9	0.87	2850.79	2804.5	0.94	0.07
36	2935.66	94.46	1.09	2968.45	2904.8	1.37	0.11
37	2981.95	95.45	0.36	2993.52	2970.38	0.45	0.02
38	3070.68	95.34	0.28	3076.46	3047.53	0.56	0.01
39	3277.06	93.12	0.23	3280.92	3238.48	1.08	0.01
40	3296.35	91.75	2.06	3354.21	3280.92	1.82	0.12

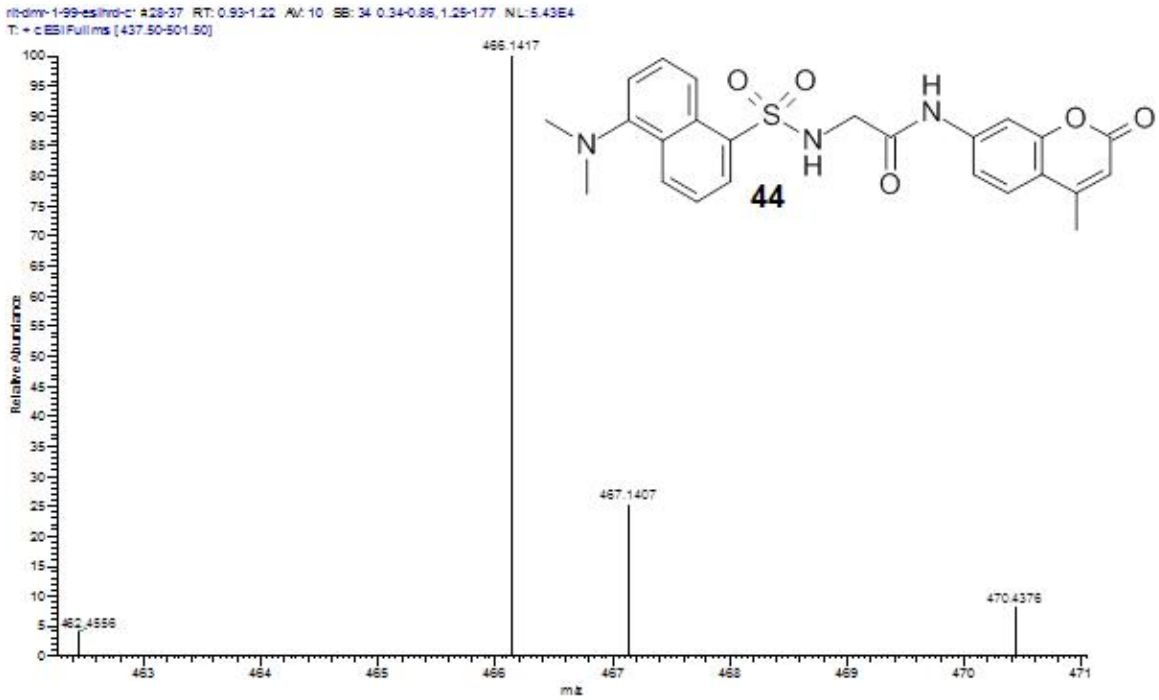

Mass	Relative Intensity	Theoretical Mass [ppm]	Delta	RDB	Composition
466.14169	32.5	466.1431	-3.1	14.5	<<C24 H24 O5 N3 S1 >>
		466.1445	-5.9	14.0	<<C26 H26 O6 S1 >>
		466.1386	6.7	23.0	<<C33 H22 O1 S1 >>
		466.1458	-8.8	19.0	<<C27 H22 O2 N4 S1 >>
		466.1372	9.5	23.5	<<C31 H20 N3 S1 >>

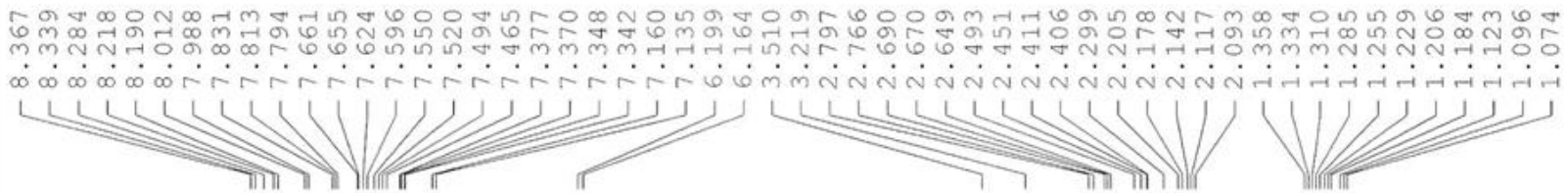
8.367
8.339
8.284
8.218
8.190
8.012
7.988
7.831
7.813
7.794
7.661
7.655
7.624
7.596
7.550
7.520
7.494
7.465
7.377
7.370
7.348
7.342
7.160
7.135
6.199
6.164
3.510
3.219
2.797
2.766
2.690
2.670
2.649
2.493
2.451
2.411
2.406
2.299
2.205
2.178
2.142
2.117
2.093
1.358
1.334
1.310
1.285
1.255
1.229
1.206
1.184
1.123
1.096
1.074

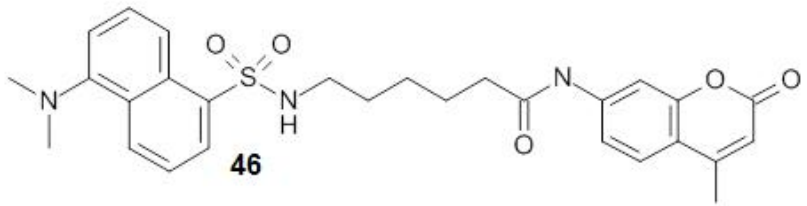
O
O
S
N
H
N
O
O
O

46

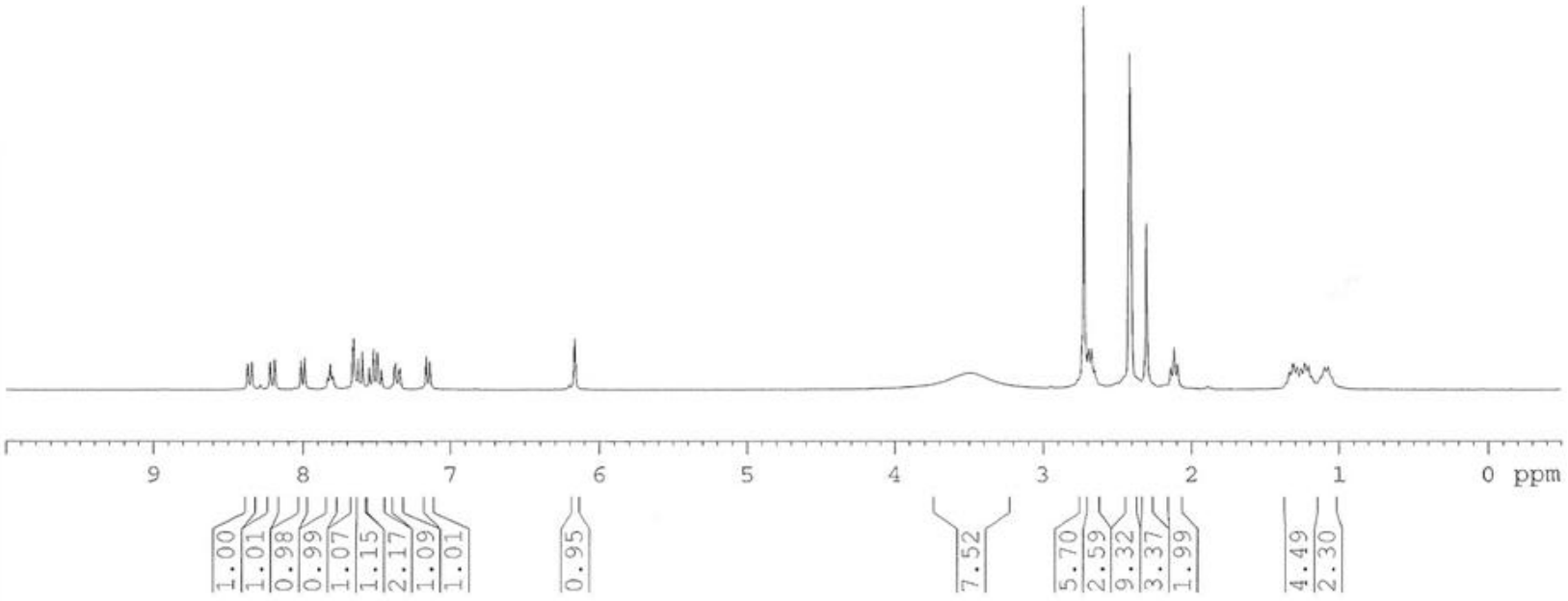
9
8
7
6
5
4
3
2
1
0 ppm
1.00
1.01
0.98
0.99
1.07
1.15
2.17
1.09
1.01
0.95
7.52
5.70
2.59
9.32
3.37
1.99
4.49
2.30

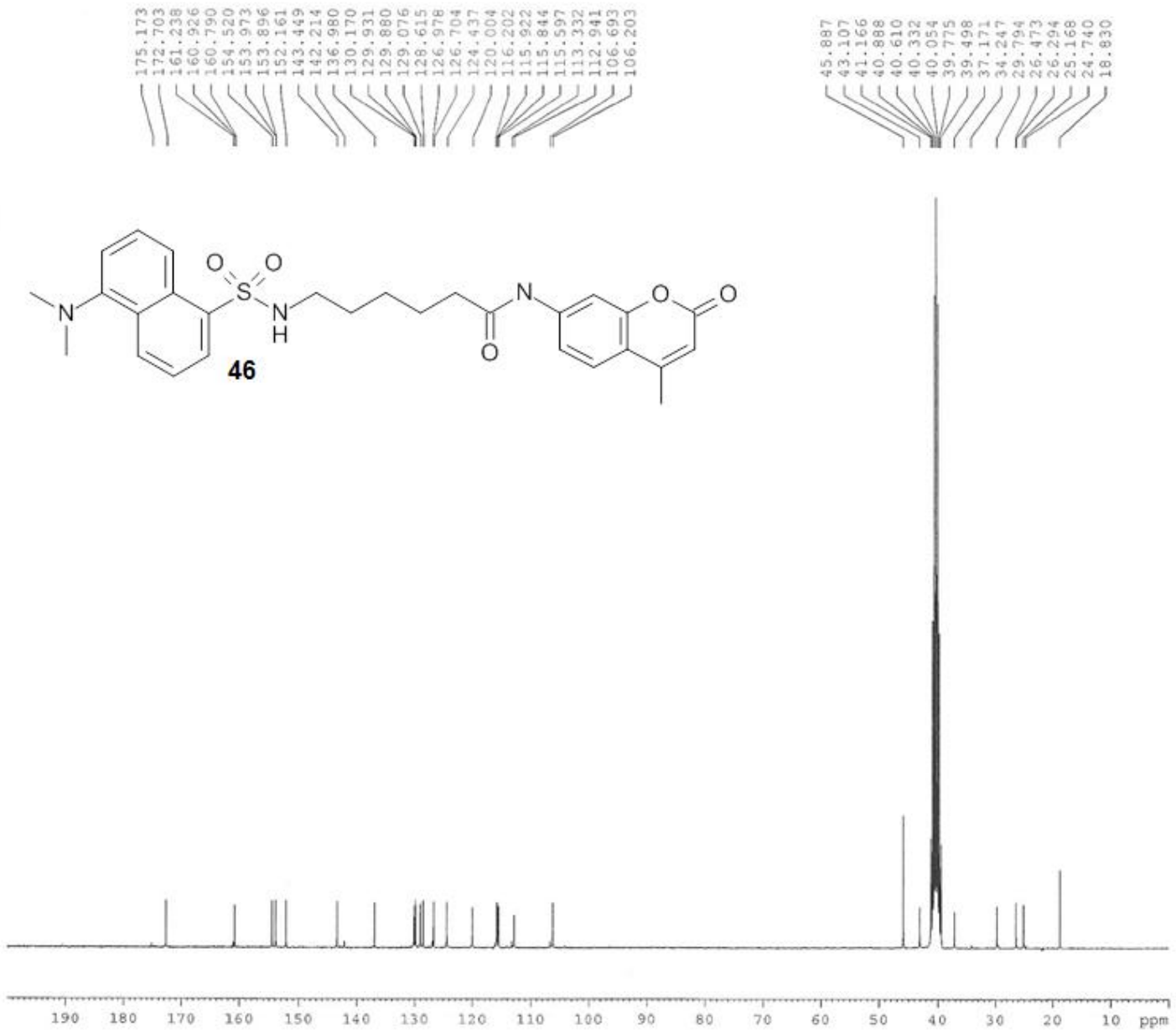
175.173
172.703
161.238
160.926
160.790
154.520
153.973
153.896
152.161
143.449
142.214
136.980
130.170
129.931
129.880
129.076
128.615
126.978
126.704
124.437
120.004
116.202
115.922
115.844
115.597
113.332
112.941
106.693
106.203
45.887
43.107
41.166
40.888
40.610
40.332
40.054
39.775
39.498
37.171
34.247
29.794
26.473
26.294
25.168
24.740
18.830
O
O
S
N
H
N
O
O
O
46
190
180
170
160
150
140
130
120
110
100
90
80
70
60
50
40
30
20
10
ppm

SHIMADZU

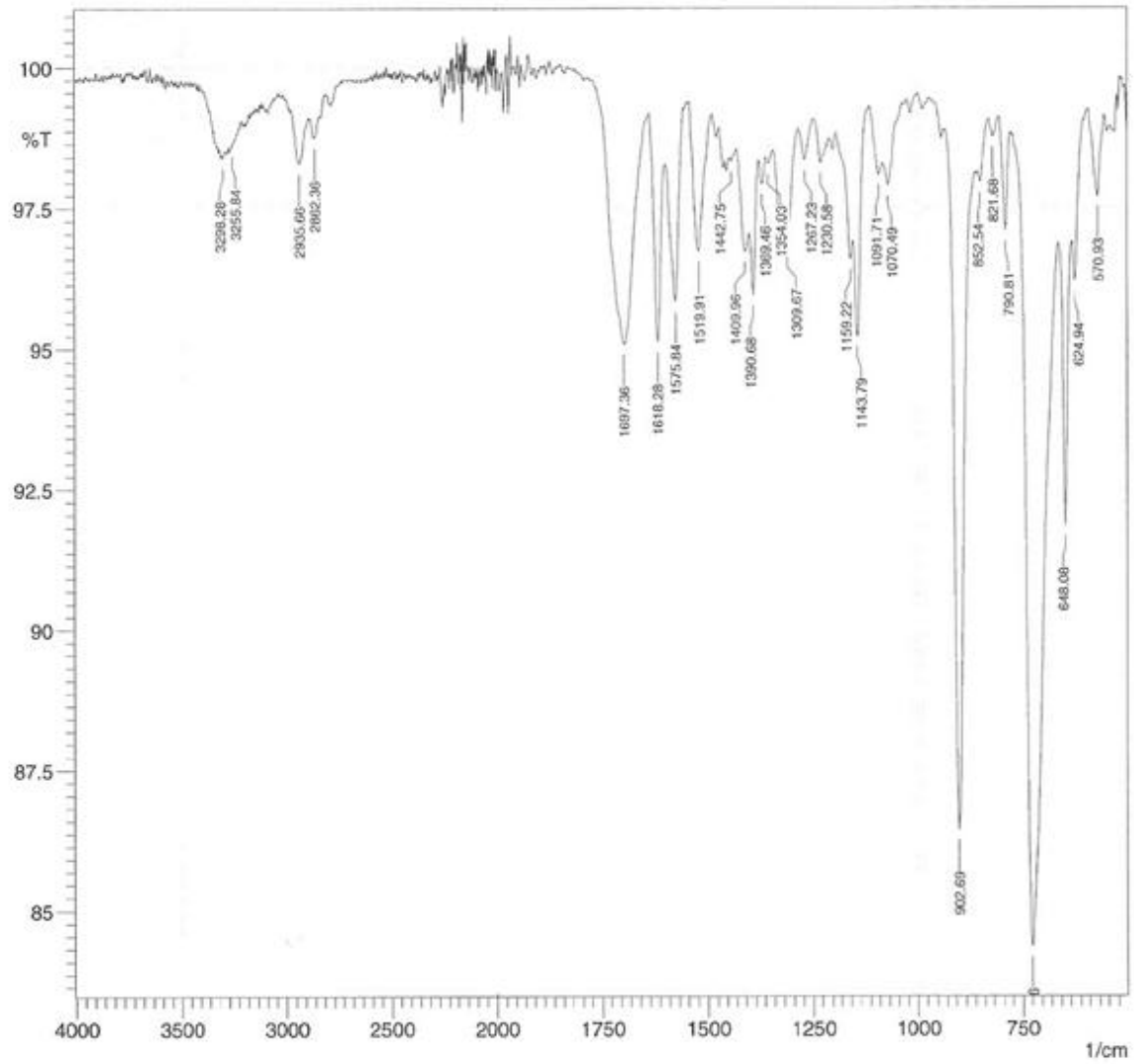

	Peak	Intensity	Corr. Inte	Base (H)	Base (L)	Area	Corr. Are
1	570.93	97.706	1.471	592.15	555.5	0.249	0.118
2	624.94	96.202	1.217	630.72	607.58	0.251	0.052
3	648.08	91.853	5.016	663.51	632.65	0.691	0.265
4	727.16	84.36	13.595	777.31	665.44	3.873	2.809
5	790.81	97.096	1.855	806.25	779.24	0.226	0.103
6	821.68	98.765	0.325	831.32	808.17	0.109	0.018
7	852.54	97.965	0.397	858.32	833.25	0.167	0.018
8	902.69	86.432	12.109	935.48	864.11	1.823	1.355
9	1070.49	97.904	0.663	1082.07	1037.7	0.272	0.049
10	1091.71	98.095	0.456	1114.86	1083.99	0.198	0.033
11	1143.79	95.228	2.31	1153.43	1116.78	0.413	0.13
12	1159.22	96.591	0.48	1193.94	1155.36	0.362	0.017
13	1230.58	98.303	0.616	1246.02	1211.3	0.21	0.042
14	1267.23	98.345	0.634	1282.66	1247.94	0.195	0.043
15	1309.67	96.823	1.907	1342.46	1284.59	0.592	0.266
16	1354.03	98.286	0.157	1359.82	1344.38	0.11	0.006
17	1369.46	97.93	0.404	1375.25	1361.74	0.113	0.015
18	1390.68	95.954	1.518	1398.39	1377.17	0.273	0.061
19	1409.96	96.73	0.814	1429.25	1400.32	0.343	0.056
20	1442.75	98.333	0.097	1446.61	1431.18	0.106	0.004
21	1519.91	96.73	2.543	1541.12	1490.97	0.456	0.292
22	1575.84	95.839	2.98	1598.99	1556.55	0.495	0.271
23	1618.28	95.121	3.578	1635.64	1600.92	0.464	0.263
24	1697.36	95.084	4.359	1770.65	1637.56	1.465	1.157
25	2862.36	98.753	0.078	2866.22	2839.22	0.126	0.005
26	2935.66	98.296	0.885	2978.09	2893.22	0.473	0.17
27	3255.84	98.609	0.04	3257.77	3234.62	0.13	0.002
28	3298.28	98.397	0.084	3304.06	3288.63	0.105	0.003

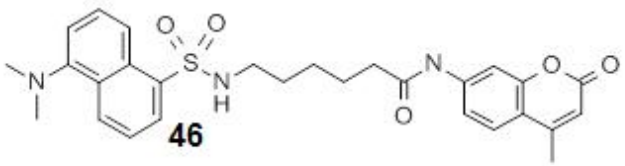

46

Date/Time; 9/16/2011 11:06:11 AM
No. of Scans; 50
Resolution; 4 [1/cm]
Apodization; Happ-Genzel

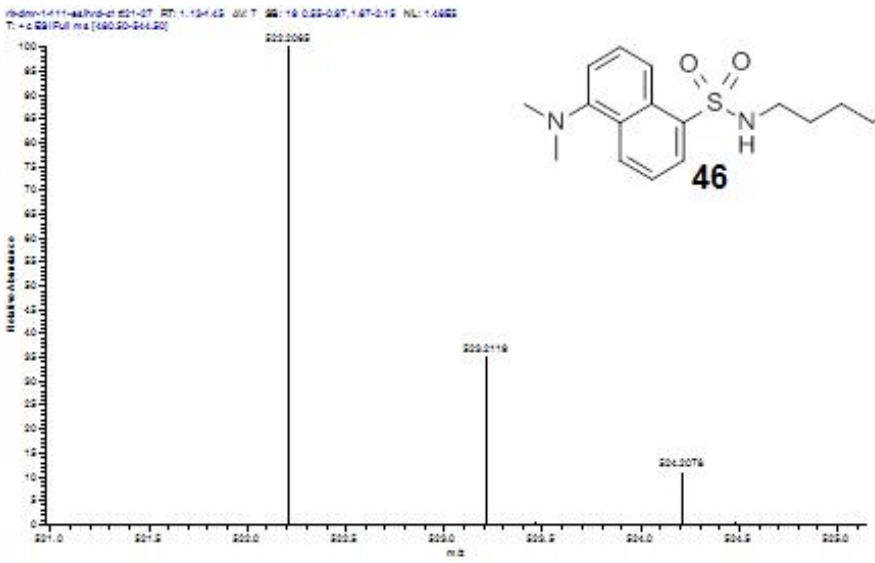

SPECTRUM - List Clipboard Mode

Data points: 1

Mass	Relative Intensity	Theoretical Mass	Delta [ppm]	RDB	Composition
522.20654	97.9	522.2071	-1.0	14.0	<<C30 H34 O6 S1 >>
		522.2057	1.6	14.5	<<C28 H32 O5 N3 S1 >>
		522.2084	-3.6	19.0	<<C31 H30 O2 N4 S1 >>
		522.2097	-6.1	18.5	<<C33 H32 O3 N1 S1 >>

Mass	Relative Intensity	Theoretical Mass	Delta [ppm]	RDB	Composition
522.20654	97.9	522.2071	-1.0	14.0	<<C30 H34 O6 S1 >>
		522.2057	1.6	14.5	<<C28 H32 O5 N3 S1 >>
		522.2084	-3.6	19.0	<<C31 H30 O2 N4 S1 >>
		522.2097	-6.1	18.5	<<C33 H32 O3 N1 S1 >>